A RAND NOTE

Numerical Simulation of Hypersonic Aerodynamics and the Computational Needs for the Design of an Aerospace Plane

S. K. Liu

RAND

The research reported here was sponsored by the United States Air Force under Contract F49620-91-C-0003. Further information may be obtained from the Long Range Planning and Doctrine Division, Directorate of Plans, Hq USAF.

Published 1992 by RAND
1700 Main Street, P.O. Box 2138, Santa Monica, CA 90407-2138

A RAND NOTE

N-3253-AF

Numerical Simulation of Hypersonic Aerodynamics and the Computational Needs for the Design of an Aerospace Plane

S. K. Liu

Prepared for the
United States Air Force

RAND

PREFACE

This Note records the results of a review and analysis of the status of the computational fluid dynamic (CFD) modeling techniques related to the National Aerospace Plane (NASP) operation. It was undertaken as a task in the study, "The National Aerospace Plane (NASP): Development Issues for Follow–on Systems," performed within the Technology Applications Program of Project AIR FORCE. The research sought to evaluate independently the degree of uncertainty and the technical risk involved in predicting the NASP performance using numerical simulation of aerothermal and chemical/combustion processes. This Note covers the technical review portion and identifies the areas for research emphasis so that the predictive reliability of the NASP's potential performance parameters can be improved.

Sponsored by the Air Force Directorate of Program Planning and Integration (SAF/AQX), the project has also required close cooperation with the NASP Joint Project Office (JPO).

This study should interest those concerned with the aerospace plane development in general, and hypersonic CFD modeling in particular.

SUMMARY

Computational fluid dynamic (CFD) simulations are now gradually replacing many ground experiments, becoming one of the major design tools for aerospace engineers. There are several reasons for using CFD models:

- Technical: Computational limits on speed and memory are rapidly decreasing with time, but the limits on experimental facilities (wall effects, distortion, etc.) have not decreased,
- Economical: Computer speed has increased faster than its cost,
- Energy saving: Wind tunnel experiments consume vast amounts of energy,
- Convenience: Computational results are immediately obtainable but experimental results are difficult to measure, calibrate, and interpret.

Potential application and major hypersonic aerodynamic issues that may be addressed by CFD modeling are:

- L/D (lift/drag) ratio of a given airframe configuration,
- The aerodynamic heat distribution vs maneuverability,
- Performance parameters of the supersonic ramjet (SCRAMJET),
- Aerodynamic stability within the NASP flight envelope,
- Boundary layer transition,
- Boundary layer/shock interaction,
- Other viscous effects.

For transonic or low Mach number aircraft design, engine and airframe simulations are usually made separately. But for the hypersonic plane, the entire aircraft has to be schematized into a single model, because the highly integrated hypersonic plane design requires dynamic coupling of the engine and the airframe. A model containing the entire aircraft and the internal

combustion computation process in a SCRAMJET engine would eliminate problems associated with the specification of redundant model boundary conditions. Consequently, there is a tradeoff between a lower spatial resolution for both airframe and the SCRAMJET simulation and a higher level of predictive uncertainty for a given computational resource.

To construct a CFD model covering a complete hypersonic plane with reasonable grid–space resolution, the model needs substantial computing resources. At the present time, a model with 900,000 grid points can be simulated with the state–of–the–art computer system, but certain tradeoffs have to be made. Simple and less–efficient numerical integration schemes have to be employed so that only limited neighboring computational points reside within the computer's main memory at a given time. Extensive data–swapping has to take place between the CPU and the external memory units. As a tradeoff, a simulation will take a longer time depending on the numerical scheme and the computational hardware involved.

In a CFD model, the friction coefficient is usually expressed as a function of the computed velocity profile perpendicular to the wall, whereas the heat transfer coefficient is usually expressed as a function of the computed temperature gradient perpendicular to the wall. Consequently, it is important to provide proper boundary conditions at the wall so that the effect of interdependency is minimized during the computation of the aerothermal field around the NASP.

For the past 35 years, the speed and memory of the most powerful U.S. computers have increased an order of magnitude every seven years. The present speed limit of the arithmetic unit is between one and two billion floating point operations per second (FLOPS) depending on the degree of vectorization of the code.

At present, a typical computer system used for large–scale CFD simulation has approximately 16 million words of main memory with possibly one or more external memory units, typically 8–mega words each. Supercomputers are nearly all vector machines. On the average, the relative improvement in speed of a typical CFD code is approximately six times after vectorization.

Beginning in the spring of 1989, CFD codes are expected to be simulated on CRAY's Y–MP/832, which offers two to three times the performance of

the X–MP. The system has 8 CPUs, operates on a 6–nanosecond clock cycle, and has a central memory capacity of 32 million 64–bit words. The next wave of supercomputers being developed by companies such as CRAY and NEC will be five times faster. They are expected to be introduced within five years.

Since there are more unknowns than just the number of (Navier Stokes) equations for turbulent flows, it is necessary for CFD models to "close" the information gap using turbulence modeling. Theoretically, higher–order turbulence models are more universally applicable than the lower–order models under various aerodynamic conditions. However, this has not always been the case in hypersonic applications. Most published models for NASP application use a zeroth–order closure scheme (see Table 4, Sec. 5, for example). This particular low–order scheme can make better predictions than many higher–order models in benchmark tests. Simpler models (usually with fewer constants), if designed by experienced aerodynamicists, can sometime outperform higher–order models with more "closure constants." Therefore, lab and design experiences also play an important part in CFD modeling. At present, areas with low predictive reliability in turbulence modeling that should be emphasized in future research include

1. Improvement in prediction of the location and length of the laminar–turbulent boundary transition zone, particularly in the upper hypersonic flight range. The uncertainty in the transition process translates directly into uncertainties in the prediction of NASP performance, weight, and other control parameters. It also influences the ability to predict engine inlet characteristics.

2. Validation of higher–order turbulent closure models to reduce the level of uncertainties in the area of low predictive reliabilities, such as:

- Strong aerodynamic curvature.
- Intermittency and large structures in the flow.
- Rapid compression or expansion.
- Kinematically influenced chemical reaction.

- Low Reynolds number effects.
- Strong swirl.
- Turbulence, which is strongly influenced by body force acting in a preferred direction.
- Uncertainties in boundary–condition specification.
- Compressibility effects on turbulence.
- Dynamic stability and intermittency in the high–wave–number turbulent eddies in the SCRAMJET combustion process.
- Improvement in the modeling of compressible turbulence, particularly near the engine inlet where boundary layer and shock layer may induce substantial density variability and unstability.

3. Improvement in conserving mass, momentum, and energy in the numerical schemes for solving the Navier Stokes equations involving nonorthogonal grid transformation. Need effective methods for handling sharp gradient and discontinuity.

4. Improvement in treatment of boundary conditions, particularly in an interdependent, nested modeling system in which different grids are used. Need effective numerical scheme for handling nonreflective boundary conditions associated with, for example, a three–dimensional full Navier Stokes (FNS) numerical solver. Reverse flow must be addressed effectively.

5. Development of quantitative estimates of reductions in computational accuracy near the nose and leading edges when implicit schemes (e.g., alternating direction implicit) are combined with the coordinate tranformation.

6. In–depth analysis of various hypotheses associated with turbulence modeling and the universality of turbulence closure constants.

7. Development of methodologies for the quantitative assessment of uncertainties in the hypersonic CFD simulations. It is important that

the uncertainties in the simulation results be estimated and published as a function of the vehicle speed and location along the vehicle so that designers and policymakers can make reasonable assessment of the vehicle's projected performance.

There is no need for "turbulence closure" if a prototype aircraft is represented by a model containing the number of grid points approaching the $9/4^{th}$ power of the highest flight Reynolds number. For the anticipated range of flight Reynolds number of NASP, say 10^7, it would need a computer at least 10^5 times more powerful than the present system. Consequently, turbulence modeling will still be needed for the foreseeable future. The present trend is to build higher–order "stress–component" type models. The simplest stress–component model solves seven extra partial differential equations in addition to the basic Navier Stokes equations of motions and continuity.

Many of the present CFD models are based on the "parabolized" Navier Stokes equations (PNS), which makes the numerical solution process much simpler and more efficient. The parabolization technique neglects the convective–diffusive process parallel to the aircraft surface. For NASP applications, many layers are generally used to resolve the normal gradient by means of stretched coordinates, so that parabolization is often justified. However, comparison of PNS and FNS solutions should be made to evaluate the importance of the eliminated convective terms in the governing equations to justify the use of a PNS code.

The majority of the present CFD models for hypersonic aircraft use the finite–difference scheme schematized over a boundary–fitted coordinate system. Coordinate transformation becomes one of the major efforts in CFD modeling. Combination of the (simpler) finite–difference method (FDM) and the coordinate transformation replaced the finite–element method (FEM), which enjoyed some popularity during the 1970s because of its geometric flexibility. Since the finite–element models need to invert extremely large matrices involving the variables of the entire aircraft, they are computationally much less efficient than the finite–difference models. The present trend is to use the most straightforward numerical scheme, so that

only a few points reside within the CPU. By doing so, a hypersonic aircraft can be schematized into a very large number of grid points.

In terms of modeling accuracy, with the maximum allowable spatial resolution, the present accuracy of CFD models at the lower hypersonic range ($M \cong 6$) is 5 to 7 percent in terms of pressure. When the predicted values are compared with the experiments, the larger deviations are located near the sharper geometric transitions. This indicates that higher spatial resolutions will likely improve the simulation results. A higher–order turbulence model may also improve the results around the curved surfaces. Both imply the need for bigger and faster computers.

As far as hypersonic laminar–turbulent transition, it may be years before we have either the data or the model to go beyond crude semi–empirical models. Similarly, not enough is known about compressible turbulence to establish suitable closure models for hypersonic flows, including the possibility of large turbulent structures or perhaps even relaminization from a turbulent state.

Judging by past trends, by the year 2000 the expected speed of the fastest computer for hypersonic aircraft applications will be in the neighborhood of 10–50 billion floating point operations per second. However, if the heat dissipation problem is drastically reduced by superconductive material, the potential CPU speed may substantially improve in the future.

Because of the lack of suitable verification data at high speed, CFD codes' ability to predict depends to a great extent on the universality of their turbulence models. In other words, the values of the "closure constants" used in these models would have to stay the same within their predictive range. However, several well–known universal constants in fluid mechnics (e.g., the Kolmogorov's universal constant) were found to be variable. In Kolmogorov's case, when a 3–D turbulence is reduced to a 2–D turbulence, a localization adjustment factor is needed when computing the spectral distribution of turbulent energy near a wall. Hypersonic modeling may be affected if parabolization is involved.

At present, major hypersonic CFD research is conducted in government research centers. To apply CFD methodologies effectively in hypersonic aircraft design, these modelers not only have to work with experienced

designers in the industry but also have to work with material engineers to extend fluid–dynamic models into "aerothermoelastic" design codes. Furthermore, it is urgent that an effective government/industry relationship be established at the technical level so that research codes developed in government labs can become production code that designers can use. It is also important that the uncertainties in the CFD simulation results be estimated and published as a function of the vehicle speed and location along the vehicle (tip to tail), so that the NASP design teams and policymakers can estimate the consequences of these uncertainties on vehicle performance.

ACKNOWLEDGMENTS

The author is indebted to the following RAND colleagues for their help during the course of this study: J. Aroesty, B. Augenstein, I. Blumenthal, J. Bonomo, G. Donohue, D. Frelinger, T. Garber, E Harris, J. Hiland, D. Orletsky, S. Pace, J. Rosen, L. Rowell, J. Stucker, P. Bedrosian, A. Boren, and G. Coughlan. The author expresses appreciation to U. B. Mehta of NASA Ames, and to S. R. Chakravathy, U. C. Goldberg, and J. W. Haney of Rockwell International for valuable discussions.

CONTENTS

FIGURES

TABLES

GLOSSARY

A, B = Jacobians of flux vectors F and G

A^+ = a turbulent closure constant in Baldwin-Lomax zero-equation model

a^{-1} = the amount of fluid/fragment interfacial area per unit volume

ADI = Alternating Direction Implicit (scheme)

3AF = three-factor approximate factorization (scheme)

AFWAL = Air Force Wright Aeronautical Laboratories

a_n = Fourier coefficient in spectral method

ARC = Ames Research Center

BL = boundary layer

b_n = Fourier coefficient in spectral method

BWB = blended-wing-body

c = speed of sound or subscript for concentration-related flux vectors

C = mass concentration

C^* = a programming language use for connection machines

CAD = computer-aided design

C_{cp} = Clauser constant

CDC = Control Data Corporation

c_k, c_ϵ = turbulence modeling constants

CNS = compressible Navier Stokes

C_d = tubulent closure constant for dissipation

C_D = drag coefficent

C_o = Courant number

C_f = skin friction coefficient

CFD = computational fluid dynamics

C_L = lift coefficient

CPU = central processing unit

d = body diameter

D = binary diffusion coefficient

DCR = dual combustor RAMJET

DEC = Digital Equipment Corp. (VAX machines)

del = deformation operator

D_s = diffusion coefficients in a coupled dynamic/chemistry model

e = total SGS energy per unit mass

ETA10 = the latest model of CYBER series supercomputer (ETA Corp, production stopped in spring 1990)

f_{12} = interfacial friction between two fluids

FDS = flux difference splitting

FCT = flux-corrected transport

FFT = fast Fourier transform

F, G, H = vector flux

F_{Kleb} = a turbulence modeling parameter (zero-equation model) involving Klebanoff intermittency factor

FLOPS = floating-point operations per second

FNS = full Navier Stokes

FVS = flux vector splitting

F_{wake} = a parameter in turbulence modeling (zero-equation model) involving the difference between the max and the min total velocity

g_{11}, g_{22} = components of the contravariant metric tensor, or g^{jk}

g_v = acceleration due to gravity

h = enthalpy

H_0 = total enthalpy

HFF = Ames hypervelocity free-flight facility

HGG = hyperbolic grid generator

HGV = hypersonic glide vehicle

i,j,k = integer index

I = inter-fluid source term in a two-fluid model

I_{sp} = specific impulse

I/O = input/output

J = Jacobian of a transformation

JFM = *Journal of Fluid Mechanics*

k = sub-grid-scale turbulent kinetic erergy, ergs/unit mass

K = a subscript

K_n = Knudsen number, = $1.26 \sqrt{\gamma} \frac{M}{Re}$

L = characteristic length

LACE = liquid air cycle engine

LaRC = Langley Research Center

LDV = laser Doppler velocimetry

Le = Lewis number, which represents the relative rate of diffusion of mass and heat

LHS = left-hand side (of an equation)

LO_x = liquid oxygen

M = Mach number

m, M = integer index

NAS = numerical aerodynamic simulator

NASP = national aerospace plane

NDV = NASP-derived vehicle

n, N = integer index

N_s = number of species

ODE = ordinary differential equation

p = static pressure

PARIS = commands (used together with C^* language for increasing processing speed in connection machines

PBR = Ames pressurized ballistic range

PDE = partial differential equation

Pe = Peclet number = Pr x Re (Prandtl No. x

Reynolds No.)

p^i = control functions in grid generation

PNS = parabolized Navier Stokes

Pr = Prandtl number, which is the ratio of rate of diffusion of vorticity and of heat

Pr_t = turbulent Prandtl number

q = heat flux

R = volume fraction of two-fluid model

R_e = free stream Reynolds number

RHS = right-hand side (of an equation)

RHYFL = Rockdyne Hypersonic Facility (a shock tube)

RMS = root-mean-square

RNS = reduced Navier Stokes

R_x = mass diffusion term such as in a species equation

R_i = Richardson number, a measure of vertical dynamic stability

R_{cr} = critical Richardson number

S = source term within fluid

S_c = Schmidt number, which represents the relative rate of diffusion of vorticity and mass

SGS = sub-grid-scale

SSD = solid-state storage device

t = time

T = static temperature

te = trailing edge

$[\ ]^T$ = transposed form of a vector

TIM = time iterative marching

TKE = turbulent kinetic energy

TLNS = thin-layer Navier Stokes

TVD = total variation diminishing

U = dependent variable

UNS = unsteady Navier Stokes

UPS = upwind PNS solver

VAST = vector and array syntax translator (for CFD code vectorization)

u, v, w = velocity components in the x, y, z, direction

u',v' w'= velocity fluctuation components

$\bar{u}$, $\bar{v}$, $\bar{w}$ = diffusion velocity components for air species in the x, y, x direction

W = weighting function in a moving adaptive grid system

$\dot{W}$ = transposed form of air chemistry source term

X-30 = an experimental aerospace plane

Y_{max} = the y-distance at which F_{max} occurs, in turbulence modeling

y^+ = law-of-the-wall distance (i.e., $\sqrt{\rho_w \tau_w} y/\mu_w$)

∇ = Cartesian gradient vector operator

Δx = grid spacing

δ = characteristic length of viscous layer; boundary layer thickness

δ_{ij} = Kronecker delta

ϵ = eddy viscosity or isotropic part of turbulent energy dissipation in a turbulence model

λ = second viscosity coefficient, or conductivity

Γ = diffusion coefficient within one fluid of a two-fluid model

μ = first viscosity coefficient, dynamic viscosity

μ_t = turbulent eddy visicosity

ν = kinematic viscosity

ω = vorticity

$\dot{\omega}$ = air chemistry source term

ρ = density

ρ^* = density of the lighter of the two fluids in a two-fluid model

$\bar{\rho}$ = average density

$\tilde{\rho}$ = variation of density

ϕ = fluid property

γ = gas specific heat ratio (1.4 for perfect gas)

ξ,η,ζ = constants in the transformed space, $x = x(\xi,\eta,\zeta)$, $y = y(\xi,\eta,\zeta)$, $z = z(\xi,\eta,\zeta)$

σ_ϵ, σ_k = turbulence modeling constants

τ = body thickness

τ_{ij} = shear stress components

1. INTRODUCTION

Advances in computational fluid dynamic (CFD) methods and the increasing capabilities of computers will play a crucial role in the development of the National Aerospace Plane (NASP). Because it is not yet practical to conduct continuous flight experiments at speeds much above Mach 8, aerodynamic behavior and the potential performance of the NASP beyond this speed have to be predicted using the CFD methods without sufficient verification data. Therefore, the degree of certainty or the confidence limits associated with CFD predictions for various NASP applications are at this moment difficult to quantify (Mehta, 1990b). This is particularly true for the newly developed computational codes based on the full Navier Stokes (FNS) equations with finite–rate chemistry. It is a challenging task to prove the validity of supersonic combustion processes and the performance parameters associated with the SCRAMJET engine at upper hypersonic speed ranges using a computer simulation.

Since CFD models are based on numerical solutions of a set of governing equations (under certain assumptions over a finite–grid network), to simulate the aerospace plane's integrated external flow field and propulsion system, a numerical model must cover several different flight regimes. Although much progress has been made in solving aerodynamic design problems, many new developments are still needed before the complete three–dimensional equations for unsteady compressible viscous flow can be solved routinely with high enough resolution and certainty in the entire operating range of the NASP.

OBJECTIVE

The research reported in this Note sought to evaluate independently the degree of uncertainty and the technical development risk involved in predicting NASP performance using numerical simulation of the highly integrated air frame/propulsion system. This Note presents a technical review and a summary of four interrelated fields.

ORGANIZATION OF THIS REPORT

Section 2 gives the hypersonic environment within which the NASP is expected to operate. It summarizes governing dynamic equations and reviews many forms of the reduced equation sets. Section 3 reviews the important numerical schemes upon which CFD codes are based. It discusses advantages and disadvantages as well as the computational requirement associated with each numerical scheme. It also covers one of the important characteristics of the hypersonic aerodynamic process –the existence of a shock wave in the flow field– as well as the use of a numerical technique and finite computational grid to resolve this shock wave.

Section 4 addresses a new technical field in computational fluid dynamics: the grid generation technique. An essential as well as a time–consuming step in CFD modeling is to generate a proper grid around an air frame or through a duct system. Theoretically, each time a numerical integration step is carried out over a transformed grid system, a certain amount of mass will be lost. The aspects of conservation of mass, energy, and momentum associated with a transformed computational domain are also discussed in this section.

Section 5 discusses the computational needs for various types of turbulence modeling. Inasmuch as the speed and the size of present–day computers cannot yet represent the flow field with high enough resolution, we still need to model sub–grid–scale turbulence. Turbulent flow will occur within the flight regime of the aerospace plane and the supersonic combustion process of the SCRAMJET engine. The modeling of turbulence is essential in predicting the advective process of momentum and heat transfer within the boundary layer of the aerospace plane. This in turn determines the potential performance and the temperature distribution throughout the NASP. This section also describes the zeroth–, first–, and second–order as well as stress–component turbulence closure schemes. Computational needs for various types of turbulence modeling are discussed in this section.

Section 6 discusses the trends in development of computers that have been used to carry out CFD modeling. To use a CFD model effectively, good hardware and software support are essential. Code development has to match the type of machine for efficient simulations. Programming and CFD modeling can be carried out more effectively by using proper computers. Some predictions are also included.

Section 7 summarizes CFD modeling needs and discusses its uncertainties. It is beyond the scope of this Note to give a quantitative analysis of technical risk associated with predicting the NASP performance using CFD simulation. This Note does, however, point out several aspects pertaining to the needs in NASP design using CFD.

Section 8 presents conclusions.

2. HYPERSONIC ENVIRONMENT AND THE GOVERNING NAVIER STOKES EQUATIONS

Numerical models designed to simulate the external aerodynamics or the duct flow (of SCRAMJET for example) of an aerospace plane should rest on a set of appropriate governing equations. These equations must:

- Include essential physical parameters in the basic formulation,
- Operate under appropriate assumptions and limits, and
- Have the necessary initial and boundary conditions for the computation.

To make a reasonable assessment of the computational needs, the range of the aerospace plane's operational parameters is discussed first. This discussion includes speed, skin temperature, air–density range, and other physical factors that are essential to the plane's aerodynamics.

THERMO– AND AERODYNAMIC OPERATING RANGE OF THE AEROSPACE PLANE

The aerospace plane is propelled by both RAMJET and SCRAMJET air–breathing engines at different speed ranges. The primary difference between the two engines is that air passes through the RAMJET at subsonic speeds and through the SCRAMJET at supersonic speeds. In a RAMJET, air is slowed down to about Mach 0.2; fuel is then added. At hypersonic speeds, the SCRAMJET is designed to compress and decelerate the incoming air to about Mach 1. Adding heat to the duct slows air further. The resulting back pressure creates a shock wave in the inner diffusor behind the inlet through but ahead of the combustion chamber. At around Mach 6 (1800 m/s), inlet temperature is approximately 2540 ^{O}F (Mackley, 1986). At that speed, the inlet air speed is slowed to about 1500 m/s. Air speed at the hydrogen injector is also around 1500 m/s. Hydrogen resides in the combustor for approximately one millisecond.

Unlike conventional aircraft, the fuselage of the aerospace plane has to supply part of the compressional surface for the engine. The same is true for the aft portion of the plane and exhaust nozzle for propulsion. Therefore, the aerodynamic computation of the engine and fuselage not only has to be dynamically coupled but also properly posed, otherwise it may create redundancy in specifying the boundary conditions.

The external temperature of the aerospace plane during supersonic cruise varies at different flight regimes within the air–breathing operational range. Figure 1 superimposes the continuous flight corridor (Masson and Gazley, 1956) over the aerospace plane's flight envelope. The maximum ranges of external temperature at various points of the aerospace plane are estimated (Korthals–Altes, 1987) and appear in Table 1.

Table 1

The Maximum Range of External Temperature at Various Points of the Aerospace Plane

Location	Estimated max. temp.
Nose	3260 ^{o}F
Outside of the crew cabin	2000 ^{o}F
Fuselage structure	1800 ^{o}F
Outside passenger and cargo area	1600 ^{o}F
Outside liquid–hydrogen tanks	1400 ^{o}F
Wing structure	2650 ^{o}F
Air inlet and propulsion unit	1600 ^{o}F
Control surface	3250 ^{o}F
Leading edges	2650 ^{o}F

The equilibrium skin temperature listed here is the temperature at which the convective heat transfer to the surface equals the radiation heat transfer from the surface.

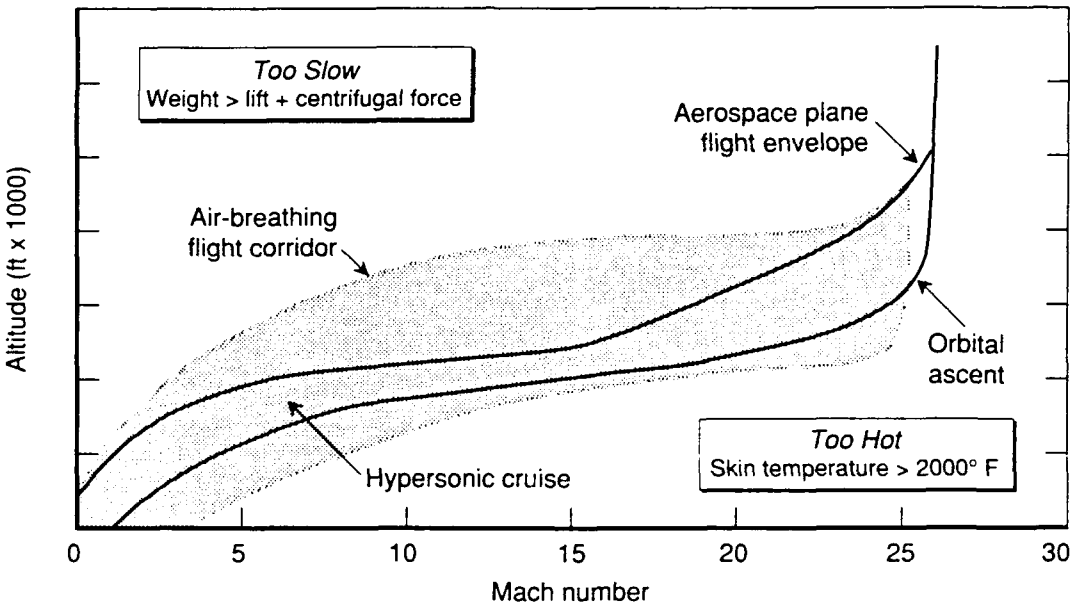

SOURCE: Adapted from Masson and Gazley (1956).

Fig.1—Assumed Prototype NASP/NDV Characteristics and the Flight Envelope of the Aerospace Vehicle

The range of Reynolds number per foot of characteristic length within the flight regime is from 10^4 to 10^8. Boundary–layer transition from laminar flow to turbulent flow will probably occur along the hypersonic body. The type of fluid flow for the numerical modeling will include a viscous shock layer and viscous boundary layer. In the air–breathing flight regime, the air–density ratio relative to the sea–level value and the mean free path is reflected in Table 2.

Table 2

The Air–Density Ratio Relative to the Sea–Level Value
in the Air–Breathing Flight Regime

Altitude (ft)	Mean Free Path (ft)	Air Density Relative to Sea Level
0	2.18×10^{-7}	1
100000	1.61×10^{-5}	1.35×10^{-2}
200000	8.45×10^{-4}	2.57×10^{-4}
300000	1.25×10^{-1}	1.75×10^{-6}

From Table 2, the Knudsen number within the aeroplane's air–breathing operating range is between 2.18×10^{-7} to around 0.1 per foot of characteristic length (body dimension or boundary–layer thickness). In a strict sense, flow with the Knudsen number greater than unity should be classified as rarefied gas flow which is not in a continuum regime. Therefore, it might not be properly described by the compressible Navier Stokes equations. Certain fully merged layer regimes can only be classified as near–continuum, and the Navier Stokes

equations should be used only for crude estimates of the local skin friction and heat transfer over that area. However, experimental evidence indicates that the Navier Stokes equations have an appreciably wider range of empirically justified validity than their theoretically defensible range. Our analysis will cover the aerodynamics of the air–breathing flight regime of the aerospace plane that can be described by the Navier Stokes equations.

FLOW COMPUTATION IN THE SCRAMJET

A major component of the aerospace plane is the supersonic–combustion RAMJET (SCRAMJET). SCRAMJET adds heat either to product gases or by direct injection of the fuel into the supersonic air stream with simultaneous mixing and burning in the combustion chamber at supersonic flows. The ideal SCRAMJET cycle is based on Rayleigh flow in which friction losses are neglected. The thermo–gas dynamic processes involved are (a) heat addition at supersonic speeds (Rayleigh flow), (b) isentropic nozzle expansion to atmospheric pressure, and (c) heat rejection at constant pressure by exhaust to the atmosphere.

A unique characteristic of the SCRAMJET engine is that the ratio of kinetic jet energy to input heat ranges from approximately 1.5 to 3.0 (Ferri, 1964). In fact, a SCRAMJET is the only propulsion system capable of generating relative jet kinetic energy to input energy ratios greater than unity (turbojet's ratio is 0.3 and rocket's 0.4). The idealized overall efficiency of a SCRAMJET system is generally quite high and increases with increasing flight Mach numbers. On the other hand, phenomena such as combustion–shock wave interaction and frictional effects may set limitations and constraints on the simplified SCRAMJET cycle. The addition of heat to the combustion process creates combustion waves (detonation or deflagnation). Combustion and shock wave interaction in a supersonic RAMJET system is quite complex, particularly if frictional effects and chemistry are also considered. Most important is the question of whether adequate mixing can occur in a reasonable length, or will the SCRAMJET be inefficient in practice? These aspects need extensive analysis using models containing all the essential variables.

In designing a SCRAMJET, the area of the combustor has to be increased

slightly to prevent thermal choking. But the amount of increase must be carefully controlled so as not to extinguish the flame. The overall system efficiency of a SCRAMJET is very sensitive to internal skin friction loss (Waltrup et al., 1979; Schetz et al., 1987). The internal flow dynamics of a SCRAMJET engine can be characterized by a strong nonuniform supersonic inflow followed by a nozzle with no contraction (throat) as in rockets, RAMJETs or jet engines. Therefore, to simulate the flow characteristics within the SCRAMJET accurately, a numerical model must be able to resolve the strong convective components with chemical reaction effects present in significant amounts at the end of the combustor.

Because of the strong convective acceleration and possible separation within the SCRAMJET engine's combustion system, simplified numerical schemes often used for NASP's external flow simulations (e.g., PNS, discussed in Sec. 3) may not be suitable for SCRAMJET. For gas chemistries, a numerical model should at least include the molecules formed with H, N, C, and O. The potential performance of a SCRAMJET engine depends to a great extent on the calculation of its nonuniformity of flow, and the turbulent mixing/combustion process. These aspects put stringent demands on the turbulence modeling computational resource and require sufficient data for model verification.

Until recently, modeling of combustion processes in a SCRAMJET engine was often assumed to be mixing–controlled combustion (complete reaction). Based on this assumption a two–dimensional unsteady Navier Stokes code (TWODLE) has been developed at NASA Langley for simulating SCRAMJET combustion flow in the NASA modular SCRAMJET engine. This CFD code is formulated to compute the combustion of hydrogen/air mixture using a complete reaction model in which instantaneous reaction is assumed at any point where both fuel and air are present. Boundary conditions at the wall are assumed to be adiabatic and noncatalytic (White et al., 1987). Chemical reactions in a SCRAMJET combustion process are generally controlled by kinetics and not mixing. However, under certain conditions it may be that both reaction time and mixing time are critical. NASA Langley, together with Johns Hopkins University Applied Physics Laboratory, recently developed a 9–species, 18–equation finite–rate chemistry code named SPARK to simulate the hydrogen–air combustion to describe the important reactions of various SCRAMJET designs (White et al., 1987).

Time–dependent solutions of chemically reacting flow in SCRAMJET are often quite "stiff" numerically. In other words, the characteristic time scale associated with the chemical reactive flow varies widely. The wide range in time scale comes from the fact that to resolve the fine details of the flow field, the computational grid needs to be small to have higher spatial resolution thus resulting in a very small time step (see Sec. 3).

GOVERNING EQUATIONS FOR THE THREE–DIMENSIONAL FLOWS

The three–dimensional Navier Stokes equation in a Cartesian coordinate system in a conservation–law form (Anderson et al., 1984) is as follows:

$$\frac{\partial U}{\partial t} + \frac{\partial F}{\partial x} + \frac{\partial G}{\partial y} + \frac{\partial H}{\partial z} = 0$$

$$U = \begin{bmatrix} \rho \\ \rho u \\ \rho v \\ \rho w \\ E_t \end{bmatrix} \qquad F = \begin{bmatrix} \rho u \\ \rho u^2 + P - \tau_{xx} \\ \rho u v - \tau_{xy} \\ \rho u w - \tau_{xz} \\ (E_t + p)u - u\tau_{xx} - v\tau_{xy} - w\tau_{xz} - q_x \end{bmatrix}$$

$$G = \begin{bmatrix} \rho v \\ \rho v u - \tau_{xy} \\ \rho v^2 + p - \tau_{yy} \\ \rho v w - \tau_{yz} \\ (E_t + p)v - u\tau_{xy} - v\tau_{yy} - w\tau_{yz} - q_y \end{bmatrix}$$

$$H = \begin{bmatrix} \rho w \\ \rho w u - \tau_{xz} \\ \rho w v - \tau_{yz} \\ \rho w^2 + p - \tau_{zz} \\ (E_t + p)w - u\tau_{xz} - v\tau_{yz} - w\tau_{zz} - q_z \end{bmatrix}$$

where U = dependent variable;

F, G, H = flux vector;

E_t = total energy per unit volume;

p = static pressure;
q = heat flux;
τ = viscous stress components;

The complete Navier Stokes equation is highly nonlinear, and it does not possess any known analytical solution. At the present time it can be solved only approximately using numerical methods. Solutions to the Navier Stokes have many applications in aerodynamic design. For example, the skin friction coefficients for a given design can be computed with proper initial and boundary conditions. The skin friction coefficient C_f can be defined as:

$$C_f = \frac{\mu_w \left(\frac{\partial u}{\partial y}\right)_w}{\rho_\infty u_\infty^2}$$

$$= \frac{\mu_\infty \left(\frac{\mu_w}{\mu_\infty}\right) \frac{\partial u}{\partial y} L}{\rho_\infty u_\infty^2 L}$$

$$= \frac{\left(\frac{\mu_w}{\mu_\infty}\right) \frac{\partial\left(\frac{u}{u_\infty}\right)}{\partial\left(\frac{y}{L}\right)}}{\frac{\rho_\infty}{\mu_\infty} u_\infty L}$$

$$= \frac{\mu^*_w \dfrac{\partial u^*}{\partial y^*}}{R_e}$$

where $$y^* = \frac{y}{L}$$

$$\mu^* = \frac{\mu_w}{\mu_\infty}$$

$$u^* = \frac{u}{u_\infty}$$

R_e denotes the free stream Reynolds number. The derivative represents the velocity profile normal to the surface. These velocities are the computed velocities resolvable by a model's grid network. Similarly, a local heat transfer coefficient can also be estimated as a function of the computed local temperature gradient.

Models based on the complete set of Navier Stokes equations require substantial computational resources. To improve the computational efficiency, the variables on the continuous physical space are first mapped onto a discrete, transformed network for modeling. For most practical applications in hypersonic aerodynamics, a thin–layer approximation further improves the computational efficiency.

PARABOLIZATION AND THE REDUCED FORMS OF NAVIER STOKES EQUATIONS

Even though the governing Navier Stokes equations provide an excellent description for fluid flow, they are of an elliptic type for which the numerical techniques are lengthy and cumbersome. They often require iterative solutions.

The presence of thin shock and shear layers makes it difficult and costly to solve within an acceptable level of accuracy. But, if one can neglect all the stream–wise viscous diffusion terms and modify the stream–wise convective flux vector to permit stable time–like marching of the equations downstream from the initial data, then mathematically the nature of the Navier Stokes equation changes from elliptic–type to parabolic–type. The equations can then be solved by advancing an initial "plane" of data in space rather than by advancing an initial "cube" of data in time. The modeling efficiency drastically increases.

From the physical point of view, parabolization neglects the diffusion process parallel to a surface but retains all three momentum equations and makes no assumption about the pressure. The diffusion term involving derivatives parallel to the surface for the high Reynolds number turbulent flows near the vorticity–generating surface is usually extremely small. Many layers are needed to resolve the normal gradient by means of stretched coordinates, so that the thin–layer approximation is often justified. In fact, many of the hypersonic aerodynamic computational schemes presently available are of the parabolized Navier Stokes (PNS) type. Detailed derivation of the PNS equations from the complete Navier Stokes equations can be found in Rudman and Rubin (1968) or in text books such as Anderson et al. (1984).

There are several other simplified forms which deviate slightly from PNS. Barnett and Davis (1985) added the stream–wise dependence to PNS by means of a pressure relaxation scheme. This reduced Navier Stokes (RNS) method is valid for air flows in which the stream–wise interaction is weak. The same is true for the thin layer Navier Stokes equations (TLNS) introduced by Pulliam (1984). In TLNS, the viscous terms containing derivatives in the directions parallel to the body surface are neglected in the unsteady NS equations, but all other terms in the momentum equations are retained. By retaining the terms that are normally neglected in boundary–layer theory, separated and reverse flow regions can still be calculated (Anderson et al., 1984).

Numerical models based on the simplified Navier Stokes equation have played a key role in the design of future aerospace planes because they reduce the computational effort by at least an order of magnitude. On the other hand, a simplification scheme such as the "zonal modeling" technique may also create potential computational problems. For example, there are potential

incompatibilities in establishing the mutual boundary conditions for the patched models, particularly when the flow fields of these models are dynamically coupled, as in the case of the aerospace plane.

Like many other types of the Navier Stokes–based numerical models, sometimes substantial efforts are required to establish a proper boundary condition so the interior solution is not influenced by the reflective boundaries. Theoretically, computers will never be large enough that the model boundaries can be placed to represent the truly far field unless we know the solution beforehand. To establish a dynamically suitable non–reflective boundary in a moving coordinate system with shock is understandably quite complex.

Past experiences in Navier Stokes modeling have indicated that more accurate numerical schemes generally need better treatment at the boundaries. This is because higher–order (more accurate) numerical schemes involve higher spatial derivatives that need to be specified at the boundaries during the integration process. As a consequence, models based on different solution schemes require different boundary treatments. They will be discussed together with the schemes themselves in the Sec. 3.

THREE–DIMENSIONAL SYSTEM IN A TRANSFORMED SPACE

The shape of most aerodynamic bodies consists of curved surfaces. Consequently, the Navier Stokes equation formulated on a Cartesian coordinate system loses its resolving power in aerodynamic applications. To improve computational efficiency, it is more desirable to formulate the equation in curvilinear coordinates. An arbitrary shape in the physical domain can be mapped onto a rectangular, discrete computational domain through coordinate transformation. The transformed space is usually, but not necessarily, a rectangle. It could be a circular disk or a sphere such as the earth ellipsoidal coordinate (Liu and Leendertse, 1987). The great majority of the coordinate system generation methods are based on solving partial differential equations using a coordinate transformation from the physical domain to an orthogonal computational domain (see Fig. 2). Using this approach, local refinements of the mesh can be achieved by introducing an appropriate mesh control function into

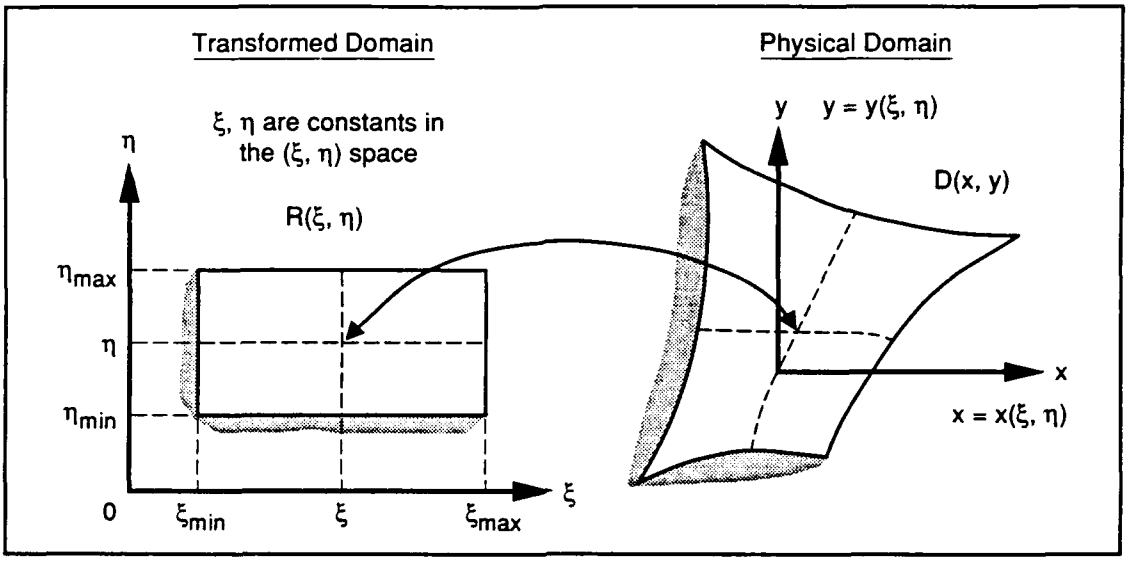

Fig. 2—Mapping of the Physical Domain on a Rectangle Via Coordinate Transformation

the governing equations. Boundary fitted coordinate generation methods are discussed in Sec. 4.

Three–dimensional, mass–averaged, Navier Stokes equations in the transformed space (ξ,η,ζ) for the dependent variable U, are:

$$\frac{\partial U}{\partial t} + (\xi_x,\xi_y,\xi_z)\begin{bmatrix}\frac{\partial F}{\partial \xi}\\ \frac{\partial G}{\partial \xi}\\ \frac{\partial H}{\partial \xi}\end{bmatrix} + (\eta_x,\eta_y,\eta_z)\begin{bmatrix}\frac{\partial F}{\partial \eta}\\ \frac{\partial G}{\partial \eta}\\ \frac{\partial H}{\partial \eta}\end{bmatrix} + (\zeta_x,\zeta_y,\zeta_z)\begin{bmatrix}\frac{\partial F}{\partial \zeta}\\ \frac{\partial G}{\partial \zeta}\\ \frac{\partial H}{\partial \zeta}\end{bmatrix} = 0$$

$$F = \Big[\rho u, \rho u^2 - \tau_{xx}, \rho uv - \tau_{xy}, \rho uw - \tau_{xz}, \rho eu - \gamma\left(\frac{\mu}{Pr} + \frac{\epsilon}{Pr_t}\right)\frac{\partial e}{\partial x} - (u\tau_{xx} + v\tau_{xy} + w\tau_{xz})\Big]^T$$

$$G = \Big[\rho v, \rho uv - \tau_{yx}, \rho v^2 - \tau_{yy}, \rho vw - \tau_{yz}, \rho ev - \gamma\left(\frac{\mu}{Pr} + \frac{\epsilon}{Pr_t}\right)\frac{\partial e}{\partial y} - (u\tau_{yx} + v\tau_{yy} + w\tau_{yz})\Big]^T$$

$$H = \Big[\rho w, \rho uw - \tau_{zx}, \rho vw - \tau_{zy}, \rho w^2 - \tau_{zx}, \rho ew - \gamma\left(\frac{\mu}{Pr} + \frac{\epsilon}{Pr_t}\right)\frac{\partial e}{\partial z} - (u\tau_{zz} + v\tau_{zy} + w\tau_{zz})\Big]^T$$

$$\tau_{ij} = (\mu+\epsilon)(\text{def}\,\bar{u})_{ij} - \left[\frac{2}{3}(\mu+\epsilon)(\nabla.\bar{u}) + P\right]\delta_{ij}$$

where an eddy viscosity model is assumed and where:

δ_{ij} = Kronecker delta;
del = deformation operator;
ϵ = eddy viscosity;
Pr = Prandlt number;
Pr_t = turbulent Prandtl number;
F,G,H = vector flux ;
U = dependent variables;

ξ,η,ζ = constants in the (ξ,η,ζ) space, $x=x(\xi,\eta,\zeta)$, $y=y(\xi,\eta,\zeta)$, etc.

For the orthogonal three–dimensional transformed system, $g_{12} = g_{13} = g_{23}$; $g_{ij} = 0$ $(i \neq j)$.

The quantity g_{ij} in curvilinear coordinates specifies the geometry considered and constitutes the matrix tensor of that space. g_{ij} is proportional to the cosine of the angle between a coordinate line along which the curvilinear coordinate ξ^i varies (the other two coodinates being constant along such a line).

The Laplacians

$$\nabla^2\xi = (g_{11}g_{22}g_{33})^{-.5}\frac{\partial}{\partial\xi}(\sqrt{g_{22}g_{33}/g_{11}})$$
$$\nabla^2\eta = (g_{11}g_{22}g_{33})^{-.5}\frac{\partial}{\partial\eta}(\sqrt{g_{11}g_{33}/g_{22}})$$
$$\nabla^2\zeta = (g_{11}g_{22}g_{33})^{-.5}\frac{\partial}{\partial\zeta}(\sqrt{g_{11}g_{22}/_{33}})$$

For two–dimensional orthogonal system

$$\nabla^2\xi = (g_{11}g_{22})^{-.5}\frac{\partial}{\partial\xi}(\sqrt{g_{22}/g_{11}})$$
$$\nabla^2\eta = (g_{11}g_{22})^{-.5}\frac{\partial}{\partial\eta}(\sqrt{g_{11}/g_{22}})$$

It must satisfy the condition within the flow field:

$$\frac{\partial}{\partial x}(\xi_x\sqrt{g_{11}/g_{22}}) + \frac{\partial}{\partial y}(\xi_y\sqrt{g_{11}/g_{22}}) = 0$$
$$\frac{\partial}{\partial x}(\eta_x\sqrt{g_{22}/g_{11}}) + \frac{\partial}{\partial y}(\eta_y\sqrt{g_{22}/g_{11}}) = 0$$

or

$$\frac{\partial}{\partial\xi}(x_\xi\sqrt{g_{22}/g_{11}}) + \frac{\partial}{\partial\eta}(x_\eta\sqrt{g_{11}/g_{22}}) = 0$$
$$\frac{\partial}{\partial\xi}(y_\xi\sqrt{g_{22}/g_{11}}) + \frac{\partial}{\partial\eta}(y_\eta\sqrt{g_{11}/g_{22}}) = 0$$

Two–dimensional orthogonal systems must satisfy these conditions on the boundaries:

$$\xi_x = \eta_y\sqrt{g_{22}/g_{11}} \qquad \xi_y = -\eta_x\sqrt{g_{22}/g_{11}}$$
$$x_\eta = -y_\xi\sqrt{g_{22}/g_{11}} \qquad y_\eta = x_\xi\sqrt{g_{22}/g_{11}}$$

If the system is orthogonal, it has the least extra terms in the transformed PDE to account for the curvature of transformation and the centrifugal force of the flow. One characteristic of the orthogonal system is the vanishing of the off–diagonal elements of the matrix tensor.

Therefore, the basic orthogonally transformed equations are, if we define Jacobian of the coordinate transformation,

$$J = \frac{\partial x}{\partial \xi}\frac{\partial x}{\partial \eta} - \frac{\partial x}{\partial \eta}\frac{\partial y}{\partial \xi} = \sqrt{g}$$

where

$$g = g_{11}g_{22}$$
$$g_{11} = g_{\xi\xi} = \left[\frac{\partial x}{\partial \xi}\right]^2 + \left[\frac{\partial y}{\partial \xi}\right]^2$$
$$g_{22} = g_{\eta,\eta} = \left[\frac{\partial x}{\partial \eta}\right]^2 + \left[\frac{\partial y}{\partial \eta}\right]^2$$
$$J = \left[\left[\frac{\partial x}{\partial \xi}\right]^2 + \left[\frac{\partial y}{\partial \eta}\right]^2\right]^{.5} = \sqrt{g} = \sqrt{g_{11}g_{22}}$$

which measures the area of a cell (volume in a three–dimensional system).
$\sqrt{g_{ii}/g_{jj}}$ = cell aspect ratio which measures the ratio of the length of the sides.

THREE–DIMENSIONAL DYNAMIC SYSTEM COUPLED WITH NONEQUILIBRIUM CHEMISTRY

When the aerospace plane reaches high altitudes where the atmosphere is

characterized by low–density effects and reacting gas chemistry, to simulate the flow field properly the governing reacting gas chemistry equations have to be dynamically coupled to the Navier Stokes equations. Recently Hoffman et al. (1988) made some tests using the simple Baldwin/Lomax zero equation turbulence model (Sec. 5) in the full Navier Stokes equation formulation dynamically coupled with nine chemical equations for air. According to Hoffman et al., nine species (include electron density) have been found to be important in the dynamic coupling. However, when the equation set is solved using an implicit numerical scheme to remove the chemistry stiffness problem, the size of the block matrix becomes very large. For example, even with the simplest turbulent closure scheme (i.e., zeroth–order scheme, see Sec. 5), the size of the block matrix becomes 14 x 14 in which five are Navier Stokes components. Using the strong conservation form, in Cartesian space the equation set is as follows:

$$\frac{\partial U_c'}{\partial t} + \frac{\partial F_c'}{\partial x} + \frac{\partial G_c'}{\partial y} + \frac{\partial H_c'}{\partial z} = \dot{W}$$

where

$U_c' = [\rho_1, \ldots\ldots, \rho N_s, \rho u, \rho v, \rho w, e]^T$

$\rho_1, \rho_2, \ldots\ldots, N_s$ = density of the species

N_s = number of species

ρ = total density = $\sum_{s=1}^{N_s} \rho_s$

u, v, w = Cartesian velocity components

$\dot{W}$ = chemistry source term, $= [\dot{\omega}_1, .., \dot{\omega}_{N_s}, 0,0,0,0]^T$

$\dot{\omega}_1, .. \dot{\omega}_{N_s}$ = source term for each species

F_c', G_c', H_c' = coupled dynamics/chemistry flux vectors each with an invicid and a viscous part.

$$F_c' = \begin{bmatrix} \rho_1 u \\ \vdots \\ \rho N_s u \\ \rho u u + p \\ \rho u v \\ \rho u w \\ u(e+p) \end{bmatrix} + \begin{bmatrix} \rho_1 \bar{u}_1 \\ \vdots \\ \rho_{N_s} \bar{u}_{N_s} \\ -\mu_B \left[\frac{\partial u}{\partial x} + \frac{\partial v}{\partial y} + \frac{\partial w}{\partial z}\right] - 2\mu \frac{\partial u}{\partial x} \\ \tau_{xy} \\ \tau_{xz} \\ u\left[-\mu_B \left[\frac{\partial u}{\partial x} + \frac{\partial v}{\partial y} + \frac{\partial w}{\partial z}\right] - 2\mu \frac{\partial u}{\partial x}\right] + v\tau_{xy} + w\tau_{xz} - \lambda \frac{\partial T}{\partial x} + \sum_{s=1}^{N_s} \rho_s h_s \bar{u} \end{bmatrix}$$

$$G_c' = \begin{bmatrix} \rho_1 v \\ \vdots \\ \rho N_s v \\ \rho v u \\ \rho v v + p \\ \rho v w \\ v(e+p) \end{bmatrix} + \begin{bmatrix} \rho_1 \bar{v}_1 \\ \vdots \\ \rho_{N_s} \bar{v}_{N_s} \\ \tau_{yx} \\ -\mu_B \left[\frac{\partial u}{\partial x} + \frac{\partial v}{\partial y} + \frac{\partial w}{\partial z}\right] - 2\mu \frac{\partial v}{\partial y} \\ \tau_{yz} \\ u\tau_{yx} + v\left[-\mu_B \left[\frac{\partial u}{\partial x} + \frac{\partial v}{\partial y} + \frac{\partial w}{\partial z}\right] - 2\mu \frac{\partial v}{\partial y}\right] + w\tau_{yz} - \lambda \frac{\partial T}{\partial y} + \sum_{s=1}^{N_s} \rho_s h_s \bar{v} \end{bmatrix}$$

$$H_c' = \begin{bmatrix} \rho_1 w \\ \vdots \\ \rho N_s w \\ \rho w u \\ \rho w v \\ \rho w w + p \\ u(e+p) \end{bmatrix} + \begin{bmatrix} \rho_1 \bar{w}_1 \\ \vdots \\ \rho_{N_s} \bar{w}_{N_s} \\ \tau_{zx} \\ \tau_{zy} \\ -\mu_B \left[\frac{\partial u}{\partial x} + \frac{\partial v}{\partial y} + \frac{\partial w}{\partial z}\right] - 2\mu \frac{\partial w}{\partial z} \\ u\tau_{zx} + v_{xy} + w\left[-\mu_B \left[\frac{\partial u}{\partial x} + \frac{\partial v}{\partial y} + \frac{\partial w}{\partial z}\right] - 2\mu \frac{\partial w}{\partial z}\right] - \lambda \frac{\partial T}{\partial z} + \sum_{s=1}^{N_s} \rho_s h_s \bar{w} \end{bmatrix}$$

In each of the above vectors F'_c, G'_c, H'_c, the left–hand–side member represents the invicid part and the right–hand–side member represents the viscous terms.

Furthermore, $\bar{u}_1,\ldots, \bar{u}_{N_s}$ are diffusion velocities for species 1 through N_s in the x direction. Similarly, $\bar{v}$ and $\bar{w}$ are diffusion velocity components in the y and z direction. In numerical simulations, these diffusion velocity components are often assumed to be proportional to the local concentration gradient of the species. To estimate the rate of diffusion, diffusion coefficients such as D_s are used.

In a strict sense, to model chemical reactions, one has to consider the nonequilibrium internal energy modes. The total internal energy is the sum of the energy due to translation, rotation, vibration, chemical disassociation/association, electronic state, and the kinetic energy in the air flow. However, for the Navier Stokes equation to be valid, it is often assumed that the translation and rotational modes are in equilibrium.

A significant portion of the energy of air behind the bow shock may be associated with the dissociation of molecules into atoms. Dissociation effects begin at about Mach 10. When the chemical reaction rates are fast (i.e., equilibrium), the heat transfer process is independent of the mode of transfer (by conduction or diffusion). However, in modeling high–speed, low–density flows, the boundary conditions at the wall often have to consider the efficiency of the wall in catalyzing the recombination of atoms into molecules. The efficiency has a significant effect on heat transfer. Chemical kinetics of catalytic surface reactions in a hypersonic viscous shock layer of a nonequilibrium gas has been studied by Chung (1961). Wray (1962) considered seven–species ionization and Bittker and Scullin (1984) and Hoffman et al. (1988) formulated a nine–species air chemistry reaction model with wall catalysis.

One problem of modeling low–density real gas flow is the "curse of dimensionality," i.e., the size of the matrix grows rapidly with the number of species being considered. This is particularly true when higher–order turbulence closure schemes are used in the model. These aspects are discussed in Sec. 5.

3. NUMERICAL SCHEMES

Perhaps the most important factor that determines the computational requirement in modeling is the principal scheme used for the integration of the governing Navier Stokes equation. For a given physical problem the numerical scheme determines not only the solution accuracy but also the requirements in computer memory, the amount of arithmetic operations, and the treatment at the model's boundaries. In this section we will cover the state–of–the–art scheme, the most popular scheme, and those with the highest potential for future aerospace plane applications considering the trend of computer developments. Only the basic numerical scheme will be treated here. The method of coordinate transformation is discussed in Sec.4

FINITE DIFFERENCE METHODS

Explicit Scheme

The original explicit finite difference scheme proposed by MacCormack (1969) was the primary modeling algorithm for nearly a decade until other relatively more efficient schemes became more popular. However, because of its simplicity, the basic scheme enjoys extensive use. For example, the majority of recent numerical studies involving SCRAMJET simulations still use this simple and straight forward algorithm. The major advantage of this method is its ease to program and to debug. Its major disadvantage is the stability conditions that limit the permissible size of the forward integration time step.

The MacCormack explicit scheme is a predictor–corrector type of algorithm. It uses a split–operator technique, which is second–order accurate in time and space. When it was first used for the Euler equation, artificial diffusion was employed thus permitting the prediction of shocked flows. Recently, the scheme has been used for the following NASP applications:

- Hypersonic turbulent mixing and reaction of hydrogen fuel and air near the injectors of a SCRAMJET (Weidner and Drummond, 1982);
- The SCRAMJET flow field over a rearward facing step with a transverse H_2 injector that includes the detail binary diffusion of hydrogen and air along with variable Lewis number (Berman and Anderson, 1983);
- The SCRAMJET flow field with no strut, one strut, and multiple struts (Kumar, 1982);
- Wing fuselage aerodynamic interaction (Shang, 1984).

The explicit numerical algorithm contains essentially a predictor and a corrector part. For illustration purposes, we only use the simplified governing equation (see Eq. (2.10)) in the conservation–law form:

$$\frac{\partial U}{\partial t} + \frac{\partial G}{\partial y} = 0 \tag{3.1}$$

The solution of dependent variables in the direction normal to the surface (normal gradient) are solved by two steps in succession:

1. Predicting new values of $u^{(p)}_{i,j}$ from the current solution $u_{i,j}$

$$u^{(p)}_{i,j} = u_{i,j} - \frac{\Delta t}{\Delta y}\left(G_{i,j} - G_{i,j-1} \right) \tag{3.2}$$

2. Correcting the predicted value

$$u^{(c)}_{i,j} = \frac{1}{2}\left[u_{i,j} + u^{(p)}_{i,j} - \frac{\Delta t}{\Delta y}\left[G^{(p)}_{i,j+1} - G^{(p)}_{i,j} \right] \right] \tag{3.3}$$

The $u^{(c)}_{i,j}$ becomes the "current value" of u for the net prediction step, and so on. The stability conditions associated with this explicit scheme in the x and y direction are, respectively:

$$\Delta t_x \leq \frac{\Delta x}{|u| + c + \left(\frac{1}{\rho}\right)\left[\left[\frac{(2\gamma\mu)}{Pr\Delta x}\right] + \left[\frac{(-\lambda\mu)^{.5}}{\Delta y}\right]\right]} \tag{3.4}$$

$$\Delta t_y \leq \frac{\Delta y}{|v| + c + \left(\frac{1}{\rho}\right)\left[\left[\frac{(-\lambda\mu)^{.5}}{\Delta x}\right] + \left[\frac{(2\gamma\mu)}{Pr\Delta y}\right]\right]} \tag{3.5}$$

where

c = speed of sound;

γ = ratio of specific heat of gas;

λ, μ = viscosity coefficients;

Pr = Prandtl number.

For NASP applications, a typical SCRAMJET model (e.g., 30 x 109 nodes) using an explicit scheme takes 30,000 time steps to reach a steady–state internal flow condition. Using a first–generation vector machine such as the Control Data Cyber 203 (equivalent to a CDC 7600 non–vector machine), it takes approximately one to two hours for the numerical integration process (Weidner and Drummond, 1982).

Vectorization of the computer code can also improve efficiency. When the explicit scheme is vectorized and run on a CRAY–1 vector mechine (rated at 160 million floating point operations per second, FLOPS), the vectorized program outperforms the original scalar code by a factor of 8.31 (Shang, 1984). Using the original explicit scheme, a typical wing–fuselage aerodynamic interaction simulation (56,730 grid points, M=6) requires about 1.4 hour CPU time on a CRAY–1 (Shang, 1984).

The basic explicit scheme has alsc been modified and coupled to a general interpolants algorithm (GIM, Prozen et al., 1977) designed to take advantage of a "pipeline" feature on certain computers such as the CDC STAR 100 machine. To compute hypersonic flows ($M \geq 5$), a factor of 6 (in speed) was obtained as compared to the equivalent scalar machine (CDC 7600).

In all of the above computations; the explicit scheme is coupled to the

algebraic turbulence models proposed by Baldwin and Lomax (1978) and discussed in Sec.5

Even though the scheme is unconditionally "stable" according to linear stability analyses (Beam and Warming, 1976; Pulliam and Steger, 1980), experience indicates that the scheme with centered spatial differences has only limited range of Courant numbers C_o (Thomas, 1988). In a Cartesian context, the limiting Courant number is

$$C_o = \frac{\Delta t}{\dfrac{\Delta \xi}{|\lambda|_{max}}}$$

where

$$|\lambda|_{max} = |\dot{\xi} + \vec{u}\cdot\nabla\overset{\Lambda}{\xi}_i| + c\,|\nabla\overset{\Lambda}{\xi}|$$

for perfect gas
where

$c =$ the local speed of sound

$C_o =$ the Courant number

$\Delta t =$ the maximum allowable time step

$u =$ the vehicular velocity

$|\lambda|_{max} =$ the largest eigenvalue of the invicid flux vector Jacobian matrix.

In the stream–wise direction, the alternating direction implicit (ADI) scheme is limited to a Courant number of unity (i.e., one). In the direction normal to the body, a much higher Courant number can be used. In addition, the implicit ADI scheme's stability is sensitive both to spatial resolution of the grid and to the degree to which the instantaneous solution departs from the real one (Thomas, 1988). To satisfy this, the initial time steps for the

integration must be small. Tassa and Conti (1987) suggested using different time steps for each grid point as time proceeds. For example, for a two–dimensional flow, to determine the variable time step size, the averaged eigenvalues in two directions have to be evaluated.

Implicit–Explicit and Hybrid Schemes

When used for viscous or turbulent flows, the explicit method described above is penalized by the stiffness of the discrete Navier Stokes approximation. Sometimes it is very inefficient in simulating flow in the flight Reynolds number range. In the explicit method, unknown variables are solved using known variables that are explicitly defined from the earlier steps in a marching manner. In the implicit methods, however, unknowns are first grouped together before they are solved simultaneously, usually by means of a matrix inversion technique.

Implicit methods can often be designed so they are not subject to certain linear stability conditions. Therefore, they are often more efficient than their explicit counterpart by being able to use larger permissible time steps.

In fact, the efficiency of aerodynamic modeling is also governed by other factors. For example, at high Reynolds numbers the magnitude of the inertial force described by the hyperbolic terms of the Navier Stokes equations is much larger than the viscous force described by parabolic terms. A numerical scheme can be made more efficient by splitting the equations into a hyperbolic and parabolic part. MacCormack (1976) proposed a method that solves the hyperbolic part explicitly by using characteristic theory and solves the parabolic part by using implicit parabolic method. Both methods are fully conservative and stable. According to MacCormack, under the thin layer assumption, the velocity component normal to the solid surface is very small compared to the streamline direction. As a consequence, the stability condition involving the normal velocity is much less restrictive than the parabolic part. The stability condition for the explicit part is:

$$\Delta t \leq \frac{\Delta y}{|v|} \tag{3.6}$$

The parabolic part solves the simple tridiagonal matrix and is unconditionally stable. The semi–implicit scheme requires roughly 1/6 of the time of the explicit scheme. Knight (1984) also developed a hybrid method that combines the explicit scheme, described earlier, and an implicit scheme for the viscous sublayer and transition wall regions of the turbulent boundary layers. When the hybrid algorithm is coded in the SL/1 vector programming language (developed at NASA Langley), the computational efficiency improved by a factor of 16 to 21 as compared to a vectorized version of the MacCormack time–split alogorithm.

Alternating–Direction Implicit Scheme

The most adapted multi–dimensional implicit method is the ADI algorithm introduced by Douglas (1955), Peaceman and Rachford (1955), and Douglas and Gunn (1964). The ADI scheme was modified and applied for the compressible Navier Stokes equation (Beam and Warming, 1976). The scheme is second–order accurate, non–iterative, and linearly unconditionally stable. Even though the scheme is a three–time–level scheme, it requires only two–time–level of data storage. The algorithm allows the spatial cross–derivative terms to be included efficiently in a spatially factored manner.

Being perhaps the most popular implicit scheme for any application, particularly in modeling multi–dimensional fluids, it consists of essentially an explicit and an implicit portion. Starting from the specified initial field, the two portions are applied in an alternating manner in the process of integration.

Several codes other than the one posed by Beam and Warming (1976) are based on the general ADI scheme (Steger, 1977; Pulliam and Steger, 1980; Schiff and Steger, 1980). The generalized ADI scheme, when used for solving a hyperbolic nonlinear two–dimensional system in conservation–law form, is

$$\frac{\partial u}{\partial t} + \frac{\partial F(u)}{\partial x} + \frac{\partial G(u)}{\partial y} = 0 \tag{3.7}$$

where

u = unknown p–component vector;

F, G = given vector functions of the components u;

$u(t) = u(n\Delta t) = u^n$.

Let Jacobian matrices $A=\frac{\partial F}{\partial u}$; $B=\frac{\partial G}{\partial u}$; F= Au and G=Bu. (3.8)

The second–order recursion algorithm can be grouped in the following sequences:

$$u^{\overline{n+1}}_{j,i} = u^n_{j,k} - \left[\frac{\Delta t}{4\Delta y}\right]\left[B^n_{j,k+1}\,u^n_{j,k+1} - B^n_{j,k-1}u^n_{j,k-1}\right] \tag{3.9}$$

$$\frac{\Delta t}{4\Delta x} A^n_{j+1,k}\,u^{\overline{\overline{n+1}}}_{j+1,k} + u^{\overline{\overline{n+1}}}_{j,k} - \left[\frac{\Delta t}{4\Delta x}\right] A^n_{j-1,k}\,u^{\overline{\overline{n+1}}}_{j-1,k}$$

$$= -\left[\frac{\Delta t}{4\Delta x}\right] A^n_{j+1,k}\,u^{\overline{n+1}}_{j+1,k} + u^{\overline{n+1}}_{j,k} + \left[\frac{\Delta t}{4\Delta x}\right] A^n_{j-1,k}\,u^{\overline{n+1}}_{j-1,k} \tag{3.10}$$

$$\frac{\Delta t}{4\Delta y} B^n_{j,k+1}\,u^n_{j,k+1} + u^{n+1}_{j,k} - \left[\frac{\Delta t}{4\Delta x}\right] B^n_{j,k-1}\,u^{n+1}_{j,k-1} = u^{\overline{\overline{n+1}}}_{j,k} \tag{3.11}$$

$$u^{\overline{n+1}}_{j,k} = u^n_{j,k} - \left[\frac{\Delta t}{4\Delta y}\right]\left[G^n_{j,k+1} - G^n_{j,k-1}\right] \tag{3.12}$$

Predictor–Corrector Type Implicit Scheme

In the solution process, an ADI implicit scheme, as discussed in Sec. 3, usually involves the inversion of tri–diagonal matrices. Because of the recursion and inversion procedures associated with an implicit scheme, it may require nearly twice as many operations per integration step as an explicit scheme. Since the permissible time step size for the implicit scheme is usually much larger than the explicit scheme, it thus justifies the increase in the number of operations. It would be, on the other hand, more desirable to design an implicit scheme that reduces the number of operations per integration step. MacCormack (1982) proposed a scheme that is basically implicit, but it allows explicit operation in the region away from the aircraft where mesh spacing is larger. The method is based on a predictor–corrector principle. In the process, it solves block bi–diagonal matrix systems rather than the block tri–diagonal one associated with the standard ADI scheme. Therefore, for the overall efficiency for hypersonic applications, this scheme outperformed the pure ADI code discussed previously. The method is stable for unbounded Δt and second–order accurate under the condition that the following term remains bounded:

$$(\mu/\rho)\left[\frac{\Delta t}{\text{Min}(\Delta x^2,\Delta t^2)}\right] \tag{3.13}$$

In practical computations in the Re range between $3x10^5$ to $3x10^7$, simulation codes based on this method can make stable simulations with Courant number as high as 1000 (MacCormack, 1982). Considering the governing Navier Stokes equation in the conservation form as:

$$\frac{\partial U}{\partial t} + \frac{\partial F}{\partial x} + \frac{\partial G}{\partial y} = 0 \tag{3.14}$$

The equation may be numerically integrated in time by a predictor–corrector sequence outlined as follows:

1. Prediction step:

$$\begin{cases} \Delta U^{n}_{i,j} = -\Delta t\left[\dfrac{\Delta_+ F^{n}_{i,j}}{\Delta x} + \dfrac{\Delta_+ G^{n}_{i,j}}{\Delta y}\right] \\ \left[I-\Delta t\dfrac{\Delta_+ |A|\ \cdot}{\Delta x}\right]\left[I-\Delta t\dfrac{\Delta_+ |B|\ \cdot}{\Delta y}\right]\delta U^{\overline{n+1}}_{i,j} = \Delta U^{n}_{i,j} \\ U^{\overline{n+1}}_{i,j} = U^{n}_{i,j} + \delta U^{\overline{n+1}}_{i,j} \end{cases} \quad (3.15)$$

2. Correction step:

$$\begin{cases} \Delta U^{\overline{n=1}}_{i,j} = -\Delta t\left[\dfrac{\Delta_- F^{n+1}_{i,j}}{\Delta x} + \dfrac{\Delta_- G^{\overline{n+1}}_{i,j}}{\Delta y}\right] \\ \left[I+\Delta t\dfrac{\Delta_- |A|\ \cdot}{\Delta x}\right]\left[I+\Delta t\dfrac{\Delta_- |B|\ \cdot}{\Delta y}\right]\delta U^{n+1}_{i,j} = \Delta U^{\overline{n+1}}_{i,j} \\ U^{n+1}_{i,j} = \dfrac{1}{2}\left[U^{n}_{i,j} + U^{\overline{n+1}}_{i,j} + \delta U^{n+1}_{i,j}\right] \end{cases} \quad (3.16)$$

where A and B are the Jacobians of vectors F and G defined by $A=\partial F/\partial U$, $B=\partial G/\partial U$. I is identity matrix. The upstream and downstream differencing operators are defined by:

$$\frac{\Delta_+ Z_{i,j}}{\Delta x} = \frac{Z_{i+1,j} - Z_{i,j}}{\Delta x} \ ; \ \frac{\Delta_- Z_{i,j}}{\Delta x} = \frac{Z_{i,j} - Z_{i-1,j}}{\Delta x} \quad (3.17)$$

for variables in the x direction; the same is true for the y direction.

Here, only the essence of the numerical scheme is outlined. Since this scheme may be the highest potential for the aerospace plane application in the near future, several of its operational aspects will be discussed herein. These include stability, memory requirement, and the relative speed as compared with the other schemes, particularly with respect to the traditional ADI implicit scheme discussed in Sec. 3

- Stability limit: Even though the scheme is *linearly* unconditionally stable, the Navier Stokes equations are highly nonlinear, so the stability limit for various applications varies. Numerical experiments using parabolized codes indicate that the practical limits are between Courant number of 100 to 1000. The maximum limit for the predictor–corrector explicit scheme is around 1.5.
  When the Courant number exceeds 5000, the skin–friction coefficients computed using this method become inaccurate. However, on fluid systems with free surfaces, the order of accuracy of the computed velocity distribution begins to drop when the Courant number exceeds 3 using the ADI scheme.

- Memory requirement: The predictor–corrector scheme requires 30 percent less computer memory than the ADI scheme because it does not need to store the entire block tri–diagonal matrix system. Instead, it forms block bi–diagonal systems and inverts with one sweep while storing only two 4 x 4 matrices at a time. For the same reason, ADI schemes involve longer computer codes than this scheme.

- Integration speed: Theoretically, since this scheme involves only bi–diagonal matrices as opposed to tri–diagonal matrices, it should be much faster than the ADI scheme. But in practice, the speed gain is somewhat less dramatic, particularly when the computational grid–network is evenly spaced so that only the implicit mode is involved during the integration process. Another major factor that reduces the speed is that for every integration time step, the |B| matrix on the right–hand–side (RHS) has to be inverted twice. The same is true for all of the RHS terms. Strict theoretical analysis indicates that two block bi–diagonal systems can be inverted about 10 percent faster than one block tri–diagonal systems. It may be concluded that for the predictor–corrector type of implicit scheme to be more efficient than the ADI scheme, the former must contain more points that can be computed explicitly. In other words, the grid spacing in the far field should be much larger than the spacing near the aircraft. This is usually the case, however.

FINITE–ELEMENT METHODS

Before the finite–element method was used for aerodynamic computation, it was used mainly to analyze static structure systems. As early as 1956 the method was employed in aircraft frame analysis. Geometric flexibility has been the primary feature of the finite–element scheme. The finite–element method is often used because it yields good accuracy on a coarse computational grid. The method has received somewhat less attention lately because good spatial resolution can be obtained by using an efficient finite difference scheme coupled with a coordinate transformation technique. For NASP applications, the finite–element method competes directly with the finite difference/coordinate transformation technique as the primary aerodynamic design tool in the higher speed range.

The finite–element method was originally formulated for linear problems until it combined the method of weighted residuals (Finlayson, 1972) and the Galerkin criterion (Galerkin, 1915), and it then became capable of handling problems described by the complete nonlinear partial differential equations such as the Navier Stokes equations. For time integration, explicit schemes always seem to use the finite–element method.

The recent establishment of an implicit finite–element solution algorithm (Baker and Soliman, 1979, 1983) has substantially advanced the solution technique. Using von Neumann linearized stability analysis, the Baker–Soliman algorithm is fourth–order phase accurate with third–order dissipation in the large Reynolds number range. The principle of the Baker–Soliman (1979) implicit scheme is based on the Galerkin weighted residual formulation. For parabolic and hyperbolic partial differential equations, the method first generates linear, quadratic, and two cubic polynomials. A finite–difference procedure is then used to solve the resultant ordinary differential equation system.

From a theoretical point of view, modelers who use the finite–element

method, emphasize that the method will provide a thoroughly structured procedure to transform the Navier Stokes equation into a large orderly equation system written on the selected discrete variables via calculus and vector–field theory. For nonlinear aerodynamic problems, the finite element formulation is usually associated with the inversion of large matrices, which is deemed to be computationally undesirable. Not so well developed in the hypersonic fluid–dynamic modeling field as the finite–difference method, the finite element method does appear to give robust and accurate algorithms. Software support for the finite–element models are relatively limited at the present time. Recently Bivens (1989) made some assessments on the reliability of using finite element techniques.

SPECTRAL AND PSEUDO–SPECTRAL METHODS

Relatively speaking, numerical methods such as the finite–difference methods (FDM) or the finite–element method (FEM) generally use lower–order difference approximation for derivatives. As a consequence, phase errors result. Representing the derivatives with spectral method drastically reduces these kind of errors.

Historically, it has been a standard technique to seek a solution to a dynamic equation as a series of known functions, so that each spectral component in the decomposition of the solution is easier to solve than the complete solution, usually via an analytical method. Laplace and Fourier transforms were often used to reduce the degree of transcendency for solving numerous differential equations. (Through transformation, partial differential equations become ordinary differential equations, for example.)

The spectral method was first used on a sphere by expansion of a flow field in a series of surface harmonics (Silberman, 1954). The main difficulty in employing the spectral technique at that time seemed to be the considerable amount of arithmetic operation, and the computer memory required to store the iteration coefficients for each mode. In the pseudospectral method (Orszag, 1970a), the mode equations are not actually transformed as they are in the spectral method (Orszag, 1970b), but the derivatives are evaluated by

the fast Fourier transforms (FFT). The FFT method, which requires only N $\log_2 N$ operations per time step, has improved the operation substantially as compared to the conventional Fourier transformation, as long as the N is a power of 2. This is called the Cooley–Tukey algorithm. In the computation, N is the number of modes or the cut–off frequency to be considered. Theoretically, spectral simulation is infinite–order more accurate than the other numerical methods in the aerodynamic computation because errors decrease more rapidly than any finite power of 1/N as the N goes to infinity. The higher the value of N, the more resolution the model will have, but at the cost of higher computational effort, however. The original FFT algorithm of Cooley and Tukey can handle series only with the cut–off frequency N being the power of 2, which is quite inconvenient in some cases. More recently, with an arbitrary–radix algorithm available, the amount of arithmetic operation is still much more economical than the conventional Fourier transform.

For aerodynamic problems with periodic boundary conditions, a Fourier spectral method is particularly efficient and accurate. It can also be used in conjunction with multi–dimensional Navier Stokes equations using spectral approximation in one of the spatial directions. For certain applications, this approach has been shown to be more accurate than other numerical methods as indicated from theoretical analysis. For example, when computing an aerodynamic flow field passing a cylinder or hemispheric cylinder, Fourier spectral approximations can be used to compute appropriate derivatives in its circumferential direction and a finite–difference scheme in the other directions. Using a spectral approximation of the derivatives in the convective terms, it is possible to achieve a particular level of accuracy with fewer circumferential points than is possible with a fourth–order finite difference scheme (Reddy, 1983). In the circumferential direction, the components of derivatives are approximated spectrally by the even and odd discrete Fourier transforms.

Let $f_j = f(\theta_j)$,

where $\theta_j = \frac{\pi j}{N}$, j=0,1,2,3,.....N

The derivative of f at the discrete nodes θ_j can be approximated by

$$\frac{df}{d\theta}(\theta_j) = \sum_{n=1}^{N-1} n\, a_n \cos\left(\frac{\pi j n}{N}\right), \quad j = 0,1,2,.....N$$

where the spectral coefficient a_n is

$$a_n = \frac{2}{N} \sum_{j=1}^{N-1} f_j \sin\left[\frac{\pi j n}{N}\right], \quad n = 1,2,..... N-1$$

This is quite similar to the traditional Fourier transform of the odd (sin) function. Sometimes high–order spectral schemes will develop nonlinear instabilities in strong convective air flows. Under this condition, a low–pass filter has to be used. Gottlieb et al. (1981) proposed a filter function that operates on the Fourier coefficient a_n.

The spectral method can also be used in conjunction with the transformed computational space (i.e., ξ,η,ζ). For example, a three–dimensional aerodynamic flow along a cylindrical body can be computed using a curvilinear grid, in which the coordinate ξ varies streamwise (along the body) and η in the circumferential direction. When a derivative of a component estimator $\hat{(F)}$ is calculated in the transformed direction η, (ie, $\partial\hat{F}/\partial\eta$), by the spectral method, the discrete Fourier transform consists of the usual even and odd parts. For example, in modeling the aerodynamic flow field over a missile–shaped, semi–sphere cylinder, Reddy (1983) used even functions to represent the velocity components u,w and coordinates x,z in the circumferential direction (i.e., η); odd functions represent v and y. In the stream–wise direction ξ, an implicit finite–difference scheme (Pulliam and Steger, 1980) is used. On a vector computer, the spectral method requires approximately 15 percent more time but has twice the accuracy when both were compared with wind–tunnel experiments (Hsieh, 1976). Therefore, the overall performance of this spectral method was concluded to be 40 percent more efficient than a fourth–order finite–difference scheme. However, it is

this writer's opinion that this method should be used only in one of the curvilinear coordinates; to quantify the overall efficiency may not be so straightforward. For most hypersonic aerodynamic applications, the spectral scheme has been associated with problems with periodic boundary conditions.

For incompressible subsonic aerodynamic boundary layer flow, the pseudospectral method has been coupled to the polynomial subtraction technique for the evaluation of spatial derivatives at certain nonperiodic boundary problems (Lee and Shi, 1986). Their technique is essentially to subtract the polynomial portion of the solution to form a periodic function. Potential NASP application includes the circular–type duct flow associated with the turbo–ramjet. It may be simulated with the pseudospectral method for higher–order accuracy than is possible with the traditional finite–difference scheme, which is usually of second or fourth order accuracy.

In terms of numerical accuracy, some theoretical comparisons are made between the spectral method and the finite–difference methods. For the sake of convenience, these comparisons are usually made with fluid dynamic problems in which accurate analytical solutions exist. One such problem is the aerodynamic flow around a sphere. A simple case is that the flow is first subsonic, then supersonic, and finally subsonic again. This kind of flow was first analyzed by Ringleb (Ringleb, 1940), and it is also a good example of the shock–capturing technique used in the spectral method. This type is presented at the end of this section together with the shock–capturing methods associated with other numerical schemes. Recently, Canuto et al. (1988) compared solution accuracy between the spectral method and the popular second–order MacCormack finite difference scheme for the simulation of Ringleb flow. The maximum error in the computed pressure against the analytic solution for the transonic and supersonic ranges appears in Table 3.

Table 3

Maximum Error in Wall Pressure as Computed by
Spectral and Second–Order Finite–Difference Solution
(Adapted from Canuto et al., 1988)

Speed range	Grid	MacCormack	Spectral
transonic	8 x 4	2.6×10^{-2}	2.2×10^{-2}
transonic	16 x 8	1.1×10^{-2}	1.9×10^{-3}
transonic	32 x 16	3.2×10^{-3}	5.0×10^{-5}
supersonic	4 x 4	2.2×10^{-2}	7.5×10^{-4}
supersonic	8 x 8	4.1×10^{-3}	1.1×10^{-6}
supersonic	16 x 16	1.0×10^{-3}	6.6×10^{-11}

Ringleb flow was selected for the evaluation of numerical accuracy because an exact analytical solution exists for the steady, isentropic flow as was explained above.

Even though spectral methods yield more information about the exact solution than other low–order numerical schemes, when the exact solution is discontinuous or contains large gradients, the extra information is then hidden in the form of numerical oscillations. Typically, when the spectral method is used to simulate a flow with shocks, it yields an oscillatory solution. The oscillations occur not only near the shock but all over the field because the spectral method is global in nature. Like artificial dissipation terms in the finite–difference schemes, diffusion and antidiffusion terms have been added in the spectral methods (Taylor et al., 1981) for calculating shock waves, rarefaction waves, and contact surfaces. This point is discussed further below.

NUMERICAL TREATMENT OF SHOCKS

One dynamic characteristic of supersonic flow is the existence of shock waves. To resolve shock within a finite computational grid structure requires special treatment. These methods vary according to the basic numerical solution scheme associated with the simulation model. Several techniques discussed are possible.

Shock Tracking Technique

In the traditional numerical analysis, shock surface is handled like an interior boundary of discontinuity (Courant and Friedrichs, 1948). This method is more conservative in terms of physical state but it also has some drawbacks (Rizzi and Engquist, 1987). One disadvantage is that the nature and interaction of discontinuity have to be known ahead of time to set up computational points in the model to handle them properly. Because of the difficulties in programming, the method has been replaced by the other methods.

The Random Choice Method of Glimm

In solving an initial–value problem for a hyperbolic system, Glimm (1965) used a constructive random choice method similar to one developed by Godunov in 1959. The principle is to make a change in the grid function averaged for a certain number of time steps. The number varies according to the time the shock passes a grid point. The change can be done on the average time steps using an algorithm based on random numbers. The method had worked mainly in one–dimensional problems including reacting gas flow (Chorin, 1977) but it has never worked well for multi–dimensional systems. Chorin also worked on the numerical solution of Boltzmann's equation applied to the problem of shock structure in a one–dimensional flow. That specific numerical method is more accurate than the Monte Carlo

methods for solving Boltzmann's equation particularly in the high Mach number region (Chorin, 1972).

Shock–Capturing Technique

This method is used in the majority of numerical models in the hypersonic aerodynamic simulation associated with NASP analysis. Its major advantage is its simplicity in programming, which assumes no prior knowledge of the nature and the location of the shock front. The shock–capturing technique was originally proposed by von Neumann during the 1940s. Substantial progress has been made during the last two decades (Godunov, 1970; Jameson, 1989). The method is based on the principle that we have to make a compromise between the accuracy of the solution value and the accuracy of the shock location. The final result is to give up a certain degree (first order) of accuracy in the immediate vicinity of the sharp discontinuity. However, if the numerical scheme used for simulating hypersonic flow is nondissipative, numerical viscosity must be artificially added to capture the shock wave.

To add artificial viscosity, it is desirable that the shock transition layer not extend over more than a few grid spacings and that the artificial viscosity be independent of the shock strength. It is also desirable that the transition layer travel at very nearly the correct speed through the air. Sometimes it is also desirable to perform some numerical filtering to smooth out short waves caused by nonlinear instabilities in the smooth air flow away from the shock. The numerical filter will be turned off automatically when the shock wave is not present. In a numerical study of shock boundary layer interaction, MacCormack and Baldwin (1975) devised a normalized second–difference sensor using the computed pressure across three grid spaces of the form:

$$\alpha_j = \frac{| p_{j+1} - 2p_j + p_{j-1} |}{| p_{j+1} + 2p_j + p_{j-1} |} \qquad (3.18)$$

For applications in two–dimensional and three–dimensional supersonic

flows, the same principle can also be extended and is carried out dimension by dimension. The same concept can be implemented in models using total variation diminishing (TDV) schemes. General conditions on coefficients that result in total variation diminishing were proved by Jameson and Lax (1984) (see also Jameson, 1989; Yee, 1987, 1989a and 1989b; Yee and Shinn, 1986; Yee et al., 1988, 1990). TDV methods can give sharp discrete shock waves without oscillations, but, as expected, the price for obtaining a stable solution by filtering is the slight loss of accuracy of the numerical solution.

Capturing vortex sheets in a numerical simulation is somewhat more involved. Presently, no well–established technique seems to be available.

Spatial Switching for Shock Resolution in the ADI Scheme

The class of ADI schemes discussed in the previous subsection is nondissipative, so that they are not good for hyperbolic equations when shock waves occur as in hypersonic aerodynamic conditions. Some dissipative terms have to be added. One of the often–used algorithms is to let

$$-\left[\frac{\omega}{8}\right]\Delta x^4\left[\frac{\partial^4 u}{\partial x^4}\right]_j^n \cong -\left[\frac{\omega}{8}\right]\delta^4 u$$

$$= -\left[\frac{\omega}{8}\right]\left[u_{j+2}^n - 4u_{j+1}^n + 6u_j^n - 4u_j^n - 4u_{j-1}^n + u_{j-2}^n\right]$$

According to the von Neumann stability condition, a one–dimensional implicit numerical scheme is stable if the value of ω is between zero and unity. For multi–dimensional cases, some experiments have to be made. The often–used value of ω has been 0.5.

Adding a dissipative term to reduce post–shock oscillations works under certain situations. But there are cases in which adding a dissipative term has to be accompanied by another treatment for resolving shock waves. Sometime a second–order explicit step which switches difference operator from "central"

to "upwind" (one–sided) across a discontinuity can greatly reduce the spurious oscillations. The method is quite commonly adapted in CFD modeling of marine pollutant transport simulation if a pollutant with high concentration is injected into currents.

Shock–Capturing and Fitting Technique in Spectral Method

Even though the spectral method generally gives more accurate numerical results, the ability for resolving the shock is generally not as good as the time–domain numerical schemes such as the finite–difference method. In spectral simulations shock waves are usually represented as a series of oscillations. To resolve the shock, different types of smoothing filters are usually employed as a post–processing step. Commonly used filters include exponential, Lanczo, or other types of cosine filters (Canuto et al., 1988). Numerical filtering across the frequency domain between 0 and 2π usually resolves the location of the shock.

Another technique to solve the shock–induced oscillation in the spectral method is to treat the shock front as an internal computational boundary. The shape of the shock front is determined during the computation. This technique is termed shock–fitting (Moretti, 1968, 1972; Salas et al., 1982; Zang et al., 1984; Hussaini et al., 1985; Canuto et al., 1988). Up to now, the spectral shock–fitting schemes have been applied only to the numerical models based on the Euler equations, which neglect viscous terms.

Numerical Treatment of Subsonic Regions in a Supersonic Flow

When an aerospace plane flies at supersonic speed, its configuration may consist of some subsonic regions (pockets) in the generally supersonic flow. These areas could be developed as a result of gradual compression or caused by flow separation. These phenomena need special numerical treatments. The traditional approach is to use different marching codes for space and for time. Recently, Chakravarthy et al. (1988) handled this problem by using a

unified marching scheme for both space and time using the relaxation method. In their unified solution algorithm (USA code), the FNS solver is based on the total variation diminishing (TVD) formulation using the finite–volume approach. With the Baldwin/Lomax and one–equation turbulence closure method (see Sec.5), a fully upwind, not–flux–limited scheme is used in the supersonic region external to the subsonic part of the boundary layer. This region involves only a forward marching sweep. For subsonic regions, the solution is to first march forward with one or two subiterations, then to follow with a backward marching sweep. The TVD formulation as described above captures shock wave in the subsonic region.

4. GRID GENERATION AND COORDINATE TRANSFORMATION TECHNIQUES

INTRODUCTION

One major advance in the field of aerodynamic modeling has been the development of a grid–generation technique. This technique, when combined with efficient finite–difference methods, gradually evolves into a major aircraft design tool supplementary to ground experiments. The difference between a grid–generation system and a moving adaptive grid–generation system is that the former generates an aerodynamic computational network before carrying out the calculation, the latter generates grid during computation according to certain criteria such as the pressure gradient. However, the adaptive methods often use the regular grid–generation method to create the initial grid as the starting condition. At present, nearly all the NASP–related hypersonic aerodynamic computations involve grid generation of some type. In many cases, the grid system involves the segmentation of the aerodynamic flow field into subregions, with grids being generated in each subregion. Continuity is then enforced at the interface. This section reviews the methods commonly used in numerical grid generation for the NASP applications.

METHODS AND PRINCIPLES OF GRID GENERATION

An accurate description of the numerical grid generation process, according to Thompson (1984), may be described as follows:

> Difference representations on curvilinear coordinate systems are constructed by first transforming derivatives with respext to Cartesian coordinates into expressions involving derivatives with respect to the curvilinear coordinates and derivatives of the Cartesian coordinates with respect to the curvilinear (metric) coefficients. The

derivatives with respect to the curvilinear coordinates are then replaced with difference expressions on the uniform grid in the transformed region.

A grid system can usually be generated using one of the following methods (Thompson, 1984; Thompson et al., 1985, Thompson and Ferziger, 1989):

- Algebraic system,
- Conformal mapping system,
- Elliptic, parabolic and hyperbolic systems.

Three–dimensional, mass–averaged Navier Stokes equations in a transformed space are presented in Sec. 2.

ALGEBRAIC SYSTEM

In an algebraically generated grid system, the spacings are basically interpolated among boundaries. This type of generating method is well–suited when used together with computer–aided–design (CAD/interactive graphic system). The characteristics of this method are:

- Fast,
- Allows explicit control of grid distribution, or
- No inherent smoothing mechanism (even though cubic spline may be used),
- Often uses transfinite interpolation as for sculptured surfaces. This is similar as in the CAD system which primarily uses the Boolean sum projector method from the boundaries.

In one–dimensional cases, the interpolation scheme often included Lagrangean polynomial interpolation, Hermitian interpolation, cubic spline, tension spline, B–spline, etc. For two– to three–dimensional cases, transfinite

interpolations are usually applied, for example, if linear interpolation functions are needed in each curvilinear direction (2–D, N by M) from a set N + M intersecting curves. These functions are:

$$\underline{r}(\xi,\eta) = \sum_{n=1}^{N} \phi_n\left[\frac{\xi}{I}\right] \underline{r}(\xi_n,\eta) \qquad \left|\xrightarrow{\xi}\right| \qquad (4.1)$$

$$\underline{r}(\xi,\eta) = \sum_{m=1}^{M} \psi_m\left[\frac{\eta}{J}\right] \underline{r}(\xi,\eta_m) \qquad \left|\begin{array}{c}\eta \\ \downarrow\end{array}\right| \qquad (4.2)$$

The interpolation matches the function on the boundary defined by ξ=0 and ξ=I in the first equation, or η=0 and η=J in the second equation. The interpolation is transfinite if the match on the entire boundary at a non–denumerable number of points.

The general form of the transfinite interpolation, which gives algebraically the best approximation, is:

$$\underline{r}(\xi,\eta) = \sum_{n=1}^{N} \phi_n\left(\frac{\xi}{I}\right) \underline{r}(\xi_n,\eta) + \sum_{m=1}^{M} \psi_m\left(\frac{n}{J}\right) \underline{r}(\xi,\eta_m)$$

$$- \sum_{n=1}^{N} \sum_{m=1}^{M} \phi_n\left(\frac{\xi}{I}\right)\psi_m\left(\frac{\eta}{J}\right) \underline{r}(\xi_n,\eta_m) \qquad (4.3)$$

or

$$\underline{r}(\xi,\eta) = \sum_{m=1}^{M} \psi_m\left(\frac{\eta}{J}\right) \underline{r}(\xi,\eta_m) + \sum_{n=1}^{N} \phi_n\left(\frac{\xi}{I}\right)\left[\underline{r}(\xi_n,\eta) - \sum_{m=1}^{M} \psi_m\left(\frac{\eta}{J}\right) \underline{r}(\xi_n,\eta_m)\right] \qquad (4.4)$$

The first term is the result at each point in the field of the unidirectional

interpolation in the η–direction and the bracket is the difference between the specified values on the $\xi=\xi_n$ lines and the result of the unidirectional interpolation on these lines. The spline–blended norm gives the smoothest grid with continuous second derivatives according to Thompson (1984).

CONFORMAL MAPPING TECHNIQUE

Conformal mapping is a classic technique based on the principle of transformation between two regions that are conformally (one–to–one) equivalent. This class of methods includes the solution of integral equations, the expansion of power series or Fourier series, and the construction of Schwarz–Christoffel transformation (see, e.g., Sokolinkoff and Redheffer, 1966). Conformal systems have the advantage of introducing the fewest additional terms in the transformed partial differential equations. Even though systems generated by conformal mapping are inherently two–dimensional, more complicated shapes have recently been constructed (Thompson and Ferziger, 1989). Conformal mappings do not exist in three dimensions except in trivial cases. A curvilinear coordinate system generated by a conformal mapping is usually quite rigid in a way that little control can be exerted over the distribution of grid network.

Aerodynamic shapes can sometimes be transformed into analytical forms such as a circle. For example, an airfoil shape can be approximated as the image of a circle through the transformation:

$$z = \xi + \frac{1}{\zeta} \tag{4.5}$$

Under the inverse transformation, a given airfoil will map to a curve that is nearly circular. Analytical functions are also useful to generate grid near the boundaries with slope discontinuities. If algebraic methods are used, the discontinuities will propagate into the physical region, thus inducing nonsmooth grid spacings.

Complex aerodynamic shapes can be treated by a sequence of

transformations each to an analytical function in succession or in isolation through an iterative procedure (Thompson et al., 1985).

ELLIPTIC, PARABOLIC, AND HYPERBOLIC SYSTEMS

These systems are classified according to the characteristics of the generating equation. For example, Laplace and Poisson partial differential equations are of the elliptic type. This type of system is the most frquently applied among the three. It has many convenient features. One of the most important characteristics of the Laplace systems is that it guarantees a one–to–one mapping for boundary–conforming curvilinear coordinate systems on generally closed boundaries. It usually generates a very smooth grid network. The difference between a Laplace and a Poisson system is the generating equation:

$$\text{Laplace equation} \qquad \nabla^2 \xi^i = 0 \qquad (i=1,2,3) \tag{4.6}$$

$$\text{Poisson equation} \qquad \nabla^2 \xi^i = P^i \qquad (i=1,2,3) \tag{4.7}$$

P^i in Eq. 4.7 are called the control functions, which are used to control the spacing and the direction of the coordinate lines. Since the Laplacian operator lacks control functions, the coordinate lines will tend to be generally equally spaced away from the solid model boundaries near the far field. Sometime this is a desirable property. The selection of control functions for the Poisson system is described in Thompson et al. (1985).

Grid–generating systems can also be based on the numerical solutions of parabolic and hyperbolic partial differential equations. In the solution sequence, one proceeds in the direction of one curvilinear coordinate between two boundaries for the two–dimensional case and between the two boundary surfaces for a three–dimensional case.

In elliptic grid generating systems as shown above, second derivatives exist in both directions (as indicated by the ∇^2 operator). Therefore, only in an elliptic system can the entire boundaries of a general region be specified.

The hyperbolic system, on the other hand, allows only one boundary to be specified. And because of this, the hyperbolic system is faster than the elliptic system by one or two orders of magnitude. The same is true for a parabolic system in which a second derivative in one of the directions does not appear (like the heat equation). Parabolic and hyperbolic systems are similar. One major difference is that in a parabolic system, influence from the other boundary still exists in the governing equation. The speed advantage of the parabolic system over the elliptic system is roughly the same as that of the hyperbolic system. Marching grid generation using hyperbolic partial differential equations was described in some detail by Steger et al. (1977).

The Poisson generating system is perhaps the most applied elliptic system. We will discuss it here in some detail. In a Poisson (inhomogeneous elliptic) system (Eq. 4.7)

$$\nabla^2 \xi^i = P^i \quad (i=1,2,3)$$

The control functions P^i are used to control the spacing and direction of the coordinate lines. The selection of a control function for the Poisson system where P^i is

$$P^i = \sum_{j=1}^{3} \sum_{k=1}^{3} g^{jk} P^i_{jk} \tag{4.8}$$

where g^{jk} are the components of the contravariant metric tensor which are the dot products of the contravariant base vectors ($\underline{a}^i$) of the curvilinear coordinate system,

$$g^{jk} = \underline{a}^j \cdot \underline{a}^k \tag{4.9}$$

Based on this relationship, the Poisson generation system can be defined as:

$$\nabla^2 \xi^i = \sum_{j=1}^{3} \sum_{k=1}^{3} P^i_{jk} \left(\nabla \xi^j \cdot \nabla \xi^k \right) = 0 \tag{4.10}$$

When the computation is carried out in a rectangular transform space, the curvilinear coordinates ξ^i are the independent variables with the cartesian coordinates x_i as dependent variables. The more common form used as the generating system in the transformed region (Thompson et al., 1985) with three control functions is

$$\sum_{i=1}^{3} \sum_{j=1}^{3} g^{ij} \underline{r}_{\xi^i \xi^j} + \sum_{k=1}^{3} g^{kk} P_k \underline{r}_{\xi^k} = 0 \tag{4.11}$$

The two–dimensional form of the generation system with two control functions is

$$g_{22}(\underline{r}_{\xi\xi} + P \underline{r}_{\xi}) + g_{11}(\underline{r}_{\eta\eta} + Q \underline{r}_{\eta}) - 2g_{12} \underline{r}_{\xi\eta} = 0 \tag{4.12}$$

In the physical space, the system is

$$\nabla^2 \xi = \frac{g_{22}}{g} P \tag{4.13}$$

$$\nabla^2 \eta = \frac{g_{11}}{g} Q \tag{4.14}$$

For the orthogonal system ($g_{12}=g_{13}=g_{23}=0$, $g_{11}=g_{22}=g_{33}=$const.), two–dimensional ($g_{33}=1$), in physical space:($g^{12}=0$)

$$\frac{\partial}{\partial x}\left(\frac{h_1}{h_2}\frac{\partial \xi}{\partial x}\right) + \frac{\partial}{\partial y}\left(\frac{h_1}{h_2}\frac{\partial \xi}{\partial y}\right) = 0 \tag{4.15}$$

$$\frac{\partial}{\partial x}\left(\frac{h_2}{h_1}\frac{\partial \eta}{\partial x}\right) + \frac{\partial}{\partial y}\left(\frac{h_2}{h_1}\frac{\partial \eta}{\partial y}\right) = 0 \qquad (4.16)$$

where

$$h_1 = \sqrt{g_{11}} \qquad (4.17)$$

$$h_2 = \sqrt{g_{22}} \qquad (4.18)$$

g_{ii} are elements of the metric tensor. The ratio h_1/h_2 and h_2/h_1 are the attraction functions that need to be prescribed. These ratios become

$$\frac{h_1}{h_2} = \sqrt{g_{11}/g_{22}} = \sqrt{\Delta\xi/\Delta\eta} = \alpha \qquad (4.19)$$

$$\frac{h_2}{h_1} = \sqrt{g_{22}/g_{11}} = \sqrt{\Delta\eta/\Delta\xi} = \frac{1}{\alpha} \qquad (4.20)$$

A curvilinear grid network can be generated by first establishing a coarse grid using a graphic input device such as a CAD system. The ratio of $\Delta\xi/\Delta\eta$ over the computational field can be interpolated into a finer ratio where ξ and η have to be computed. The attraction function α is calculated using Eq. 4.19.

Substituting α and $1/\alpha$ for h_1/h_2 and h_2/h_2 in Eqs. (4.15) and (4.16), an orthogonal curvilinear computational grid is then generated.

Since the Jacobian of the transformation for a two–dimensional orthogonal system is

$$J = \sqrt{g_*} = \sqrt{g_{11}g_{22}} = \sqrt{g_{\xi\xi}g_{\eta\eta}} \quad \text{(area of a cell)}$$

$$= \left[\frac{\partial x}{\partial \xi}\frac{\partial x}{\partial \eta} - \frac{\partial x}{\partial \eta}\frac{\partial y}{\partial \xi}\right] = \left[\left[\frac{\partial x}{\partial \xi}\right]^2 + \left[\frac{\partial y}{\partial \eta}\right]^2\right]^{0.5} \qquad (4.21)$$

The continuity equation for a two–dimensional system with free surface is

$$\frac{\partial \zeta}{\partial t} + \frac{1}{\sqrt{g_*}} \frac{\partial}{\partial \xi} \left[(d+\zeta) u \sqrt{g_{\xi\xi}} \right] + \frac{1}{\sqrt{g_*}} \frac{\partial}{\partial \eta} \left[(d+\zeta) v \sqrt{g_{\eta\eta}} \right] = 0 \quad (4.22)$$

where the transformation coefficients $\sqrt{g_{\xi\xi}}$ and $\sqrt{g_{\eta\eta}}$ are usually located at the v and u vectors, respectively, to maintain the conservation of mass during the integration process. Within a control volume, they are located at

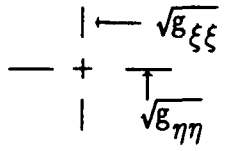

$$\frac{\partial^2 \xi}{\partial x^2} + \frac{\partial^2 \xi}{\partial y^2} = P(\xi, \eta, x, y) \quad (4.23)$$

$$\frac{\partial^2 \eta}{\partial x^2} + \frac{\partial^2 \eta}{\partial y^2} = Q(\xi, \eta, x, y) \quad (4.24)$$

NUMERICAL SOLUTION SCHEME – POISSON SYSTEM

The solution of an elliptic Poisson equation is a boundary value problem. If ξ is a prescribed function ξ_0 on the boundary, such a problem is called a "Dirichlet problem." If, instead of the value ξ, the value of $\partial\xi/\partial\nu$, the normal derivative of ξ, is prescribed on the boundary, the problem is called a "Neumann problem." Several numerical iteration methods such as the Richardson and Liebmann line iteration scheme can be used. The method developed by Peaceman and Rachford (1955) seems to be the quickest iterative method in which line iteration schemes are used in the columns and rows alternatively. The explicit description of the method is contained in the following recursion formula:

$$\xi_{i-1,j}^{(2n+1)} - (2+\rho n)\xi_{i,j}^{(2n+1)} + \xi_{i+1,j}^{(2n+1)}$$

$$= -\xi_{i,j-1}^{(2n)} + (2-\rho n)\xi_{i,j}^{(2n)} - \xi_{i,j+1}^{(2n)} + \frac{1}{p^2} f_{ij} \qquad (4.25)$$

$$\xi_{i,j-1}^{(2n+2)} - (2+\rho n)\xi_{i,j}^{(2n+2)} + \xi_{i,j+1}^{(2n+2)}$$

$$= -\xi_{i-1,j}^{(2n+2)} + (2-\rho n)\xi_{i,j}^{(2n+1)} - \xi_{i+1,j}^{(2n+1)} + \frac{1}{p^2} f_{ij} \qquad (4.26)$$

where n=0,1,2,..., and hopefully the sequence converges. The value ρn is an extrapolation parameter that is to be determined so that the method will converge as quickly as possible. Peaceman and Rachford suggest putting $\rho n = \rho k$ if $n \equiv k \pmod p$ where

$$\rho k = 4 \sin^2 \frac{(2k+1)\pi}{4p} \qquad (4.27)$$

ORTHOGONAL SYSTEMS

Orthogonal systems are important to grid generation for two major reasons. First, the truncation error associated with an orthogonal system in the difference expression is minimal. Therefore, the method is more accurate than others. Second, the orthogonal system induces fewer additional terms in the transformed partial equations to account for the effects of curvature and centrifugal forces. Therefore, the method is computationally very efficient. As a consequence, perhaps more aerodynamic applications are based on orthogonality than on any other method.

A true orthogonal system in a three–dimensional case is also very difficult to implement. For aerospace applications, orthogonality will likely be over a surface coordinate network.

MOVING ADAPTIVE GRID SYSTEMS

One of the newest developments in the field of hypersonic aerodynamic modeling is in the technique of moving adaptive grid generation. During simulation, the grid network moves as the physical solution develops. By sensing the gradient of the solution, the grid concentrates in regions of large variations.

The grid adaptation can generally be achieved by arranging the neighboring points in an identifiable order so that a continuous function can be represented, and errors evaluated and redistributed while the grid network is shifting. In doing this, however, sufficient resolution in time and space is required to minimize and to evaluate truncation error so that numerical oscillation can be avoided.

In an economical sense, the method offers better resolution at fewer points than the other nonadaptive schemes, even though somewhat more computations are involved. With the potential saving in the total number of points for a given level of accuracy, the adaptive method is still competitive with the other schemes in terms of computer time. The method is most suitable for problems for which we have no prior knowledge of their solution. However, an initial fixed grid has to be generated with the other methods.

In solving multi–dimensional aerodynamic problems such as those associated with NASP, if the variability of the solution sought is mainly in one direction, then the grid adaption can be applied with the grid location constrained to move along one direction only. The grid spacing along the region of large gradients is placed according to the principle of equi–distribution of certain weighting functions. The criterion is to select these weighting functions to be inversely proportional to the grid spacing. Therefore, larger gradients are resolved by smaller spacing. We will use this rather simple case for illustration purpose.

Let x(i) represent grid spacing and w_i denote a weighting function. The idea is that the product of the weighting function and the grid spacing would

be a constant (Thompson et al., 1985). In the transformed domain,

$$x_\xi \Delta\xi.w = x_\xi.w = \text{const.} \tag{4.28}$$

where x_ξ is grid spacing

If a velocity gradient is selected as the weighting function, it can be selected as

$$w = \left[1 + \left(\frac{\partial u}{\partial x}\right)^2\right]^{1/2} \tag{4.29}$$

The above formulation has the advantage that the resulting spacing near the far–field boundary will not be very large. Ideally, it would be more desirable to have equal spacing if the gradient is zero such as near the far field. To achieve this, one has to select a set of parameters according to the curvature of the solution gradient (Eiseman, 1985) such as:

$$w = \left[\, 1 + \beta^2 |k| \, \left[1+\alpha^2(\partial u/\partial x)^2\right]^{1/2} \right] \tag{4.30}$$

where α and β are parameters to be selected and k is the curvature of the solution curve.

Three–dimensional adaptation is much more complicated than the above example. However, the general idea is still the same. Recently, tension spring analog has been used for the three–dimensional adaptation (Nakahashi and Deiwert, 1986) in which the weighting function is treated as the tension spring constant of the three–dimensional spring system. In the system, each grid node is suspended by six tension and twelve torsion springs. Rather than solving it simultaneously, the system splits into a sequence of one–dimensional adaptations in which three–dimensional grid movements are achieved by successive applications of the one–dimensional method. The weighting function w (i.e., the tension spring constant) is derived according to the solution gradient over an arc length multiplied by a group of tension and

torsion spring coefficients. The tension spring coefficient affects the mesh spacing along each line. It is selected by considering the range of spacing change (max–min) along a line. Torsion spring constants control the damping between tension and torsion forces. As a result, larger values give a more gradual change in the mesh spacing.

ADAPTIVE MOVING FINITE ELEMENTS

This dynamically adaptive method, in essence, adds dependent variables at the location where the Galerkin weighted residual process is used. In the aerodynamic flow formulation, the entire domain is reduced into finite elements whose contributing residuals are evaluated by trial solution. At each grid point and on each element, the residual is required to be orthogonal to all the basic functions. As a result, the location of grid points becomes part of the solution. At the present time, solution methods are developed only for two–dimensional systems. For more complex systems, it seems apparent that roundoff error can play a major part in the accuracy of the result, inasmuch as the complexity of a large problem necessitates a larger number of iterations both within and per time step.

For NASP application with shocks, solution derivatives of the density field seem to be a good choice for the weighting function. Gnoffo (1983) used Mach numbers for this purpose to compute the flow field over the Galileo probe where values were computed for M=50, Re=10^5–$5\text{x}10^5$ (γ=1.4, Pr=0.72, Sotherland's law for viscosity). Experiment verification for M=6 (Libby and Cresci, 1961) was made. For the hypersonic flow simulation, the adaptation technique is based also on an equivalent spring analogy where springs connect adjacent mesh points and spring constants are a function of the user–specified gradient between the point. The scheme is coupled to the finite volume method. In the formulation, the integral form of the governing conservative laws is approximated on cells whose corners are defined by the position of grid points in physical space. On a rectangular grid, the algorithm reduced exactly to the MacCormack's explicit method (Sec. 3) which is second–order accurate both in time and space. During adaptation, certain filtering of the spring constants was involved.

Recently, Peraire et al. (1987) introduced an adaptive remeshing procedure for improving the quality of steady–state solutions to the two–dimensional Euler equation with a finite–element algorithm. The method involves an iterative step using the computed solution to determine the optimal value according to an indicator of the error magnitude and direction. The scheme has the advantage of gradually improving the quality of the solution without significantly increasing the total number of unknowns at each stage of iteration. No results are available from the three–dimensional analysis yet.

5. MODELING TURBULENCE

INTRODUCTION

One major effort in hypersonic aircraft design is to predict the location of laminar–turbulent transition. The range and the magnitude of uncertainty in the prediction increase as the Mach number increases. The uncertainty translates directly into uncertainties in the prediction of vehicle performance, weight, and other control parameters. To narrow the range of uncertainty in transition prediction, the numerical modeling of turbulent transitional processes is extremely important.

The National Research Council made an objective assessment of the capabilities and future directions in CFD (NRC, 1986). In the area of modeling turbulence, they have reached the following conclusion:

> Turbulence modeling, including modeling of the laminar–turbulent transition, is becoming a pacing technology. Present turbulent models are adquate only for use in relatively simple flows, and do poorly in flows with strong three–dimensionality, massive separation, large–scale unsteadiness, strong density gradients, strong rotation, and chemical reaction. Large eddy simulations have not yet been developed for boundary conditions, geometrics, and Mach numbers of practical interest. (NRC, 1986)

We concur with the NRC and observe that additional research in the modeling of turbulence is needed to reduce the uncertainties in predicting the performance parameters of a vehicle if CFD simulation is used as a design tool. In this section, we will examine various turbulence models used in hypersonic research and try to make some quantitative assessment of uncertainties associated with each approach.

A HISTORICAL BACKGROUND OF MODEL TURBULENCE

The original Navier Stokes equation (Navier, 1822; Poisson, 1829; Saint–Venant, 1843; and Stokes, 1845) was formulated only for describing the laminar flow field in which the momentum transfer due to viscous effects is included in the viscous terms. The amount of momentum loss or gain due to the viscous effect is proportional to the coefficient of viscosity (μ) of the fluid [gr $cm^{-1}sec^{-1}$] which is assumed constant. The equations are (see Sec. 2 for a generalization):

$$\frac{\partial u}{\partial t} + u\frac{\partial u}{\partial x} + v\frac{\partial u}{\partial y} + w\frac{\partial u}{\partial z} = -\frac{1}{\rho}\frac{\partial p}{\partial x} + \frac{\mu}{\rho}\nabla^2 u \qquad (5.1)$$

$$\frac{\partial v}{\partial t} + u\frac{\partial v}{\partial x} + v\frac{\partial v}{\partial y} + w\frac{\partial v}{\partial z} = -\frac{1}{\rho}\frac{\partial p}{\partial y} + \frac{\mu}{\rho}\nabla^2 v \qquad (5.2)$$

$$\frac{\partial w}{\partial t} + u\frac{\partial w}{\partial x} + v\frac{\partial w}{\partial y} + w\frac{\partial w}{\partial z} = -\frac{1}{\rho}\frac{\partial p}{\partial z} + \frac{\mu}{\rho}\nabla^2 w \qquad (5.3)$$

The last term in each equation contains the kinematic (molecular) viscosity. The Navier Stokes equations, including mass, energy, and species conservation, can also be derived from the kinetic theory of gases using the Chapman and Enskog procedure (Chapman and Cowling, 1939; Tsien, 1958). Presumably, they apply to reacting gas flows, both turbulent and laminar, under compressible flow conditions. For most aerodynamic modeling applications, the molecular viscosity of single component gas is often calculated using Southerland's law with appropriate constants for the species under consideration. For the case of multiple component gases such as the mixture of hydrogen and air, its binary molecular viscosity can be calculated by the Wilke's formula.

Turbulent flows, on the other hand, cannot be computed with these time–dependent Navier Stokes equations unless the flow field is resolved by a numerical model whose computational network approaches $Re^{9/4}$ grid points (Case et al., 1973). With that many points, the effects of even the smallest

turbulent eddies can then be represented entirely by these viscosity terms. For turbulent flow, it was Boussinesq (1877) who used the "eddy–viscosity" concept which assumes that the gross effects of both the turbulent and the laminar portions of the viscous effects are proportional to the mean velocity gradient. Eddy viscosity (μ_t) is analogous to the viscous stress coefficient (μ) in the laminar flow. Although μ is a fluid property, eddy viscosity depends on the velocity gradients within the flow. However, Boussinesq's eddy viscosity concept forms the foundation of turbulence theory. Together with Prandtl's contribution, the eddy viscosity type of closure methods such as the zero–equation, one–equation and two–equation turbulence models are the primary method used in the aerodynamic flow modeling. In these models, the shear stresses in the Navier Stokes equations are computed as a function of mean velocity gradient and the eddy viscosity, of the general form:

$$\tau = \rho \mu_t \frac{\partial u}{\partial y} \tag{5.4}$$

Since the eddy viscosity varies within the flow field under different situations, these zero–, one–, and two–equation models are designed to account for the variability of these coefficients, using hypotheses, assumptions, and experimental results in the process of seeking certain universal relationships. However, the ultimate solution to account for the various flow situations, would be to calculate individual stress components explicitly according to the turbulent Navier Stokes equation first established by Osborne Reynolds in 1894. The solution of these types of equations containing turbulent stress terms constitutes the multi–equation, stress–component models. This type of turbulence model will be more universal than the eddy–viscosity type of models but requires extensive computation. This will be the model of the next decade.

Formulated using mean–flow velocity components $\bar{u}$, $\bar{v}$, $\bar{w}$, and the mean pressure $\bar{p}$, the Navier Stokes equation modified by Reynolds for turbulent flow resembles the original equation. The right hand side of the equation (when μ, ρ are constants) becomes:

$$= -\frac{1}{\rho}\frac{\partial \bar{p}}{\partial x} + \frac{\mu}{\rho}\left[\frac{\partial^2 \bar{u}}{\partial x^2} + \frac{\partial^2 \bar{u}}{\partial y^2} + \frac{\partial^2 \bar{u}}{\partial z^2}\right] - \left[\frac{\partial \overline{u'^2}}{\partial x} + \frac{\partial \overline{u'v'}}{\partial y} + \frac{\partial \overline{u'w'}}{\partial z}\right] \qquad (5.5)$$

$$= -\frac{1}{\rho}\frac{\partial \bar{p}}{\partial y} + \frac{\mu}{\rho}\left[\frac{\partial^2 \bar{v}}{\partial x^2} + \frac{\partial^2 \bar{v}}{\partial y^2} + \frac{\partial^2 \bar{v}}{\partial z^2}\right] - \left[\frac{\partial \overline{v'u'}}{\partial x} + \frac{\partial \overline{v'^2}}{\partial y} + \frac{\partial \overline{v'w'}}{\partial z}\right] \qquad (5.6)$$

$$= -\frac{1}{\rho}\frac{\partial \bar{p}}{\partial z} + \frac{\mu}{\rho}\left[\frac{\partial^2 \bar{w}}{\partial x^2} + \frac{\partial^2 \bar{w}}{\partial y^2} + \frac{\partial^2 \bar{w}}{\partial z^2}\right] - \left[\frac{\partial \overline{w'u'}}{\partial x} + \frac{\partial \overline{w'v'}}{\partial y} + \frac{\partial \overline{w'^2}}{\partial z}\right] \qquad (5.7)$$

In the formula, the instantaneous velocity component (e.g., u) is the sum of the mean velocity and the turbulent velocity, namely, $u = \bar{u} + u'$ in the x–direction. These turbulent velocity components (u', v', w') have the property that their long–term (ensemble) mean value approaches zero. But the correlation terms such as $\overline{u'v'}$, etc., do not disappear even when time averages are taken. Reynolds defined these terms as the turbulent stress terms. They are as follows:

$$\tau_{xx} = \bar{\rho}\,\overline{u'u'} \quad ; \quad \tau_{yy} = \bar{\rho}\,\overline{u'v'} \quad ; \quad \tau_{zz} = \bar{\rho}\,\overline{u'w'} \quad ; \text{etc} \qquad (5.8)$$

The Navier Stokes equation modified for turbulent flow containing the "Reynold stress" terms looks quite similar to its original form:

$$\frac{\partial u}{\partial t} = u\frac{\partial u}{\partial x} + v\frac{\partial u}{\partial y} + w\frac{\partial u}{\partial z} = -\frac{1}{\rho}\frac{\partial p}{\partial x} + \frac{1}{\rho}\left[\frac{\partial \tau_{xx}}{\partial x} + \frac{\partial \tau_{xy}}{\partial y} + \frac{\partial \tau_{xz}}{\partial z}\right] \qquad (5.9)$$

$$\frac{\partial v}{\partial t} = u\frac{\partial v}{\partial x} + v\frac{\partial v}{\partial y} + w\frac{\partial v}{\partial z} = -\frac{1}{\rho}\frac{\partial p}{\partial y} + \frac{1}{\rho}\left[\frac{\partial \tau_{yx}}{\partial x} + \frac{\partial \tau_{yy}}{\partial y} + \frac{\partial \tau_{yz}}{\partial z}\right] \qquad (5.10)$$

$$\frac{\partial w}{\partial t} = u\frac{\partial w}{\partial x} + v\frac{\partial w}{\partial y} + w\frac{\partial w}{\partial z} = -\frac{1}{\rho}\frac{\partial p}{\partial z} + \frac{1}{\rho}\left[\frac{\partial \tau_{zx}}{\partial x} + \frac{\partial \tau_{zy}}{\partial y} + \frac{\partial \tau_{zz}}{\partial z}\right] \qquad (5.11)$$

The theory of turbulence, as well as the turbulent Navier Stokes equation in its original form proposed by Reynolds in 1894, has several difficulties in application because of the following (Hinze, 1959):

- When the partial differential equation for the velocity corrections of a given order are derived from the equations of turbulent fluctuation, the presence of the inertia terms causes the appearance of the velocity correlations of the next higher order, which are also unknown
- Equations of correlation on the second and higher orders constructed out of the equations of turbulent fluctuation contain the unknown terms of correlation between the pressure and velocity fluctuation
- The value of the decay term in these equations has to be determined.

ALGEBRAIC (ZERO–EQUATION) MODEL FOR THIN–LAYER APPROXIMATIONS

In this type of turbulence closure scheme, the eddy–viscosity coefficients are computed based on the Prandtl formulation in which the mixing length is specified algebraically. Since these types of models use only the partial differential equations for the mean field and no differential equation for the turbulent quantities, it is, therefore, also called the "zero equation model." These models relate the turbulent shear stress only to the mean flow conditions at each point through an algebraic relationship. The scheme

proposed by Baldwin and Lomax (1978) belongs to this type and has received the most attention in the hypersonic aerodynamic flow computation. CFD models for simulating the SCRAMJET flow field are based nearly entirely (twelve out of sixteen) on the Baldwin–Lomax scheme (see Table 4). This scheme has several major advantages in computing hypersonic air flow. We will discuss this closure scheme in some detail.

The basic approach of the Baldwin–Lomax scheme is patterned after the Cebeci method (1974). However, the Baldwin–Lomax scheme has the advantage of avoiding the necessity for finding the edge of the boundary layer. The two–layer model divides the eddy viscosity μ_t into two parts, as follows:

$$\mu_t = \begin{cases} (\mu_t)\text{inner} & y \le y_{\text{crossover}} \\ (\mu_t)\text{outer} & y_{\text{crossover}} < y \end{cases} \tag{5.12}$$

where y is the local normal distance from the wall and $y_{\text{crossover}}$ is the smallest value of y at which values from the inner and outer formulas are equal. In other words, the crossover point in y is the point at which $(\mu_t)_{\text{outer}}$ becomes less than $(\mu_t)_{\text{inner}}$. Unlike the Prandtl formulation in which the eddy viscosity is a function of the velocity gradient, the Prandtl–Van Driest formula is used for defining the eddy viscosity. In that formulation, the vorticity of the local flow field is used in the inner region:

$$(\mu_t)_{\text{inner}} = \rho l^2 |\omega| \tag{5.13}$$

$$\text{The mixing length} \qquad l = ky\left[1-\exp\left(-y^+/_{A^+}\right)\right] \tag{5.14}$$

where y is the normal distance from the wall, y^+ is the law–of–the–wall distance (i.e., $\sqrt{\rho_w \tau_w}\, y/\mu_w$), k is the von Karman constant, and A^+ is a closure contant ($A^+ = 26$). The magnitude of vorticity $|\omega|$ is defined as (for three–dimensional flow)

Table 4

Use of Turbulence Models in Recent Aerospace Plane-Related Hypersonic Simulations

Model	Numerical Method	Turbulence Closure	References
1) Supersonic flow in SCRAMJET with step, H_2 injection	2-D explicit scheme (MacCormack, 1969)	2-layer algebraic eddy viscosity (Baldwin and Lomax, 1978)	Berman and Anderson (1983)
2) 2-D analysis of SCRAMJET inlet flow field	2-D explicit scheme (MacCormack, 1969)	2-layer algebraic eddy viscosity (Baldwin and Lomax, 1978)	Kumar (1982)
3) Staged H_2 injection for SCRAMJET	Time-split algorit. (MacCormack and Baldwin, 1975)	2-layer algebraic eddy viscosity (Baldwin and Lomax, 1978)	Weidner & Drummond (1982)
4) Hypersonic lamin. flow, 15^{o}corner at M_{∞} = 14.1	Predictor-corrector implicit (MacCormack, 1982)	2-layer algebraic eddy viscosity (Baldwin and Lomax, 1978)	Lawrence et al. (1987)
5) NASA modular SCRAMJET combustor flow 2-D, PNS	Time unsplit/split MacCormack and Baldwin (1969, 1976)	Baldwin and Lomax (1978)	White et al. (1987)
6) 3-D hypersonic equilibrium flow with ablation	Beam and Warming ADI (1976)	Baldwin and Lomax (1978)	Thomas (1988)

Table 4 (Cont.)

Use of Turbulence Models in Recent Aerospace Plane-Related Hypersonic Simulations

Model	Numerical Method	Turbulence Closure	Reference
7) Low-density hypersonic real gas	MacCormack implicit (1982)	Baldwin and Lomax (1978)	Hoffman et al. (1988)
8) Separated flow, backflow turbulence	Implicit upwind-biased, TVD, appr. factorization	Modified Baldwin and Lomax (1978)	Goldberg and Chakravarthy (1988)
9) Separated flow, backflow turbulence	Implicit upwind-biased, TVD, appr. factorization	hybrid k-L one-equation model	Goldberg and Chakravarthy (1989)
10) SCRAMJET combustor & nozzle real gas	Implicit finite-volume, time-marching	Baldwin and Lomax (1978)	Nelson et al. (1989)
11) SCRAMJET flow PNS, combustor/nozzle	Implicit upwind	low Re k-ϵ two-equation	Dash et al. (1989)
12) NASA Ames all-body hypersonic aircraft model	Implicit upwind PNS solver	Baldwin and Lomax (1978)	Lockman et al. (1989)

$$|\omega| = \left[\left[\frac{\partial u}{\partial y} - \frac{\partial v}{\partial x} \right]^2 + \left[\frac{\partial v}{\partial z} - \frac{\partial w}{\partial y} \right]^2 + \left[\frac{\partial w}{\partial x} - \frac{\partial u}{\partial z} \right]^2 \right]^{\frac{1}{2}} \quad (5.15)$$

For two–dimensional flow,

$$|\omega| = \left[\left[\frac{\partial u}{\partial y} - \frac{\partial v}{\partial x} \right]^2 \right]^{\frac{1}{2}} \quad (5.16)$$

Eddy viscosity of the outer region is a function of the Clauser constant (C_{cp}), the Klebanoff intermittency factor, and other closure constants:

$$(\mu_t)_{outer} = K\, C_{cp}\, \rho\, F_{wake}\, F_{Kleb} \quad (5.17)$$

The closure constants Baldwin and Lomax used have been determined by requiring agreement with the original Cebeci formulation for constant pressure boundary layers at transonic speeds. They used C_{cp}=1.6, C_{Kleb}=0.3, and K=0.0168. F_{wake} is defined by additional parameters involving the difference between maximum and minimum total velocity in the velocity profile. F_{wake} is usually taken to be the minimum of $Y_{max}\, F_{max}$ or $C_{wake} Y_{max} U^2_{dif} / F_{max}$ where Y_{max} is the y distance at which F_{max} occurs with F_{max} being the maximum value of F(y) in a given transverse profile. The function of F(y) is given by

$$F(y) = y|\omega|(1-\exp(-y^+/A^+)) \quad (5.18)$$

U_{diff} is determined by taking the difference between the maximum and minimum velocities in a given velocity profile with $\min(U_{diff})$ equal to zero everywhere else. Therefore,

$$U_{diff} = [\, u^2 + v^2 \,]^{\frac{1}{2}} \tag{5.19}$$

The value of F_{Kleb} represents the Klebanoff intermittency factor, given by

$$F_{Kleb}(y) = \left[1 + 5.5 \left[\frac{C_{Kleb}\, y}{Y_{max}}\right]^6\right]^{-1} \tag{5.20}$$

The constants for the Baldwin and Lomax model are: $A^+ = 26.0$, $C_{cp} = 1.6$, $C_{kleb} = 0.3$, $C_{wake} = 0.25$, $k = 0.4$, and $K = 0.0168$. Prandtl (Pr) and turbulent Prandtl number (Prt) used in the original Baldwin–Lomax model (1978) are 0.72 and 0.9, respectively.

Since the model uses the normal distance from the wall as its primary parameter in determining the turbulent viscosity. If certain discontinuity (e.g., a step) exists, there will be a jump in the value of viscosity. This ambiguity sometimes requires smoothing. This can be done by a relaxation equation (Waskiewicz et al., 1980, Berman and Anderson, 1983) of the form

$$\frac{\mu_t - \mu_{te}}{\mu_{le} - \mu_{te}} = 1 - \exp\left[-\frac{\Delta x}{\lambda\ \delta_{te}}\right] \qquad x > x_{te} \tag{5.21}$$

where subscript t represents turbulent, te represents trailing edge, le denotes leading edge, δ is the boundary–layer thickness, and Δx is grid spacing of the model.

One major advantage of the zero–equation algebraic turbulence model is the simplicity of its application. It can be modified for different flow situations. An example is Goldberg's treatment for the separated flow region (Goldberg, 1986, Goldberg and Chakravarthy, 1988). The algebraic backflow model has been incorporated into a Reynolds–averaged Navier Stokes solver that uses the Baldwin–Lomax turbulence model outside of separation bubbles. The scheme has been applied to calculate the reattaching flow over a backward–facing bump. Data comparison indicates that this combination

outperforms the more complicated e–ϵ (or some times called k–ϵ) two–equation model, which is discussed below.

ONE–EQUATION TURBULENCE CLOSURE MODELS

In zero–equation models, the closure is made through the mean–velocity field. The specification of turbulence field by means of an algebraic relationship implies that generation and dissipation of turbulent energy are in balance everywhere. Therefore, the dynamic process of convection and diffusion of turbulent energy is ignored. These are, of course, important features of real turbulent flows. To include these processes, the transport of turbulent energy has to be computed explicitly via another set of partial differential equations. In fact, at the very beginning, the founders of modern tubulence theory (namely, Prandtl and Kolmogorov) suggested that turbulent viscosity be determined by way of differential rather than algebraic equations.

In the set of differential equations the dependent variable often being computed for the closure is the sub–grid–scale (SGS) turbulent energy density "e" (or sometimes called "k") within a computational cell. In most models, the following transport equation for e is used:

$$\underset{(1)}{\frac{\partial e}{\partial t}} + \underset{(2)}{U_i \frac{\partial e}{\partial x_i}} = \underset{(3)}{\frac{\partial}{\partial x_i}\left[\frac{\mu_t}{\sigma_e}\frac{\partial e}{\partial x_i}\right]} - \underset{(4)}{\overline{u_i u_j}\frac{\partial U_i}{\partial x_j}} - \underset{(5)}{\epsilon} \qquad (5.22)$$

where

(1) = local acceleration;
(2) = convection of sub–grid–scale turbulent energy;
(3) = diffusive transport of SGS energy;
(4) = energy production by shear stress;
(5) = viscous dissipation;
μ_t = turbulent viscosity, which is assumed to be a property of the local state of the turbulence;

σ_e = effective Prandtl number for the diffusion of turbulent energy.

In most one–equation models, the turbulent viscosity is determined as a function of the local energy intensity and the local mixing length (l) from the boundary via the following relationship

$$\mu_t = C_\mu \rho \sqrt{e}\, l\, \mathrm{Re} \tag{5.23}$$

The rate of viscous dissipation is determined by the local energy density according to the following relationship,

$$\epsilon = C_d \frac{\rho e^{\frac{3}{2}}}{l} \mathrm{Re} \tag{5.24}$$

where C_d is one of the closure constants (approximately 0.9), and l is the local mixing length, which is usually proportional to the distance from the solid wall.

The sequence of closure computation also involves the relationship between pressure, density, and compressibility, which is approximated by the equation of state of air. To explain the cyclic process of numerical integration in which "one" additional partial differential equation is used for SGS energy, the sequence starting from an arbitrary point in time during the process goes as follows.

The velocity fields are computed in the entire domain by the balance of pressure gradient, shear stress, and other forces including the specified far–field boundary conditions. From these velocity fields just determined, heat, SGS energy, and other essential constituents are transported and diffused. From the transport of SGS energy, the new turbulent viscosity coefficients throughout the entire flow field are determined. From these stress coefficients and other diffusion coefficients computed in a similar manner, together with the updated pressure field, a new velocity field is computed.

From the computed velocity and temperature field, the drag, lift, detailed skin friction, and heat coefficients about the entire vehicle can be computed.

TWO–EQUATION TURBULENCE CLOSURE MODELS

In essence, the one–equation turbulence model is based on the proposal made earlier that the sub–grid–scale, time–averaged, turbulent kinetic energy e (or sometimes called k)

$$e = \frac{1}{2}\left[\overline{u'^2 + v'^2 + w'^2}^{t}\right] \tag{5.25}$$

is determined from the solution of a convective transport partial differential equation similar to the transport of heat. In the above equation, u', v' and w' are turbulent "random fluctuations" around the time–averaged mean velocities. The major shortcomings of the one–equation model are: 1) the influence of convection and diffusion on the small–scale turbulent random velocities is not accounted for; and 2) the viscosity μ_t vanishes whenever $\partial u/\partial y$ is zero. To avoid these problems we need one more equation to describe the transport of the length scale l. The turbulent viscosity μ_t is determined in the same way as in the one–equation model, namely,

$$\mu_t = c_\mu \rho e^{\frac{1}{2}} l \tag{5.26}$$

In other words, the length scale l is calculated by a differential equation rather than prescribing it algebraically. In most two–equation models, the length scale is determined indirectly via a variable z

$$z = e^m l^n \tag{5.27}$$

where m and n are constants that vary according to the model proposed by a different modeler, as shown in Table 5.

Table 5

Closure Constants Proposed by Different Modelers in Two–Equation Turbulence Modeling

Proposer	z	m, n
Kolmogorov (1942)	$z = e^{\frac{1}{2}} l^{-1}$	$m = \frac{1}{2}$, $n = -1$
Chou (1945)	$z = e^{\frac{3}{2}} l^{-1}$	$m = \frac{3}{2}$, $n = -1$
Rotta (1951) Spalding (1967a)	$z = l$	$m = 0,\ n = 1$
Rodi and Spalding (1970)	$z = e\, l$	$m = 1,\ n = 1$
Spalding (1969)	$z = e\, l^{-2}$	$m = 1\ ,\ n = -2$

The transport equation of e and z can be rearranged to have the similar form

$$\rho \frac{De}{Dt} = \frac{\partial}{x_i}\left[\frac{\mu_t}{\sigma_e}\frac{\partial e}{\partial x_i}\right] + e\left[\frac{\mu_t}{e}\left[\frac{\partial u_i}{\partial x_i}\right]^2 - c_\mu \frac{\rho^2 e}{\mu_t}\right] \qquad (5.28)$$

$$\rho \frac{Dz}{Dt} = \frac{\partial}{\partial x_i}\left[\frac{\mu_t}{\sigma_\epsilon}\frac{\partial z}{\partial x_i}\right] + z\left[c_{\epsilon 1}\frac{\mu_t}{e}\left[\frac{\partial u_i}{\partial x_i}\right]^2 - c_{\epsilon 2}\frac{\rho^2}{\mu_t}\right] \quad (5.29)$$

In these equations, c_μ, σ_e, σ_ϵ, $c_{\epsilon 1}$, $c_{\epsilon 2}$, etc., are turbulent closure constants. They have to be determined by fitting them against experimental data. A set of optimally fitted turbulent closure constants are listed in Table 6.

Conventional two–equation models formulated using e–z (or or sometimes called k–ϵ) generally are inaccurate for boundary layers in an adverse pressure gradient. Wilcox has recently (1988) proved that the use of "wall functions" (Rodi, 1981) tends to mask the shortcomings of such models and is inadequate for flows with mass injection. Under the latter case, skin friction predicted by the k–ϵ model is as much as 50 percent higher than measured (Wilcox, 1988). Using a singular perturbation method, Wilcox proposed a multiscale model with no viscous damping of the model's closure coefficients which gives improved accuracy for flow with surface mass addition.

Strictly speaking, the one–equation modeling approach is not as general as the two–equation model. In practice, however, this method allows a modeler to select an algebraic function for the length scale according to the specific physical process guided by experimental data and field observations. The one–equation approach thus avoids the problematic z–equation (see Goldberg and Chakravarthy, 1989), which is needed to prescribe the length scale in the two–equation model. This advantage was reported by Liu and Leendertse (1978, 1987, 1990) in three–dimensional CFD Navier Stokes models of geophysical fluid dynamic systems.

Table 6

Optimally Fitted Turbulence Closure
Constants in CFD Modeling

c_μ	σ_k	σ_ϵ	$c_{\epsilon 1}$	$c_{\epsilon 2}$	Reference
0.09	1.00	1.30	1.44	1.92	Launder & Spalding (1974)
0.09	1.00	1.30	1.44	1.92	Launder & Sharma (1974)
0.09	1.00	1.30	1.45	2.00	Hassid and Poreh (1978)
0.09	2.00	3.00	1.81	2.00	Hoffman (1975)[a]
0.09	0.90	0.95	1.35	2.00	Dutoya & Michard (1981)
0.09	1.00	1.30	1.35	1.80	Chien (1982)
0.084	1.69	1.30	1.00	1.83	Reynolds (1976)[a]
0.09	1.00	1.30	1.43	1.94	Launder et al. (1973)
0.09	2.00	(Not directly compatible)			Wilcox and Rubesin (1980)
0.09	1.00	1.30	1.44	1.92	Warfield and Lakshminarayana (1987)

[a] Model constants have to satisfy the relationship
$c_{\epsilon 1} = c_{\epsilon 2} - (k^2/\sigma_\epsilon c_\mu^{1/2})$ so that the ϵ equation reduces to zero.

STRESS–COMPONENT CLOSURE MODELS

At the present time, the most complete set of turbulent closure equations is the "mean Reynolds stress" approach, which was proposed by Chou (1945) and Davidov (1959, 1961). The formulation includes the transport and diffusion of length scale l, $\overline{u'v'}$, $\overline{u'^2}$, $\overline{u'v'}^2$ terms, and results in 3 equations for mean flow components, 1 equation for continuity, 3 equations for shear stresses, 3 equations for normal stresses, 10 equations for triple correlations, for a total of 20 equations for a homogeneous aerodynamic systems. The turbulent stress component formulated originally by Chou, in compact tensor notation, for double velocity correlation, takes the following form:

$$-\frac{1}{\rho}\frac{\partial \tau_{ik}}{\partial t}-\frac{1}{\rho}\left[U_{i,j}\tau^{j}_{k}+U_{k,j}\tau^{j}_{i}\right]-\frac{1}{\rho}U^{j}\tau_{ik,j}+\left[\overline{u^{j}u_{i}u_{k}}\right]_{,j}$$

$$=-\frac{1}{\rho}\left[\overline{p_{,i}u_{k}}+\overline{p_{,k}u_{i}}\right]-\frac{\nu}{\rho}\nabla^{2}\tau_{ik}-2\nu g^{mn}\,\overline{u_{i,m}u_{k,n},} \quad (5.30)$$

Ten equations for triple correlations are:

$$\frac{\partial \overline{u_{i}u_{k}u_{l}}}{\partial t}+U_{i,j}\,\overline{u^{j}u_{i}u_{l}}+U_{k,j}\,\overline{u^{j}u_{l}u_{i}}+U_{l,j}\,\overline{u^{j}u_{i}u_{k}}+U_{l,}\overline{u^{j}u_{i}u_{k}}+$$

$$U^{j}\left[\overline{u_{i}u_{k}u_{l}}\right]_{,j}+\left[\overline{u^{j}u_{i}u_{k}u_{l}}\right]_{,j}=-\frac{1}{\rho}\left[\overline{p_{,i}u_{k}u_{l}}+\overline{p_{,k}u_{l}u_{i}}+\overline{p_{,l}u_{i}u_{k}}\right]$$

$$+\frac{1}{\rho^{2}}\left[\tau^{j}_{i,j}\tau_{kl}+\tau^{j}_{k,j}\tau_{li}+\tau^{i}_{l,j}\tau_{ki}\right]+\nu g^{mn}\left[\overline{u_{i}u_{k}u_{l}}\right]_{,mn}$$

$$-2\nu g^{mn}\left[\overline{u_{i,m}u_{k,n}u_{l}}+\overline{u_{k,m}u_{l,n}u_{i}}+\overline{u_{l,m}u_{i,n}u_{k}}\right] \quad (5.31)$$

The continuity equation is:

$$u^j_{,j} = 0 \tag{5.32}$$

Since, in tensor notation, a subscript preceded by a comma denotes the covariant derivative, the continuity equation in scaler notation is then,

$$\frac{\partial u_1}{\partial x_1} + \frac{\partial u_2}{\partial x_2} + \frac{\partial u_3}{\partial x_3} = 0 \tag{5.33}$$

defining $q^2 = \overline{u_j u^j}$ = the variance or the RMS of the velocity fluctuation, $\tau^j = \tau^j(x^1x^2x^3)$, (j=1,2,3).

The triple and quadruple correlation technique is essentially a method of successive approximation to the solution of the turbulence problem by solving (PDEs) for each component of Reynolds stress. The approximation takes the following order:

Initial approximation: Reynolds equations of mean motion, which contain the unknown apparent stresses

Second approximation: Solve the equations of mean motion and of the double correlation by making certain approximations to the triple–velocity correlations in the equations

Third approximation: Solve the equations of mean motion and both the double and triple correlations simultaneously by assuming approximations for the quadruple correlations.

The above implies that there will always be more unknowns than the available equations. Or one can obtain an approximation at a certain level with some remaining lower–order unknown terms, thus the term "turbulence closure."

For three–dimensional turbulence closure computations, in addition to the

dynamic and chemical balance equations, there are six components of the Reynolds stresses $u_i u_j$ and three flux (scalar) components plus one transport equation for the scalar concentration fluctuations, for a total of 10 additional partial differential equations to solve. The application of the stress–component turbulence modeling is, therefore, still very limited due to its computational demand. Some simplification can be made to the PDE such that they reduce to algebraic expressions but still retain the fundamental characteristics of the basic approach. In the transport equations, if the gradients of the dependent variables (e.g., rate of change, convection, and diffusion) are eliminated by model approximations, the differential equations can then be converted into algebraic expressions (Launder et al., 1975; Launder and Spaulding, 1974). Warfield and Lakshminarayana (1987) made some tests with this approach.

Difficulties associated with the length–scale equation often cause the poor performance of the two–equation turbulence models. Since the stress component model uses a similar length–scale equation, this type of model may not necessarily give better predictions over the one– or two–equation model. However, this remains to be seen.

TWO–FLUID MODEL OF TURBULENCE AND COMBUSTION

In many turbulent combustion processes (e.g., within a SCRAMJET engine), two interacting fluids of different states (e.g., velocities) are assumed to exist within a finite–control volume. The dynamic and chemical processes of the interspersed gas fragment within the flame can sometime be represented more faithfully by using a two–fluid model of the flame than a single fluid formulation.

Introduced originally by Shchelkin (1943) and Wohlenberg (1953), the theory of two–fluid model of turbulence has recently been advanced to use the analytical tools for two–phase flows (Spalding, 1986; Fan, 1988). If R represents the volume fraction, the mean density of the fluid is

$$\bar{\rho} = R_1\rho_1 + R_2\rho_2 \tag{5.34}$$

When analyzing the two–fluid flow, the averaged fluid property ϕ can be defined in two ways:

1. the time (or volume) average: $\bar{\phi} = R_1\phi_1 + R_2\phi_2$ (5.35)

2. the mass–weighted average: $\hat{\phi} = \dfrac{(R_1\rho_1\phi_1 + R_2\rho_2\phi_2)}{\bar{\rho}}$ (5.36)

The momentum transfer or interfluid friction in the turbulent closure can be expressed as f_{12} :

$$f_{12} = c_f\, a^{-1} \rho^* \mid V_1 - V_2 \mid \tag{5.37}$$

where f_{12} represents the interfacial friction between the two fluids, c_f is a dimensionless proportionality constant, a^{-1} is the amount of fluid/fragment interface area per unit volume of space, ρ^* is the density of the lighter of the two fluids, and $|V_1 - V_2|$ is the local time–averaged relative speed of the two fluids. The area/volume quantity (i.e., a^{-1}) is taken as being proportional to the volume fraction product R_1R_2, so that it vanishes when either fluid disappears. During the dissipation of turbulence, the turbulent fluid can transfer to the nonturbulent fluid. On the other hand, the nonturbulent fluid can become turbulent as a result of the volumetric entrainment process.

The basic governing equation for the mean flow contains two fluids co–existing in one space:

$$\frac{\partial(R_k\rho_k\phi_k)}{\partial t} + \frac{\partial(R_k\rho_k U_{kj}\phi_k)}{\partial x_j} = \frac{\partial}{\partial x_j}\left[R_k \Gamma_{\phi k} \frac{\partial \phi_k}{\partial x_j} \right]$$

$$+ \frac{\partial}{\partial x_j} \left[\phi_k D_{\phi k} \frac{\partial R_k}{\partial x_j} \right] + S_{\phi k} + I_{\phi k} \qquad (5.38)$$

where

k = subscript denoting fluid 1 or fluid 2
j = subscript representing coordinate
Γ = turbulent or laminar diffusion coefficient within one fluid
D = coefficient of diffusion transport of dependent variable due to the fluctuations of velocity and volume fraction
S = within–fluid source term
I = inter–fluid source term

At present, the fluid model has been formulated for analyzing a tubulent premixed combustion process. Documented computer programs for one– and two–phase flows such as the PHOENICS code are available from the London Imperial College.

MODELING COMPRESSIBLE TURBULENCE

In modeling turbulence, the compressibility effect can generally be neglected if the ratio between time–averaged air density ($\bar{\rho}$) and the variation of density associated with the turbulent fluctuation ($\tilde{\rho}$) is small, i.e.,

$$\tilde{\rho} / \bar{\rho} << 1 \qquad (5.39)$$

This is approximately the same order of u'^2 / c^2 (Hinze, 1959), which is the square of the Mach number of the turbulence. In compressible turbulent flow, the mean motion is affected not only by turbulence shear stresses but also by stresses generated from double and triple correlations involving the density fluctuation $\tilde{\rho}$. In hypersonic compressible–flow jets, variation in density occurs from pressure differences. Only limited information is available on the effect of compressibility of air on the mechanism of turbulent

air flow in a boundary layer. Near boundaries, the reduction in high velocity causes a conversion into heat through compression. Heat generated by the compressional process does not distribute uniformly within the boundary layer. The temperature variation due to this process changes fluid's properties. A transport of heat occurs by the molecular and turbulent diffusion processes. The turbulence eddy entrainment rate of the compressible turbulent flow is less than that of the corresponding incompressible flow. The effect of the shock wave on the rate of energy transport into or out of turbulence eddies is not well understood at this time. For compressible turbulence, the fundamental spectral laws that govern the partition and the cascade of turbulent energy as proposed by Kolmogorov may need revision (Dimotakis, 1989). Recent research on compressible turbulence includes mainly theoretical studies such as the three–dimensional structures of compressible shear layer (Papamoschou, 1989), and the theory of sonic eddy (Breidenthal, 1990). In the latter theory, the effect of Mach number on turbulent shear flow is expressed via the concept of sonic eddy. Thus, obviously, it may be some time before our understanding of compressible turbulence models can be refined and verified, and proper models used to calculate hypersonic flows. This will require a combination of measurements, analyses, and theory.

AREAS OF LOW PREDICTIVE RELIABILITY IN MODELING TURBULENCE

In this section, we have reviewed the necessity for modeling turbulence in the CFD simulation of hypersonic aerodynamic flows. In some cases, the basic theory of turbulent flow *per se* cannot truthfully describe the complicated physical phenomena of fluid turbulence. In some cases, we are limited by the capacity of the present day computer, so that CFD models do not have high enough resolution to simulate turbulent flow at high Reynolds number. Other difficulties involve the lack of sufficient data to verify many turbulent models such as those proposed just for the simpler two–equation model (as tabulated in Table 5). As we have quoted at the beginning of this

section, the NRC conclusions on the present status of turbulence modeling suggest that extensive research is still needed before we have sufficient confidence in CFD predictions particularly in areas without verification data.

From our study, we have summarized a list of difficult subjects and areas with low predictive reliability in turbulence flow. Table 7 lists these. Several of these areas are associated with anisotropic, nonhomogeneous turbulence, which induces hydrodynamic instability. The combustion process in a SCRAMJET engine may involve nonhomogeneous tubulence if steps or blocks are used for inducing more complete mixing at such high speed. The problem of hydrodynamic stability has been studied for decades by many well-known scientists in the fluid dynamic field. We do not yet have a final conclusion on the basic stability criterion for the nonhomogeneous turbulence problem (see Table 8). It has long been recognized that energy dissipation in turbulence must be intermittent in space. Recently, the spectral method has been used in conjunction with supercomputers to study the intermittency in turbulence with 2 million (128^3) grid resolution (Hosokawa and Yamamoto, 1990). Direct simulation methods have also been used to study the effect of Mach number on the stability of plane supersonic wake (Chen et al., 1990), so that the physics of linear, nonlinear, and three-dimensional stages of laminar-turbulent free-shear flow transition is better understood. In the area of mixing and combustion, in incompressible flows, the mixing layer is generally convectively unstable. Similar information is not available for the compressible mixing layer for which temperature effects are important. Recent experimental results (Jackson and Grosch, 1990) suggest a way to derive from linear stability theory a "convective Mach number" (proposed originaly by Bogdanoff, 1983) for a compressible mixing layer for multispecies gas. This provides a convenient way for studying the stability of compressible free shear layer. In supersonic combustion jet engine design, it is important to understand the behavior of compressible turbulent shear layers. With progress in numerical modeling, computing capability, and more experimental data, our understanding of fluid turbulence will certainly improve, which would also lead to higher predictive reliability for supporting aircraft design.

A key unresolved issue is the analysis of the laminar-turbulent transition process, first for the low-speed case and ultimately for the high-speed case of

Table 7

Modeling Turbulence:
Difficult Subjects and Areas With Low Predictive Reliability

Strong aerodynamic curvature
Intermittency and large-scale flow structure
Rapid compression-expansion (k-ϵ model needs modifications)
Kinematically influenced chemical reaction
Low Reynolds number effects
Strong swirl
Aerodynamic turbulence is strongly influenced by body force acting in a preferred direction (k-ϵ model no longer valid)
Uncertainties in setting the boundary condition
Large-density fluctuations -> high Mach number

Table 8

Modeling Nonhomogeneous Turbulence:
Stability Criterion for Stratified Shear Flow

R^*_{cr}	Proposed by	Year	Conditions and Assumptions
1.0	Richardson	1920 (Roy. Soc. 20,354)	Boussinesq approximation (deviation of ρ is neglected except in buoyancy force) Eddy diffusion for heat=momentum
1.0	Taylor	1931 (1915) (Sci. Paper 2,240)	Same
2.0	Prandtl	1930 (Springer)	Taylor in 1931 suggested multiplying by 0.5 to obtain 1.0
1/4	Miles	1961 (JFM 10,496)	Dynamically attainable motions using energy consideration
1/4	Chandrasekhar	1961 (Clarendon, Oxford)	Same
1/4	Howard	1961 (JFM 10, 509)	Same
1.0	Abarbanel, Holm, and Ratiu	1986 (Roy. Soc. 318,349)	Proved $R > 1$ is sufficient for Liapunov stability of 3-D stratified shear flow Boussinesq approximation
1.0	Miles	1986 (Phy. Fld. 29,3470)	Amended Chandrosekhar's flaw in energy derivations of 1961

*Richardson number $R \equiv -\frac{g}{\rho}\frac{\frac{\partial p}{\partial z}}{\left[\frac{\partial u}{\partial z}\right]^2} > R_{critical}$

interest to NASP designers. At present, there is little analysis or data to guide or prediction of transition, except for the use of linear stability and the classic e^N method that has been useful in lower–speed flows. Unfortunately the e^N method gives little useful detail beyond the location of transition, and presumably only for flows that have disturbance similar to those that were in the original database for determining "N". Many analysts have suggested that uncertainties in the location of transition on the forebody of a NASP vehicle could entail uncertainties of as much as 200 percent in vehicle weight. What is also suspected is that the spatial and temporal characteristics of the transition process, in terms of intermittency, unsteadiness, and three–dimensionality, and even the presence of a large unsteady flow structure, can markedly affect inlet behavior and the ability of the forebody–inlet combination to perform properly. Transition is still an experimental art form and there are limited data to guide analysts. It may be years before we obtain the needed statistical data to properly determine the characteristics of hypersonic flow fields. Other issues involve the possibility of relaminization in high–speed flow and the behavior of the hypersonic turbulent shear layers.

Density fluctuation should play an important role in very–high–speed turbulent boundary layers, but there are almost no useful data to guide the formulation of CFD models reflecting such phenomena. In addition, little is known about the statistics of turbulent fluctuations and the occurrence of large–scale fluid structures in hypersonic flow. Such large eddy structures exist in other types of turbulent boundary flow. Even more troublesome than our present lack of understanding of the hypersonic turbulent boundary layer is the lack of data and understanding concerning the hypersonic turbulent mixing process that occurs in the engine. Current data are limited but suggest that the efficiency of mixing of two streams decreases rapidly as the Mach number of the high–speed stream increases, that large–scale fluctuations are likely to occur, and that compressible shear layers may be far more stable than previously thought. Thus, shear layers may, if left to their devices, be more laminar than is desirable. This suggests that means may be needed to augment compressible mixing, perhaps using small eddy–generating devices. These devices might produce small shock waves (shocklets) that could assist

eddy formation and promote mixing. The resulting temporal fluctuations in the engine flow path could influence inlet performance by feeding disturbances upstream through the thick boundary layers, leading to inlet buzz or unstart.

As far as inlet performance is concerned, there is also little evidence that inlet dynamics, which can be affected by the forebody flow upstream and the combustor flow downstream, can yet be modeled by CFD in a realistic way. Furthermore, the need to operate SCRAMJET at full-length scale to allow for complete mixing, and the effects of combustion instabilities and other fluctuations on inlet unstart, suggest that without a full-scale test that includes combustion, we will not have confidence in our ability to diagnose the cause of inlet malfunction. All of these performance-related questions need to be addressed by CFD modeling in the near future.

6. SUPERCOMPUTERS, PARALLEL PROCESSING, AND VECTOR PROGRAMMING

INTRODUCTION

Most NASP–related CFD simulations use supercomputers. This section attempts to evaluate the following aspects of NASP–related subjects in super computing:

(1) NASP–related CFD modeling in the past two decades.
(2) Present hardware/software capability and costs.
(3) Technical limitations in hardware, software, and the future trend of hardware/software development available for NASP research/design support.

Looking back in the history of computers, numerical weather prediction and nuclear reactor simulation are two of the driving forces for the development of, and also major users of, the early computers. Both involve numerical solutions of the Navier Stokes equations. At each stage of the development, these simulations were performed on the largest computers available at the time. However, most of those large computers were "scalar" machines designed for general purposes, particularly for business data processing. One of the earliest group of numerical simulations involving the solution of the "parabolized" Navier Stokes equations (PNS) for hypersonic aerodynamic flows were conducted at RAND using general purpose IBM business computers (Cheng et al., 1970). Using scalar machines for solutions of vector quantities, the integration process is carried out sequentially, which is not as efficient as if it were conducted in parallel.

Special machines were designed based on this parallel principle. ELLIAC–4, which consists of 64 parallel processors, is one of the earliest examples. But these special–purpose machines were expensive and time–consuming to build since they were not mass–produced.

SUPERCOMPUTERS AND PARALLEL PROCESSING

Since the mid-70s, manufacturers such as Control Data and Texas Instruments began to build machines for scientific computations. Control Data started with the STAR series, which was the predecessor of its Cyber series vector machines. Since the introduction of CRAY-1 in 1976, the total number of "supercomputers" has grown to a total of 180 machine from several computer makers. Most hydrodynamic codes run on these machines, including NASP-related hypersonic simulations.

Hypersonic simulations run faster on vector machines. Technically, the major reason is that in traditional sequential machines, the system contains a memory, an instruction processor, an arithmetic processors and an input/output system. In the memory, data and instructions occupy unique addresses. Operations instructions have to carry addressing information to access the required operands in the memory. The final computational speed is determined by the slowest component that controls the machine's cycle time. Vector processors, on the other hand, operate by a pipeline procedure that performs many arithmetic operations concurrently with a single vector instruction, thus achieving much higher system throughput.

Data-swapping between CPU and the external memory units is also a routine operation in CFD modeling. During numerical integration of the Navier Stokes equations, the portion not being actively handled is usually stored temporarily in the external memory unit. Traditionally, external magnetic disk units are used. Some supercomputers, such as the X-MP, offer solid-state storage devices as an alternative, which are about 30 times faster than the magnetic units. External memory units are usually configured in blocks of 8-mega bits. The efficiency and overall throughtput of a CFD simulation depends on a combination of hardware and the simulation program in which the block size of the data transfer usually also matters.

In February 1988, Cray introduced the model Y-MP/832, which offers two to three times the performance of X-MP. The Y-MP has 8 CPUs and a central memory capacity of 32 million words. With eight CPUs, the Y-MP/832 has twice the number of processors and memory as the X-MP.

Each CPU operates on a 6–nansecond clock cycle. At clock speeds of six billionths of a second, the machine can thus handle 32 million 64–bit words in central memory. Abour ten Y–MP were delivered in 1989. The other supercomputer, Control Data's CYBER–205, has a cycle time of 20 ns which is about half the speed of Cray's X–MP.

A new machine (i.e., ETA–10) introduced in Control Data is comparable to the Cray's Y–MP. The ETA–10 was introduced in June 1987. The system is a highly vectoring, parallel–processor, with virtual memory. A major difference between ETA–10 and other supercomputers is the instruction set of its central processing unit. Unlike most supercomputers which increased speed by reducing the instruction set (RISC), the ETA 10 can be qualified as a VCISC–a very complex instruction set computer. Designed mainly for large–scale computational fluid dynamic and structure applications, consequently, the use of vectors is inherent both in the hardware and the instruction set. Each CPU contains in addition to the scalar processor a dual–pipe line vector processor, both of which operate completely in parallel. Each CPU is a 44–layer printed single circuit board. The ETA 10 system can contain one to eight processors each with a 32 megabytes of local memory. The performance benchmark for the single–processor model–P (air–cooled, 24–ns clock) is equivalent to 44 times the speed of the popular Micro VAX II. The faster model ETA 10–G is liquid nitrogen cooled with a 7–nanosecond clock and has a rated speed of 94 MFLOPS when equipped with a single CPU. The delivery date for ETA 10–G was in December 1988. The price basic configuration is $1 M for the 24–ns ETA10–P and $13.5 M for the 7–ns ETA10–G. Because of financial difficulties, the production of ETA–10 machines stopped in the spring of 1990.

The next model being developed at Cray Research is said to be five times faster. However, some R&D and cost overrun problems may delay its introduction. Recently, Cray's older systems have begun to be challenged by comparatively low–cost mini–supercomputers such as Convex (of Texas), Elxsi (of California), Multiflow Computer Corp. (of Connecticut), and Floating Point Systems (of Oregon). These machines cost approximately half a million dollars while the Cray's new Y–MP is in the $20 million range.

Many predict that the number of mini–supercomputers will grow to five times between 1987 to 1992. But others feel that the market is already saturated as of 1988. Figure 3 illustrates the computational speed of major main frame computers over the last three decades while Fig. 4 gives a general idea of the correlation between the computer's speed and the hardware cost.

According to the designer of Cray–2, Steve Chen (personal communication, 1988), the next generation of vector machines which is being developed by his IBM–supported Super Computer Corporation will have a processing speed of nearly one hundred times the Y–MP. The targeted date for introduction will be approximately five years from now.

VECTOR PROGRAMMING AND THE VECTORIZATION OF CFD CODES

Even though some compilers can perform automatic vectorization, the final processing speed of most CFD codes depends on a programmer's knowledge of the machine's architecture, so that optimum concurrency can be obtained. Numerical schemes used in CFD modeling also influence its processing speed. In many cases, explicit time integration schemes vectorize naturally because they are an algebraic operation. Implicit numerical integration schemes require additional preparation since matrix calculations are involved.

Most vector processors contain vector pipelines. Cyber–205 contains either one, two, or four vector pipelines, each of which is fed from a vector stream unit. The top speed of the four–pipe unit is 400 mega–FLOPS after the initial start–up period.

In CFD modeling, the objective is to write and compile the numerical code to suit the machine's architecture. Therefore, the modeler should have detailed knowledge about the hardware system as well as aerodynamics and aircraft design criteria. Most CFD simulations are carried out by supercomputers equipped with either an array or vector processor.

Unlike a vector processor, which is either an integral part of the CPU or

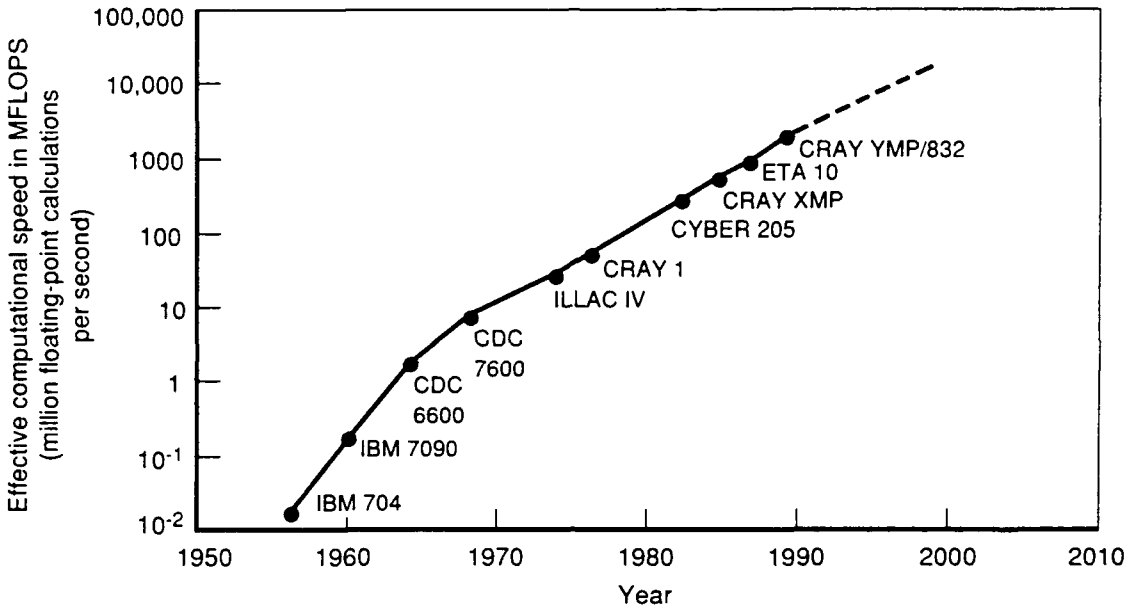

Fig. 3—Computational Speed of Major Mainframe Computers over the Last Three Decades

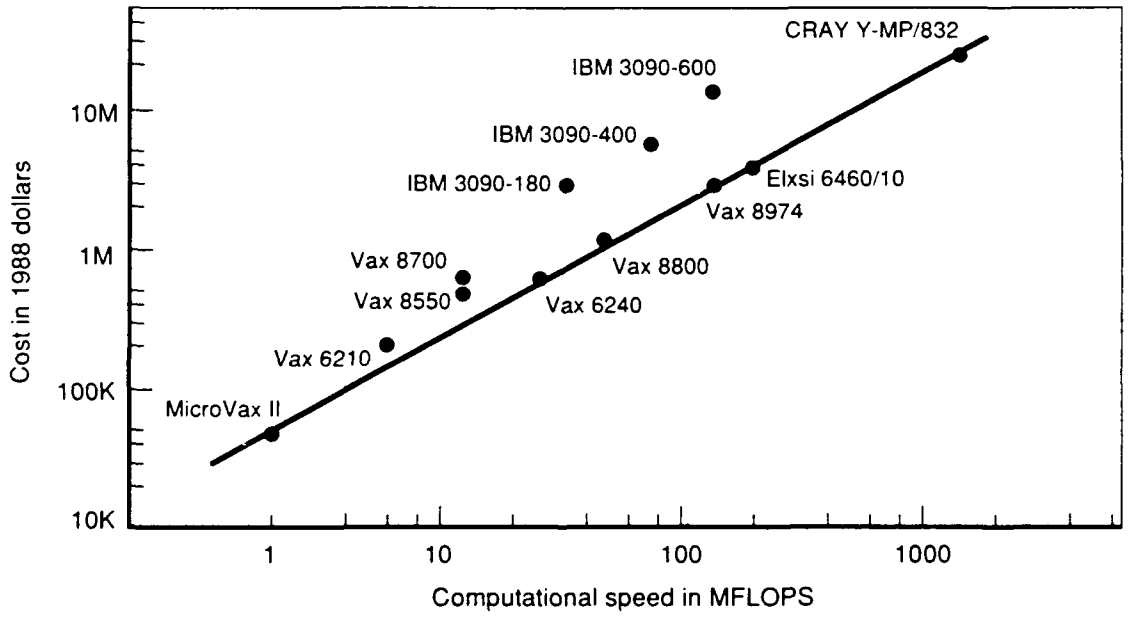

Fig. 4—Computational Speed Versus Cost from Micro-Mini to Super Computers

resides on the same data bus, array processors connect to the I/O bus of a computer. The speed of an I/O bus can be an order of magnitude slower than the CPU bus. So the simulation speed is much slower on an array processor unless the array is extremely large, which is usually the case for PNS or FNS codes. Array processors must also pay an additional speed penalty for the initialization step as well as having to interact with the host CPU.

There are basically two ways to design a vector processor: memory–to–memory architecture or the load/store architecture. The Control Data family of supercomputers uses the memory–to–memory method which loads data directly into arithmetic units on the vector board from main memory without the need for vector registers or the so–called cache. The advantage of this architecture lies in its suitability for very large datasets.

One way of implementing the load/store architecture is called the "synchronous method," which is adapted by Cray and IBM 3090. In this method, a cache is used. During CFD simulation, calculations are carried out following the main, scalar CPU until a vector call is encountered. While the vector is being processed, the CPU is in a wait state. The CPU's wasted idle time is directly proportional to the size of the vector. The newest machines from Convex and DEC (C240 and VAX 9000, around the spring of 1990) have adapted the asychronous load/Store method. This type of architecture allows the main CPU to perform in parallel with the vector processor if the operations in the CPU do not depend on the results from the vector processor.

In terms of programming software, FORTRAN is still the most popular scientific programming language. There are special utility programs used by many super– and mini–supercomputer manufacturers, such as ETA, and CYBER (CDC), to vectorize FORTRAN programs to take advantage of the vector processing hardware. One vectorization utility is called VAST (vector and array syntax translator) and is produced by Pacific Sierra Research. To give a simple example, if a constant is to be added to every element of an array using scalar FORTRAN, th. llowing DO loop is needed.

```
      DO 10 I=1,2000
10    A(I) = A(I) + X
```

When this operation is performed on an ETA10 which contains hardware specially designed for vector operation, the ETA VAST-2 can transform the above scalar operation into:

$$A(1,2000) = A(1,2000) + X$$

The FORTRAN compiler of ETA10 would recognize this vector operation and will generate the appropriate machine instructions to load the vector processor and add the constant to all elements of the array simultaneously. The vectorized code would take about only 1/2000th the time to complete the operation.

Since vectorization can be accomplished in several ways for a complex program, the preprocessor must determine the most efficient one. Even though the vectorization preprocessor can be a powerful tool, it sometimes can give unwanted vectorizations resulting in harmful side effects. Programmers sometimes have to give directives in the source file that help syntex translators such as VAST make the vectorization.

CFD MODELING ON ARRAY COMPUTERS AND CONNECTION MACHINES

An array computer consists of many microprocessors that perform identical computations. The concept is originated from von Neumann. ILLIAC IV, which consists of 64 (8x8) processing elements, is the earliest example of a general-purpose array computer. Even though each processor in the ILLIAC IV is quite powerful, the size of the array is too small to perform practical calculations in CFD modeling. In 1976, RAND proposed to build a Navier Stokes array computer consisting of 10,000 identical microprocessors arranged in an 100x100 array (Gritton et al., 1977). The concept was to perform CFD simulations on an array computer that is

designed only to solve the Navier Stokes equation with great efficiency. They proposed to solve the three–dimensional Navier Stokes equations in primitive variables and the Poisson equation for pressure via Fourier transformation in the span–wise direction. With 100x100 array of microprocessors and 128 Fourier components, the processing speed was expected to be several orders faster than a sequential machine. The main reason for this difference is that during a simulation, most of the hardware in the sequential processor sits idle. In a parallel machine, calculations are carried out at every processor simutaneously.

Several general–purpose, massively parallel processors such as the one built at the Thinking Machine Corp. (Hillis, 1985) are presently being developed and used for CFD modeling. For example, the Naval Research Laboratory has two machines presently dedicated to CFD simulations. The smaller one (nicknamed Bambi) consists of 8000 floating–point processing chips in a 4K+4K congifuration. The larger one (nicknamed Godzilla) has 16,000 floating–point processing chips in a 8K+8K configuration. Each processor has 2K words of memory. Navier Stokes solutions coded on these massively parallel connection machines are usually written in C* language, which is quite similar to FORTRAN. Usually, C* language is used together with PARIS or CMIS commands to increase the processing speed. Large connection machines can sometime outperform supercomputers. For example, a 256x128x128–grid, three–dimensional fluid simulation of complex shock interaction, when carried out using the 16K Connection Machine at the Naval Research Laboratory, takes 20 seconds per time step. The identical problem would take 80 seconds per time step on a Cray X–MP (Boris et al., 1989). This implies that the speed of the 16K connection machine is equivalent to the speed of Cray's Y–MP.

Recent computations of fully compressible two–dimensional Navier Stokes equations (1024 x 2048 grid) on the large parallel connection machine CM2 at the University of Colorado achieved a speed of 1,500 Mega–FLOPS (1.5 G–FLOPS, Biringen et al., 1989). The benchmark test was carried out using the MacCormack second–order explicit scheme for the simulation of a square wave propagating outward through a square domain with radiation boundary conditions for 24,000 integration time steps. Coded in C* and

PARIS, the execution speed in the parallel connection machines slows down substantially when implicit schemes are used because of the involvement of matrix operations.

Presently, on connection machines, the finite–difference scheme is more efficient than the spectral method (Sec. 3) for lower accuracy modeling such as second– or fourth–order accuracy. When the required accuracy increases, the pseudospectral method is better, particularly for simpler geometric shapes. Recently many CFD simulations of the hydrodynamics of symmetrical and spherical systems have been studied using parallel spectral methods on connection machines (Pelz, 1989).

7. ASPECTS OF MODELING NEEDS AND UNCERTAINTIES IN HYPERSONIC SIMULATION

REQUIREMENTS ON THE COMPUTATIONAL SPEED AND MEMORY

CFD models are based on the approximated (numerical) solutions of the governing equations over the finite–grid network. Consequently, the finer the grid, the more accurate the numerical solutions are. There are tradeoffs between speed and computer memory requirements. To obtain the best estimate of the flow field around an aircraft, we often trade computational speed for higher spatial resolution with the largest machine available. To do this, we sometimes have to use a less efficient but more straightforward numerical method such as the explicit scheme. This type of scheme requires fewer variables residing within the machine's main memory at the same time. Variables that are not involved reside in the machine's external memory units waiting to be called upon. More "time–efficient" and sophisticated integration methods such as the implicit method would require more variables in the main memory simultaneously. At the present time, the largest computer's main memory and speed can allow simulations with a half–million to a million grid points if the simplest explicit scheme is used. In this type of scheme, only five neighboring grid points are contained in the CPU at a given time during the time and spatial marching (integration) process. A paging process is involved in which cyclic data blocks move in and out of the CPU and the external high speed storage device.

With the maximum allowable resolution using the method described above, the accuracy of the CFD approach at lower Mach range is around 5 to 7 percent. For example, in a simulation involving an X24C–10D experimental plane, the estimated values of the lift and drag coefficients, using the CFD method as compared with experiments at M=5.95, are 4.71 percent and 6.71 percent, respectively (Shang and Scherr, 1985). This simulation was made with the parabolized Navier Stokes equation coded with an explicit scheme (MacCormack, 1969) coupled with a zeroth–order algebraic turbulence closure technique (Baldwin and Lomax, 1978).

When the computed values are compared with the measurements, the larger deviations are located near the sharper geometric transitions. This indicates that higher spatial resolution will improve the accuracy. A higher–order turbulence model will also improve results around curved surfaces. All of this indicates a need for bigger and faster computers.

Within the foreseeable future, the computational speed of the computer is likely to follow the previous trend, namely, to increase 3 to 5 times in 3 to 4 years. The present computational speed limit is around 1 billion floating point operations per second (FLOPS). In projecting future speeds of supercomputers, the improvements can be made in several ways. In terms of hardware development, the speed improvement due to the increase in chip density is expected to increase by tenfold every seven years (Fig. 3). Supercomputers can also increase their processing speed through parallelism in architectural design, and the I/O speed can be increased by the use of super–conductive material, just to name a few possibilities.

For the NASP and the NASP–derived system applications around the year 2000, the expected computational speed is in the neighborhood of 10–20 billion FLOPS. A system with this capability could carry out CFD simulations for an external aircraft configuration consisting of 10 million grid points assuming the use of numerical techniques similar to those described above.

REQUIREMENTS ON THE SPECIFICATION OF BOUNDARY CONDITIONS

The use of CFD is based on the solution of boundary value problems. To obtain a solution, boundary conditions have to be specified. Any inaccuracy in specifying the proper boundary condition propagates into the computational field. But if one knows the exact conditions at the boundary, he would already have the solution to the problem. This is a well–known difficulty in the field of numerical modeling. One solution would be to set the boundaries of the model as far as possible from the aircraft so that its influence will be very small near the far–field boundaries. This approach

would need a large computational capacity. The next solution is to design a sophisticated numerical scheme at the model's boundaries in such a way that the dynamic effects (e.g., shock) originated at the aircraft would leave the boundaries without reflecting back into the model domain. This type of boundary treatment is called the "radiation boundary condition." It means that the energy within the model can radiate out of the model through its boundaries.

To make the boundary condition completely radiative is easier said than done. One major difficulty is to design a numerical scheme at the boundary which can "sense" all outgoing (pressure) waves of various frequencies and let them pass through. Furthermore, it is even more difficult to design such a scheme if "zonal modeling" techniques are used. In such a method, several models are patched together to form an entire aircraft. Mutual boundaries are located throughout the system and all of them need to be treated. Since the boundaries interconnect, special numerical schemes are therefore needed to overcome the redundancy in their specification. This is also true in the specification of the radiation boundary conditions for an adaptive (moving) grid network. To avoid this type of problem, it is much easier to simulate the entire aircraft in a single model, if the computational resources are available.

REQUIREMENTS ON THE VERIFICATION DATA AT THE UPPER HYPERSONIC RANGE

During different stages of model development, experimental data are needed to verify the theoretical basis and the computational code of the numerical model. As the Reynolds number and air speeds increase, the accuracy of the experimental measurement decreases. The degree of difficulty of acquiring the experimental data also increases as the speed increases. Shock tubes and gun–launched models can reach high Mach range, but they all have limitations for NASP applications. Because of the lack of emphasis on the hypersonic experiments during the 1970s, hypersonic wind tunnels and other ground test facilities designed to perform continuous

free flight tests are either no longer in existence or out of commission. At present, very few ground testing facilities or wind tunnels can simulate continuous free flight conditions at Mach number higher than 8. At speeds above Mach 10, it becomes increasingly more difficult to obtain high enough temperature to avoid gas condensation with corresponding high pressure to simulate flight Reynolds number range. Recently, tetrafluoromethane (CF_4) and nitrogen (N_2) have been used (Midden and Miller, 1978) for simulating the thin shock layer, chemically reactive, and high Reynolds number effects associated with the hypersonic flows.

REQUIREMENTS ON THE UNIVERSALITY OF A MODEL'S PREDICTION CONSTANTS

Without suitable verification data at high speed, the predictability or accuracy of the CFD codes will depend upon the universality of their turbulence model. In other words, the values of the closure constants have to stay the same for these models to predict beyond the verified range of applicability. This seems to be one of the crucial issues at the present time. New CFD codes are undoubtedly versatile and powerful. At low Mach range, experimental results have been used extensively to verify and adjust turbulence closure computations. Since turbulence modeling is not system–specific in terms of geometric shape, it has been a favored method for model verification. During the adjustment process, the so–called turbulence closure "constants" have been optimally fitted for various proposed models. Some of the results, presented in Table 5, show some degree of uncertainty. At this moment, we cannot predict whether the degree of uncertainty will increase in the higher Mach range. To obtain verification data at high speed (M 8–25), measurements from shuttle reentry flight or drones launched from high–speed planes may provide some technical data for benchmarking computational codes. In turbulence modeling, areas of low predictive reliability are listed in Tables 6 and 7.

In the field of fluid mechnics, however, there are very few truly

"universal" constants. Constants often considered as universal, such as the Kolmogorov constant are later found to vary under different flow conditions. The Kolmogorov constants for the distribution of turbulent spectral energy within turbulent flow was recently found to vary in two–dimensional turbulence (Kraichnan, 1987; Qian, 1986). This finding is quite important since flows under the thin–layer approximation or flows describable by parabolized CFDs are two–dimensional turbulences. To simulate the proper laminar/turbulent transition process at high hypersonic flight speeds, models of compressible turbulence should be used. For example, the entrainment rate of compressible turbulence is lower than the corresponding incompressible turbulence. The effects of shock structure on the transport of kinetic energy in and out of a turbulent eddy is still not completely understood (Breidenthal, 1990). Furthermore, the compressibility of air at hypersonic speed may change the universally accepted concept of Kolmogorov's law of the cascade of spectral energy in the frequency domain (Dimotakis, 1989). It is still too early to know the impact of these new findings on CFD modeling.

REQUIREMENTS ON THE COOPERATION BETWEEN MODELERS AND DESIGNERS

To develop and work with CFD methods and codes, one needs an extensive background in both mathematics and computer sciences as well as fluid dynamics. Sensitivity to experimental findings is also essential. CFD modeling gradually evolves into a highly specialized field. To maintain a CFD simulation system often becomes a full–time task for a small research team. After completion of the Apollo moon–landing program and design of the shuttle reentry vehicle in the early 1970s, there has been no major design activity in hypersonics during the last one and half decades. As a consequence, most CFD modelers have limited design experience. Since computers are not yet fast and big enough to perform a complete automated design under given constraints, CFD simulations still play the role of the designer's aids, which are extremely complicated to use. To close this gap,

experienced designers have to work with the CFD simulation team. This is necessary because an experienced designer not only can give valuable guidance in the design phase but can also check to see if the computer output makes sense. As mentioned earlier, although they are powerful tools, CFD results are still only simulations.

COMPATIBILITY REQUIREMENTS BETWEEN HARDWARE AND SOFTWARE

The computational efficiency of a numerical scheme is a relative matter. It often depends on the type of hardware the code is running on. An understanding of the machine architecture is very important for code development. For example, during the numerical integration process, the control of data flow between the parallel functional unit and the hierarchically organized memory is essential. Because the computer's basic clock speed, which determines the rate of calculation, varies from machine to machine, the cycle time required for various computer functions will also vary thereby resulting in major differences in overall computational speed. Machine–specific characteristics such as the "memory cycle time," the "access time," and the "transfer rate" all require a different number of clock periods to complete. A CFD code should be designed to allow maximum concurrent operations to achieve the overall efficiency.

According to Cray Research (Shang et al., 1980), the efficiency of a FORTRAN code can be improved by:

- Avoiding a long and complicated "do loop"
- Replacing the most frequently addressed temporary scalar variable with a vector temporary variable
- Developing the code to allow maximum use of concurrent (chaining) operations. The chaining of two or more vector operations allows a vector machine to yield more than one result per clock period.

Along the same line as discussed above but more fundamental in nature, it is important to use better programming languages and operating systems. At present, the majority of aerospace engineers write CFD models in FORTRAN, which is considered to be primitive as compared to the more advanced languages such as Pascal or ADA. More efficient transfer between the database and the arithmetic unit can also be achieved by improving the operating system.

8. CONCLUSIONS

During this review the following conclusions were reached:

1. Computational fluid dynamic (CFD) models, if they are properly designed, verified, and applied, are versatile and powerful tools. With the level of resolution that can be handled by the present state–of–the–art computers, the level of verifiable simulation accuracy (in terms only of pressure distribution) is approximately within 5 to 6 percent at the intermediate speed range (Mach 0 – 8). But, it is difficult to even estimate the inaccuracies in such crucial parameters as skin frictions, heating values, and turbulent mixing. When the computed values are compared with the available data, the larger deviations are located near the sharper geometric transitions. This indicates that higher spatial resolution will improve the accuracy. A higher–order turbulence model should also improve results around curved surfaces. These improvements need bigger and faster computers. However, it may be years before we can narrow uncertainties in both the laminar–turbulent transition location and the characteristics of flows as they enter the inlet region. We may also require time to better understand the character of the mixing region with the SCRAMJET as the Mach numbers approach those of interest to NASP.

2. For better predictive accuracy and for the generality in the CFD models' predictive applicability, turbulence closure techniques need to be further improved. Experimental data at the full range of NASP speeds are needed to evaluate the closure constants. A wider range of applicability can be achieved if the constants are more universal. Universality implies higher predictive reliability into higher speed range. Closure models will nearly always be needed in CFD within the foreseeable future (e.g., until 2000) unless a major breakthrough in computing power takes place. The speed and memory of computers would have to inprove several orders of magnitude over present state–of–the–art machines considering realistic flight Reynolds number range. With improvement of this magnitude, the troublesome

"turbulence closure" step can then be completely eliminated. Given that the past rate of progress in computing power continues (i.e., 10 times in 7 years) and the NASP schedule remains unchanged, it will be necessary to continue using turbulence modeling for the entire NASP development program, as well as possibly for the NDV development program as well. To approach universality for constants, many more data must be collected at all NASP speed ranges. If this is not done, a similar level of predictive uncertainty as the present will continue to exist.

3. Because of the relatively inactive period in hypersonic research for the past 15 years, the design–supporting ground–testing facilities that were in existence have not been properly maintained or are out of commission. At present, there is an urgent need for ground–testing facilities with improved measurement techniques to provide verification data for CFD models. Complementary techniques to ground tests are needed to verify CFD simulations at the high Mach ranges where experimental data are difficult to obtain. Recent advances in flow measurements by means of laser–Doppler technology will undoubtedly improve the quality of verification data in the future. The shock tube "RHYFL" (Rockdyne Hypersonic Facility), which will be completed in the near future, has a velocity limit of Mach 16. The piston is driven by nitrogen with the testing duration of 1/1000 second. As a consequence, dynamic processes induced by transient dynamics may pose some problem. But extensive use of RHYFL will be an important part of reducing the uncertainty in the CFD simulation.

4. The numerical solution schemes used in the CFD models have improved in accuracy and efficiency during the last two decades. However, no clear distinction has developed among all the available methods as to which is the best overall method. Tradeoffs often have to be made. There are times, when less efficient but more straightforward integration schemes have been selected so that fewer spatial points reside in the CPU simultaneously. By doing this, a great number of grid points can be simulated with a single model, thus simplifying the boundary condition handling problem, even though this approach increases the simulation time (I/O process).

5. One major advancement in the field of CFD is the application of coordinate transformation schemes often employed in conjunction with the

finite–difference methods. When an implicit scheme is used together with transformed coordinates, the drop in accuracy of numerical approximation should be evaluated especially near the crucial area such as the leading edge where the Courant number is very high as a result of small grid size.

6. During the coming years, for NASP applications, emphasis on CFD research should be on the following crucial areas:

- Validation of higher order turbulence models to reduce the level of uncertainty in the areas of low predictive reliability such as rapid compression/expansion, strong swirl, kinematically influenced chemical reaction, dynamic instability.
- Improvement in modeling compressible turbulence.
- Improvement in predicting the location and the length of the boundary layer transition zone on the aerospace plane and the details of the transition process.
- Improvement in conserving mass, momentum, and energy in the numerical scheme solving the Navier Stokes equations involving grid transformation particularly curvilinear transformation.
- Treatment of boundary conditions particularly in a "nested" modeling system where different grids are used.
- More efficient cooperation between government and industry in CFD code development and validation.
- Explicitly evaluating and publishing the uncertainty in CFD simulation results as a function of the vehicle speed and position along the vehicle.

BIBLIOGRAPHY

Abarbanel, S., and E. M. Murman (1985): *Progress and Supercomputing in Computational Fluid Dynamics,* Birkhauer, Boston.

Abbett, M. J. (1973): "Boundary condition calculation procedures for inviscid supersonic flow fields," *Proc. 1st AIAA Computational Fluid Dynamics Conf.,* Palm Springs, California, pp. 153–172.

Acharya (1977): "A critique of some recent 2nd order turbulence closure models for compressible boundary layer," *AIAA,* paper 77–128.

Anderson, D. A., J. C. Tennehill, and R. H. Pletcher (1984): *Computational Fluid Dynamics and Heat Transer,* Hemisphere Publishing Company/McGraw-Hill Book Company.

Anderson, J. D. (1984): "A survey of modern research in hypersonic aerodynamics," *AIAA,* paper A84–37983.

Anderson, J. D. (1989): *Hypersonic and High Temperature Gas Dynamics,* McGraw-Hill Book Company.

Anderson, W. K., J. L. Thomas, and B. Van Leer (1985): "A comparison of finite volume flux vector splittings for Euler equations," *AIAA,* paper no. 85–0122.

Aroesty, J. (1964): "Slip flow and hypersonic boundary layer," *AIAA Journal,* Vol. 2, No. 1, pp. 189–190.

Ashford, O. M. (1985): *Prophet or Professor? The Life and Work of L. F. Richardson,* Adam Hilgler, Bristol.

Ashurst, W. T., A. R. Kirstein, R. M. Kerr, and C. H. Gibson (1987): "Alignment of vorticity and scalar gradient with strain rate in simulated Navier-Stokes turbulence," *Phys. Fluids,* Vol. 30, pp. 2343–2353.

Aubry, N., P. Holmes, J. L. Lumley, and E. Stone (1987): "Models for coherent structures in the wall layer," in Comte-Bellot and Mathieu (eds.) *Proc. Advances in Turbulence,* Springer, pp. 346–356.

Augarten, S. (1985): *Bit by Bit: An illustrated History of Computers,* Unwin, London.

Babuska, I., J. Chandra, and J. E. Flaherty (eds.) (1983): "Adaptive Computational Methods for Partial Differential Equations," *SIAM,* Philadelphia, Pennsylvania.

Babuska, I., O. C. Zienkiewicz, J. Gago, and E. R. de A. Oliveira (eds.) (1986): *Accuracy Estimates and Adaptive Refinements in Finite Element Computations,* Wiley, New York.

Bachalo, W. D., and D. A. Johnson (1979): "An investigation of transonic turbulent boundary layer separation generated on an axisymmetric flow model," *AIAA,* paper 79–1479.

Bahn, G. S. (1972): "Calculations on the autoignition of mixtures of hydrogen and air," *NASA*, report CR–112067.

Baines, M. J., and A. J. Wathen (1988): "Moving element methods for evolutionary problems, I. Theory," *Journal of Computational Physics*, Vol. 79, pp. 245–269.

Baker, A. J., and M. O. Soliman (1979): "Utility of a finite element solution algorithm for initial-value problems," *Journal of Computational Physics*, Vol. 32, pp. 289–324.

Baker, A. J., and M. O. Soliman (1983): "A finite element algorithm for computational fluid dynamics," *AIAA Journal*, Vol. 21, No. 6, pp. 816–827.

Baldwin, B. S., and H. Lomax (1978): "Thin layer approximation and algebraic model for separated turbulent flows," *AIAA*, paper 78–257.

Bardina, J., J. H. Ferziger, and R. S. Rogallo (1985): "Effects of rotation on isotropic turbulence computation and modeling," *Journal of Fluid Mechanics*, Vol. 154, pp. 321–336.

Barnett, G. D., and R. T. Davis (1985): "A procedure for the calculation of supersonic flows with strong viscous-inviscid interactions," *AIAA*, paper 85–0166.

Barry, A., J. Bielak, and R. C. MacCamy (1988): "On absorbing boundary conditions for wave propagation," *Journal of Computational Physics*, Vol. 79, pp. 449–468.

Beam, R. M., and R. F. Warming (1976): "An implicit finite difference algorithm for hyperbolic systems in conservative law form," *Journal of Computational Physics*, Vol. 22, pp. 87–110.

Beam, R. M., and R. F. Warming (1978): "An implicit factored scheme for the compressible Navier-Stokes equations," *AIAA Journal*, Vol. 16, No. 4, pp. 393–402.

Bell, J. B., P. Colella, and J. A. Trangentein (1989): "Higher order Godunov methods for general systems of hyperbolic conservation laws," *Journal of Computational Physics*, Vol. 82, No. 1, pp. 362–397.

Benek, J. A., P. G. Buning, and J. L. Steger (1985): "A 3D chimera grid embedding technique," *AIAA*, paper No. 85–1523.

Berger, M. J., and P. Colella (1989): "Local adaptive mesh refinement for shock hydrodynamics," *Journal of Computational Physics*, Vol. 82. No. 1, pp. 64–84.

Berglind, T. (1985): "Grid generation around car configurations above a flat ground plane using transfinite interpolation," *FFA*, report 139, Stockholm.

Berman, H. A., and J. D. Anderson (1983): "Supersonic flow over a rearwall facing step with transverse nonreacting hydrogen injection," *AIAA Journal*, Vol. 22, pp. 1707–1713.

Bhutta, B. A., C. H. Lewis, and F. A. Kautz (1985): "A fast fully-interactive parabolized Navier-Stokes scheme for chemically-reacting reentry flows," *AIAA*, paper no. 85–0926.

Bilbao, L. (1990): "A three-dimensional Lagrangian method for fluid dynamics," *J. of Comp. Phys.*, Vol. 91, pp. 361–380.

Biringen, S., A. Saati, and C. Farhat (1989): "Performance evaluation of an explicit Navier-Stokes solver on the Connection Machine," 42nd Annual Meeting, Fluid Dynamics Division, American Physics Society, Palo Alto, California.

Bisseling, R. H., and R. Kosloff (1988): "Optimal choice of grid points in multi-dimensional pseudospectral Fourier methods," *Journal of Computational Physics,* Vol. 76, pp. 243–262.

Bittker, D. A., and V. J. Scullin (1984): "GCKP84—General Chemical code for gas-phase flow and batch processes including heat transfer effects," *NASA,* paper 2320.

Bivens, G. A. (1989): *Reliability Assessment Using Finite Element Techniques,* Rome Air Development Center, RADC–TR–89–281, November 1989.

Blackwelder, R. F., and R. E. Kaplan (1976): "On the wall structure of the turbulent boundary layer," *Journal of Fluid Mechanics,* Vol. 76, pp. 89–112.

Blaschak, J. G., and G. A. Kriegsmann (1988): "A comparative study of absorbing boundary conditions," *Journal of Computational Physics,* Vol. 77, pp. 109–139.

Bogdanoff, D. W. (1983): "Compressibility effects in turbulent shear layers," *AIAA Journal,* Vol. 21, No. 6, pp. 926–927.

Boris, J. P., E. S. Oran, E. F. Brown, C. Li, and F. F. Grinstein (1989): "Boundary conditions for fluid dynamic simulations on the Connection Machines," 42nd Annual Meeting, Fluid Dynamics Division, American Physics Society, Palo Alto, California.

Bortner, M. H. (1969): *A Review of Rate Constant of Selected Reactions of Interest in Reentry Flow Fields in the Atmosphere,* National Bureau of Standards Technical Note 484.

Boussinesq, J. (1877): "Essai sur la theorie des eaux courantes," *Memoires présentes par division sav. a l'Academie des Sciences,* Vol. 23, pp. 380–396.

Boyd, J. P. (1987): "Spectral methods using rational basis functions on an infinite interval," *Journal of Computational Physics,* Vol. 69, pp. 112–142.

Breidenthal, R. E. (1990): "The sonic eddy—A model for compressible turbulence," *AIAA,* paper 90–0495.

Browning, G. L., and H. O. Kreiss (1989): "Comparison of numerical methods for the calculation of two-dimensional turbulence," *Math. of Computation,* Vol. 52, No. 186, pp. 369–388.

Busnaina, A. A., G. Ahmadi, and S. J. Chowdhury (1987): "Two-equation turbulence model consistent with the second law," *AIAA Journal,* Vol. 25, No. 12, pp. 1543–1544.

Bussing, T.R.A., and E. M. Murman (1987): "Numerical investigation of two-dimensional H_2-air flameholding over ramps and rearward-facing steps," *J. Propulsion,* Vol. 3, No. 5, pp. 448–454.

Cai, W., D. Gottlieb, and C. W. Shu (1989): "Essentially nonoscillatory spectral Fourier methods for shock wave calculations," *Math. of Comp.*, Vol. 52, No. 186, pp. 389–410.

Calloway, R. L. (1978): "Real gas-simulation for the Shuttle Orbiter and planetary entry configurations including flight results," *AIAA*, paper 84–0489.

Camac, M., and R. M. Feinberg (1966): "Formation of NO in shock-heated air," *Proc. 11th International Symposium on Combustion.*

Cambon, C., D. Jeandel, and J. Mathieu (1981): "Spectral modelling of homogeneous nonisotropic turbulence," *Journal of Fluid Mechanics*, Vol. 104, pp. 247–262.

Canuto, C., M. Y. Hussani, A. Quarteroni, and T. Zang (1988): *Spectral Methods in Fluid Dynamics*, Springer Verlag, New York.

Carpenter, M. H. (1988): "Effects of finite rate chemistry and viscosity on high enthalpy nozzle results," *Fourth National Aerospace Plane Technology Symposium*, 1988, pp. 133–160.

Carruthers, D. J., and J.C.R. Hunt (1986): "Velocity fluctuations near an interface between a turbulent region and a stably stratified layer," *Journal of Fluid Mechanics*, Vol. 165, pp. 475–501.

Case, K. M., F. J. Dyson, E. A. Freeman, C. E. Grosch, and F. W. Perkins (1973): *Numerical Simulation of Turbulence*, SRI, TR–JSR–73–3.

Cebeci, T., and A.M.O. Smith (1974): *Analysis of Turbulent Boundary Layer*, Academic Press, New York.

Chakravarthy, S. R. (1986): "The versatility and reliability of Euler solvers based on high accuracy TVD formulations," *AIAA*, paper no. 86–0243.

Chakravarthy, S. R., K. Y. Szema, and J. W. Haney (1988): "Unified 'nose-to-tail' computational method for hypersonic vehicle applications," *AIAA*, paper 88–2564.

Chakravarthy, S. R., K. Y. Szema, U. C. Goldberg, J. J. Gorski, and S. Osher (1985): "Application of a new class of high accuracy TVD schemes to the Navier Stokes equations," *AIAA*, paper 85–0165.

Chambers, T. L., and D. C. Wilcox (1977): "Critical examination of two equations turbulence closure model for boundary layers," *AIAA Journal*, Vol. 15, pp. 821–828.

Chapman, D. R. (1979): "Computational aerodynamics development and outlook," *AIAA Journal*, Vol. 17, No. 12, 79–0129R, pp. 1293–1313.

Chapman, S., and T. G. Cowling (1939): *The Mathematical Theory of Non-Uniform Gases*, Cambridge University Press.

Chase, D. M. (1969): "Space-time correlation of velocity and pressure and the role of convection for homogeneous turbulence in the universal range," *Acustica*, Vol. 22, pp. 303–320.

Chen, J., B. J. Cantwell, and N. N. Mansour (1990): "The effect of Mach number on the stability of a plane supersonic wake," *Phys. Fluid. A.*, Vol. 2, No. 6, pp. 984–1004.

Chen, S. Y., J. Aroesty, and R. Mobley (1966): *The Hypersonic Viscous Shock Layer with Mass Transfer*, RAND, RM–4631–PR.

Cheng, H. K. (1960): *The Shock Layer Concept and Three-Dimensional Hypersonic Boundary Layer*, Cornell Aeronautical Lab., AF–1285–A–3, Buffalo, New York.

Cheng, H. K., S. Y. Chen, R. Mobley, and C. R. Huber (1970): *The Viscous Hypersonic Slender-Body Problem: A Numerical Approach Based on a System of Composite Equations* RAND, RM–6193–PR.

Chien, K. Y. (1982): "Predictions of channel and boundary-layer flows with a low-Reynolds number turbulence model," *AIAA Journal*, Vol. 20, pp. 33–38.

Chollet, J. (1983): "Two-point closure as a subgrid scale modeling for large eddy simulations," *Fourth Symposium on Turbulent Shear Flows*, Karlsruhe, September 1983.

Chorin, A. J. (1972): "Numerical solution of Boltzmann's equation," *Comm. Pure and Appl. Math.*, Vol. 25, pp. 171–186.

Chorin, A. J. (1973): "Numerical study of slightly viscous flow," *J. Fluid Mech.*, Vol. 57, part 4, pp. 785–796.

Chorin, A. J. (1977): "Random choice methods with applications to reacting gas flow," *Journal of Computational Physics*, Vol. 25, pp. 253–272.

Chou, P. Y. (1945): "On velocity correlations and the solutions of the equations of turbulent fluctuations," *Quarterly Appl. Math.*, Vol. 3, pp. 38–54, and "Pressure flow of a turbulent fluid between parallel plates," pp. 198–209.

Chung, P. M. (1961): *Hypersonic Viscous Shock Layer of Non-Equilibrium Dissociating Gas*, NASA, TR R–109.

Coles, D. (1978): "A model for flow in the viscous sublayer," *Proc. of the Workshop on Coherent Structure of Turbulent Boundary Layers*, Lehigh University, Bethlehem, Pennsylvania.

Courant, R., and K. O. Friedrichs (1948): *Supersonic Flow and Shock Waves*, Interscience Publishers, New York.

Daly, D. J., and F. H. Harlow (1970): "Transport equations in turbulence," *Phys. Fluid*, Vol. 13, pp. 2634–2649.

Darin, N. A., and V. I. Mazhukin (1988): "An approach to adaptive grid construction for non-stationary problems," *USSR Computational Mathematics and Mathematical Physics*, Vol. 28, No. 2, pp. 99–103.

Dash, S. M. (1986): "Design-oriented PNS analysis of complete Scramjet propulsion system," *Second National Aerospace Plane Technology Symposium*, NASP CP 2012, Vol. IV.

Dash, S. M. (1986): "Turbulence modeling, chemical kinetics and algorithm related issues in CFD analysis of Scramjet components," *Second National Aerospace Plane Technology Symposium,* NASP CP 2012, Vol. IV.

Dash, S. M., and D. E. Wolf (1984): "Iterative phenomena in supersonic jet mixing problems, Part I: phenomenology and numerical modeling techniques," *AIAA Journal,* Vol. 22, pp. 905–913.

Dash, S. M., and R. D. Thorpe (1981): "A shock-capturing model for one and two phase supersonic exhaust flows," *AIAA Journal,* Vol. 19, pp. 842–851.

Dash, S. M., N. Sinha, D. E. Wolf, B. J. York, and R. A. Lee (1988): "Analysis of combustor and nozzle flowfields using zonal PNS," *Fourth National Aerospace Plane Technology Symposium,* pp. 267–292.

Dash, S. M., T. Harris, W. Krawczyk, R. Lee, N. Rajendran, N. Sinha, B. York, and D. Carlson (1989): "Three-dimensional upwind/implcit PNS computer codes for analysis of scramjet propulsive flowfields," *Sixth National Aerospace Plane Technology Symposium,* pp. 129–172.

Davidov, B. I. (1959): "On the statistical dynamics of an incompressible turbulent fluid," *Dokl. Akad. Nauk SSSR,* Vol. 127, pp. 768–770 (English trans. in *Sov. Phys. Doklady,* Vol. 4, pp. 769–772).

Davidov, B. I. (1961): "On the statistical dynamics of an incompressible fluid," *Dokl. Akad. Nauk SSSR,* Vol. 136, pp. 47–50 (Eng. trans. in *Sov. Phys. Doklady,* Vol. 6, pp. 10–12).

Davis, S. F., and J. E. Flaherty (1982): "An adaptive finite element method for initial-boundary value problems for partial differential equations," *SIAM J. on Scient. and Statis. Comp.,* Vol. 3, pp. 6–27.

De Swart, H. E., and J. Grasman (1987): "Effects of stochastic perturbations on a low-order spectral model of the atmospheric circulation," *Tellus,* Vol. 39A, pp. 10–24.

Denton, J. D. (1985): *3D Computational Techniques Applied to Internal Flows in Propulsion Systems,* AGARD–LS–140.

Dimotakis, P. E. (1989): "Turbulent free shear layer mixing," *AIAA,* paper 89–0262.

Donaldson, C. du P., and R. D. Sullivan (1972): "An invariant second-order closure model of the compressible turbulent boundary layer on a flat plate," *Aeron. Res. Assoc. of Princeton,* Rep. No. 187.

Douglas, J. (1955): "On the numerical integration of $u_{xx} + u_{yy} = u_t$ by implicit method," *J. SIAM,* Vol. 3, pp. 42–65.

Douglas, J., and Gunn (1964): "A general formulation of alternating direction methods," *Numerische Mathematiks,* Vol. 6, pp. 428–453.

Drummond, J. P., and R. C. Rogers (1988): "Simulation of supersonic mixing and reacting flow fields," *Fourth National Aerospace Plane Technology Symposium,* pp. 177–196.

Dutoya, D., and P. Michard (1981): "A program for calculating boundary layer along compressor and turbine blades," in Lewis et al. (eds.), *Numerical Methods in Heat Transfer*, Wiley, New York.

Dwoyer, D. L. (1988): "NASP CFD technology maturation plan review," *Fourth National Aerospace Plane Technology Symposium*, pp. 1–13.

Eiseman, P. R. (1985): "Grid generation in fluid mechanic computations," *Ann. Rev. of Fluid Mech.*, Vol. 17.

Engquist, B., P. Lotstedt, and B. Sjogreen (1989): "Nonlinear filters for efficient shock computation," *Math. Comp.*, Vol. 52, No. 186, pp. 509–538.

Eriksson, L. E. (1984): *A Study of Mesh Singularities and Their Effects on Numerical Errors*, FFA Tech. Note. TN 1984–10, Stockholm.

Esch, D., A. Siripong, and R. Pike (1970): *Thermodynamic Properties in Polynomial Form for Carbon, Hydrogen, and Oxygen Systems from 300K–3000K*, NASA–REL–TR–70–3.

Evans, J. S., and C. J. Schexnayder (1979): "Critical influence of finite rate chemistry and unmixedness on ignition and combination of supersonic H_2 air stream," *AIAA*, paper 79–0355.

Fan, W. C. (1988): "A two-fluid model of turbulence and its modifications," *Scientia Sinica (Series A)*, Vol. XXXI, No. 1, pp. 79–86.

Ferri, A. (1964): "Review of problems in application of supersonic combustion," *Jour. Roy. Aeronautical Soc.* Vol. 68, pp. 575–597.

Ferri, A. (1973): "Mixing controlled supersonic combustion," *Annual Review of Fluid Mechanics*, Vol. 5, Annual Reviews Inc., Palo Alto, California, pp. 301–338.

Fichtl, G. H., N. D. Reynolds, A. E. Johnston, S. I. Adelfang, W. Batts, L. Lott, P. J. Mayer, O. E. Smith, M. S. Swint, and O. H. Vaughan (1988): "Analysis of in-flight winds for Shuttle Mission STS 51–L," *Journal of Meteorology*, Vol. 27, pp. 1232–1241.

Finlayson, B. A. (1972): *The Method of Weighted Residuals and Variational Principles*, Academic Press, New York.

Fong, J., and L. Sirovich (1987): "Supersonic inviscid flow—a three-dimensional characteristic approach," *Journal of Computational Physics*, Vol. 68, pp. 378–392.

Fornberg, B. (1980): *Soc. Ind. J. Sc. Stat. Comput.*, Vol. 1, p. 386.

Gaier, D. (1974): *Lecture Notes in Mathematics*, No. 399, Springer-Verlag, Berlin.

Galerkin, B. G. (1915): "Rods and plates, series in some problems of elastic equilibrium of rod and plates," *Vestn. Inzh. Tech. (Engr. Bull.)*, USSR, Vol. 19, pp. 897–908 (English trans. 63–18924, Clearing-house, Fed. Sci. Tech. Info. Spring Field, Virginia).

Gatski, T. B., C. E. Grosch, and M. E. Rose (1989): "The numerical solution of the Navier-Stokes equations for 3-dimensional, unsteady, imcompressible flows by compact schemes," *Journal of Computational Physics,* Vol. 82, No. 2, pp. 298–329.

Gelinas, R. J., and S. K. Doss (1981): "The moving element method: application to general partial differential equation with multiple large gradients," *Journal of Computational Physics,* Vol. 40, pp. 202–249.

Gentzsch, W. (1984): *Vectorization of Computer Programs with Application to Computational Fluid Dynamics,* Vieweg, Braunschweig.

Ghil, M., R. Benzi, and G. Parisi (eds.) (1985): *Turbulence and Predictability in Geophysical Fluid Dynamics and Climate Dynamics,* North-Holland, New York.

Giannakopoulos, A. E., and A. J. Engel (1988): "Directional control in grid generation," *Journal of Computational Physics,* Vol. 74, pp. 422–439.

Gilreath, H. E. (1988): "Tangential injection in high speed flow, comparison of computational and experimental results," *Fourth National Aerospace Plane Technology Symposium,* pp. 161–176.

Glimm, J. (1965): "Solutions in the large for non-linear hyperbolic systems of conservation laws," *Comm. Pure Appl. Math.,* Vol. 18, p. 697.

Gnoffo, P. A. (1983): "A vectorized, finite volume, adaptive grid algorithm applied to planetary entry problems," *AIAA Journal,* Vol. 21, p. 1249.

Godunov, S. K. (1970): *Solution of One Dimensional Problems of Gas Dynamics with Variable Meshes,* NAUKA, Moscow, 1970.

Goldberg, U. C. (1986): "Separate flow treatment with a new turbulence model," *AIAA Journal,* Vol. 24, No. 10, pp. 1711–1713.

Goldberg, U. C., and S. R. Chakravarthy (1988): "Prediction of separated flows with a new backflow turbulence model," *AIAA Journal,* Vol. 26, No. 4, pp. 405–408.

Goldberg, U. C., and S. R. Chakravarthy (1989): "Separated flow predictions using a hybrid k-L/backflow model," *AIAA,* paper 89–0566.

Gordon, W. J., and L. C. Thiel (1982): "Transfinite mapping and their application to grid generation," in J. F. Thompson (ed.), *Numerical Grid Generation,* North Holland Publishing Company.

Gorski, J. J., S. R. Chakravarthy, and U. C. Goldberg (1985): "High accuracy TVD schemes for the k-ε equations of turbulence," *AIAA,* paper No. 85–1665.

Gottlieb, D. (1985): "Spectral methods for compressible flow problems," *Nineth International Conference on Numerical Meth. in Fluid Dynamics,* Springer-Verlag.

Gottlieb, D., and S. A. Orszag (1977): "Numerical analysis of spectral method: theory and applications," NSF Bd of Math. Sci. Monograph, No. 26, *SIAM,* Philadelphia, Pennsylvania.

Gottlieb, D., L. Lustman, and S. A. Orszag (1981): "Spectral calculation of one-dimensional inviscid compressible flows," *SIAM J. of Sci. and Sta. comp.*, Vol. 2, 1981, pp. 296–310.

Granville, P. S. (1987): "Baldwin-Lomax factors for turbulent boundary layers in pressure gradients," *AIAA Journal*, Vol. 25, No. 12, pp. 1624–1629.

Gritton, E. C., W. S. King, I. Southerland, R. S. Gaines, C. Gazley, C. Grosch, M. Juncosa, and H. Peterson (1977): *Feasibility of a Special Computer to Solve the Navier-Stokes Equations*, RAND, R–2183–RC.

Grosch, C. E., and S. Orszag (1977): "Numerical solution of problems in unbounded regions: Coordinate transforms," *J. Comp. Phys.*, Vol. 25, pp. 273–296.

Halsey, N. D. (1987): "Use of conformal mapping in grid generation for complex three-dimensional configurations," *AIAA Journal*, Vol. 25, No. 10, pp. 1286–1291.

Hancock, P. E., and P. Bradshaw (1989): "Turbulence structure of a boundary layer beneath a turbulent free stream," *J. Fluid Mech.*, Vol. 205, pp. 45–76.

Hanjalic, K., and B. E. Launder (1972): "A Reynolds stress model of turbulence and its application to thin shear flows," *J. Fluid. Mech.*, Vol. 52, pp. 609–638.

Hanjalic, K., and B. E. Launder (1976): "Contribution towards a low Reynolds-stress closure for low-Reynolds-number turbulence," *Journal of Fluid Mechanics*, Vol. 74, pp. 593–610.

Harris, T. B., W. J. Krawczyk, and N. Rajendran (1988): "Progress toward the development of 3-D implicit upwind computer codes for inlets and forebodies," *Fourth National Aerospace Plane Technology Symposium*, 1988, pp. 249–266.

Hassid, S., and M. Poreh (1978): "A tubulent energy dissipation model for flows and drag reduction," *J. Fluid Engineering*, Vol. 100, pp. 107–112.

Haworth, D. C., and S. B. Pope (1987): "Monte Carlo solutions of a joint PDF equation for turbulent flows in general orthogonal coordinates," *Journal of Computational Physics*, Vol. 72, pp. 311–346.

Herzog, S. (1986): "The large-scale structure in the near wall region of turbulent pipe flow," Ph. D. thesis, Cornell University.

Hillis, W. D. (1985): *The Connection Machine*, MIT Press, Cambridge, Massachusetts.

Hinze, J. O (1959): *Turbulence*, McGraw-Hill, New York.

Hockney, R. W., and C. R. Jesshope (1983): *Parallel Computers*, Adam Hilger, Bristol.

Hoeijmakers, H. W. (1983): *Aerodynamics of Vortical Type Flows in Three-Dimensions*, AGARD-CP 342. Paris.

Hoffman, G. H. (1975): "Improved form of the low-Reynolds number k-ε turbulence model," *Physics of Fluids*, Vol. 18, pp. 309–312.

Hoffman, J. J., R. S. Wong, T. R. Bussing, and S. F. Birch (1988): *Low Density Real Gas Flows about Hypersonic Vehicles,* Air Force Wright Aeronautical Lab., Rep. AWFAL–TR–87–3112.

Holt, M. (1984): *Numerical Methods in Fluid Dynamics, Computational Physics,* 2nd edition, Springer-Verlag, New York.

Hosokawa, I., and K. Yamamoto (1990): "Intermittency exponents and generalized dimensions of a directly simulated fully developed turbulence," *Physics of Fluids, A.,* Vol. 2, No. 6, pp. 889–891.

Hsieh, T. (1976): *An Investigation of Separated Flow about a Hemisphere-Cylinder at 0- to 19-deg. Incidence in the Mach No. Range from 0.6 to 1.5,* Arnold Eng. Dev. Center, AEOC–TR–76–12.

Hung, C. M., and R. W. MacCormak (1978): "Numerical solution of three-dimensional shock wave and turbulent boundary layer interaction," *AIAA Journal,* Vol. 16, pp. 1090–1096.

Hunt, J.C.R. (1988): "Studying turbulence using direct numerical simulation: 1987 Center for Turbulence Research NASA Ames/Stanford Summer Programme," *Journal of Fluid Mechanics,* Vol. 190, pp. 375–392.

Hussain, A.K.M.F., (1986): "Coherent structures and turbulence," *Journal of Fluid Mechanics,* Vol. 173, pp. 303–356.

Hussaini, M. Y., et al. (1985): "Spectral methods for the Euler equations, part 1: Fourier methods and shock-fitting," *AIAA Journal,* Vol. 23, pp. 64–70.

Ivanenko, S. A., and A. A. Charakhch'yan (1988): *USSR Compt. Maths. and Math. Phys.,* Vol. 28, No. 2, pp. 126–133.

Ivanov, M. Y., and V. V. Koretskii (1985): "Calculations of flows in two- and three-dimensional nozzles by the approximate factorization method," *Zh. vychisl. Mat. Fiz.,* Vol. 25, No. 9, pp. 1365–1381.

Jackson, T. L., and G. E. Grosch (1990): "Absolute/convective instabilities and the convective Mach number in a compressible mixing layer," *Physics of Fluids, A.,* Vol. 2, No. 6, pp. 949–954.

Jameson, A. (1986): *Multigrid Methods II, Lecture Notes in Mathematics Series,* in W. Hackbusch and U. Trottenberg (eds.), Springer-Verlag, New York.

Jameson, A. (1989): "Computational aerodynamics for aircraft design," *SCIENCE Magazine,* Vol. 245, pp. 361–371.

Jameson, A., and D. A. Caughey (1977): *Numerical Calculation of the Transonic Flow Past a Swept Wing,* New York University Report, COO–3077–140.

Jameson, A., and P. D. Lax (1984): *Conditions for the Construction of Multi-Point Total Variation Diminishing Difference Schemes,* Princeton University Report, MAE–1650.

Jeandel, D., J. F. Brison, and J. Mathieu (1978): "Modeling methods in physical and spectral space," *Phys. Fluids*, Vol. 21 (2), pp. 169–182.

Jones, W. P., and B. E. Launder (1972): "The prediction of laminarization with a two-equation model of turbulence," *International Journal of Heat and Mass Transfer*, Vol. 15, pp. 301–314.

Kang, S. W., and M. G. Dunn (1973): *Theoretical and Experimental Studies of Reentry Plasma*, NASA, CR–2232.

Kee, R. J., J. Warnatz, and J. A. Miller (1983): *A Fortran Computer Code Package for the Evaluation of Gas-Phase Viscosities, Conductivities, and Diffusion Coefficients*, Sandia Lab Report, SAND 83–8209.

Keller, J. B., and D. Givoli (1989): "Exact non-reflective boundary conditions," *Journal of Computational Physics*, Vol. 82, No. 2, pp. 172–192.

Knight, D. D. (1984): "A hybrid explicit-implicit numerical algorithm for the 3-D compressible Navier-Stokes equations," *AIAA Journal*, Vol. 22, pp. 1056–1063.

Kolmogoroff, A. N. (1962): "A refinement of previous hypotheses concerning the local structure of turbulence in a viscous incompressible fluid at high Reynolds number," *Journal of Fluid Mechanics*, Vol. 13, No. 1, pp. 82–85.

Korthals-Altes, S. W. (1987): "Will the aerospace plane work?" *Technology Review*, pp. 43–51.

Kraichnan, R. H. (1987): "Kolmogorov's constant and local interaction," *Phy. of Fluids*, Vol. 30, No. 6, pp. 1583–1585.

Krouthen, B. (1986): *Grid Generation for Compressor/Turbine Configurations*, FFA, TN–1986–50, Stockholm.

Ku, H. C., R. S. Hirsh, and T. D. Taylor (1987): "A pseudospectral method for solution of the three-dimensional incompressible Navier-Stokes equations," *Journal of Computational Physics*, Vol. 70, pp. 439–462.

Kumar, A. (1982): "Two dimensional analysis of a Scramjet inlet flow field," *AIAA Journal*, Vol. 20, pp. 96–97.

Lam, C.K.G., and K. A. Bremhorst (1977): "Modified form of the k-ε model for predicting wall turbulence," *Journal of Fluid Engineering*, Vol. 103, pp. 456–460.

Launder, B. E., A. Morse, W. Rodi, and D. B. Spaulding (1973): "Prediction of free shear flows—a comparison of the performaance of six turbulence models," *Proc. NASA*, Langley SP–321, pp. 361–422.

Launder, B. E., and B. I. Sharma (1974): "Application of the energy dissipation model of turbulence to the calculation of flow near a spinning disc," *Letters in Heat and Mass Transfer*, Vol. 1, pp. 131–138.

Launder, B. E., and D. B. Spaulding (1974): "The numerical computation of turbulent flow," *Comp. Method in Appl. Mech. and Engr.*, Vol. 3, p. 269.

Launder, B. E., G. J. Reece, and W. Rodi (1975): "Progress in the development of a Reynolds-stress turbulence closure," *Journal of Fluid Mechanics,* Vol. 68, pp. 537–566.

Lawrence, S. L., and A. Balakrishnan (1988): "UPS code development," *Fifth National Aerospace Plane Technology Symposium,* Paper No. 13.

Lawrence, S. L., and R. U. Jettmar (1988): "Hypersonic flow-field predictions using space-marching and time-dependent upwind codes," *Fourth National Aerospace Plane Technology Symposium,* pp. 215–234.

Lawrence, S. L., D. S. Chaussee, and J. C. Tannehill (1987): "Application of an upwind algorithm to the PNS equations," *AIAA 22nd Thermophysics Conf.,* AIAA–87–1112, Honolulu, Hawaii.

Lawrence, S. L., U. Kaul, and J. C. Tennehill (1989): "UPS code enhancement," *Sixth National Aerospace Plane Technology Symposium,* pp. 47–60.

Lax, P. D. (1973): "Hyperbolic systems of conservation laws and the mathematical theory of shock waves," *SIAM,* Philadelphia.

Lee, C. H., K. Squires, J. P. Bertoglio, and J. Ferziger (1988): "Study of Lagrangian characteristic times using direct numerical simulation of turbulence," *Sixth Symposium on Turbulence Shear Flows,* Toulouse, France.

Lee, H. N., and J. K. Shi (1986): "Pseudospectral technique for calculation of atmospheric boundary layer flows," *J. Climate and Metero.*

Lee, R. S., and H. K. Cheng (1969): "On the outer-edge problem of a hypersonic boundary layer," *Journal of Fluid Mechanics,* Vol. 38, pp. 161–170.

Lesieur, M. (1987): *Turbulence in Fluids,* Martin Nijhoff, Dordrecht.

Libby, P. A., and R. J. Cresci (1961): "Experimental investigations of downstream influence of stagnation-point mass transfer," *J. of Aero. Sciences,* Vol. 28, No. .l, pp. 51–64.

Lin, S., and J. D. Teare (1963): "Rate of ionization behind shock wave in air. Part 2. Theoretical interpretations," *Physics Fluids,* Vol. 6, No. 3.

Lin, S., R. Neal, and W. Fyfe (1962): "Rate of ionization behind shock waves in air. Part 1. Experimental results," *Physics Fluids,* Vol. 5, No. 12.

Lin, T. C., and R. J. Bywater (1983): "Turbulence models for high-speed rough wall boundary layer," *AIAA Journal,* Vol. 20, No. 3, pp. 325–333.

Liu, S. K. (1984): "Complementary stochastic methods in computational fluid dynamics," in *Finite Elements in Fluid,* Elsievier Book Company, Amsterdam and New York.

Liu, S. K., and J. J. Leendertse (1978): "Multidimensional numerical modeling of coastal seas," *Advances in-Hydroscience,* Academic Press, New York.

Liu, S. K., and J. J. Leendertse (1987): *Modeling the Alaskan Continental Shelf Waters,* RAND, R–3567–NOAA/RC, 136 pages.

Liu, S. K., and J. J. Leendertse (1990): "Computation of 3-D fluid-driven currents by response function method," in *Coastal Engineering,* Delft, The Netherlands.

Lockman, W. K., S. L. Lawrence, and J. W. Cleary (1989): "Experimental and computational flow-field results for an all-body hypersonic aircraft," *Sixth National Aerospace Plane Technology Symposium,* pp. 265–294.

Luchini, P. (1987): "An adaptive-mesh finite-difference solution method for the Navier-Stokes equations," *Journal of Computational Physics,* Vol. 68, pp. 283–306.

Lumley, J. L. (1978): "Computational modelling of turbulent flows," *Advance in Appl. Mech.,* Vol. 18, pp. 123–176.

MacCormack, R. W. (1969): "The effects of viscosity in hypervelocity impact cratering," *AIAA,* paper 69–354.

MacCormack, R. W. (1971): "Numerical solution of the interaction of a shock wave with a laminar boundary layer," *Lecture Notes in Physics,* Vol. 8, pp. 151–163.

MacCormack, R. W. (1976): *An Efficient Numerical Method for Solving the Time-Dependent Compressible Navier-Stokes Equations at High Reynolds Numbers,* NASA, TM X–73, p. 129.

MacCormack, R. W. (1982): "A numerical method for solving the equations of compressible viscous flow," *AIAA Journal,* Vol. 20, No. 9, pp. 1275–1281.

MacCormack, R. W., and B. S. Baldwin (1975): "A numerical method for solving the Navier-Stokes equation with applications to shock boundary layer interactions," *AIAA,* paper 75–1.

Mackley, E. A. (1986): An interview in *Mechanical Engineering,* June 1986, pp. 32–36.

Makatos, N. C. (1986): "The mathematical modelling of turbulent flows," *Appl. Math. Modelling,* Vol. 10, pp. 190–220.

Marvin, J. G. (1983): "Turbulence modeling for computational aerodynamics," *AIAA Journal,* Vol. 21, No. 7, pp. 941–955.

Masson, D. J., and C. Gazley, Jr. (1956), *Aeronaut. Engineering Review,* Vol. 15, pp. 46–55.

Matsuno, K., and H. A. Dwyer (1988): "Adaptive methods for elliptic grid generation," *Journal of Computational Physics,* Vol. 77, pp. 40–52.

Mehta, U. B. (1990a): "Computational requirements for hypersonic flight performance estimates," *Journal of Space and Rockets,* Vol. 27, No. 2, pp. 103–112.

Mehta, U. B. (1990b): *Some Aspects of Uncertainty in Computing Hypersonic Flight Estimates,* NASA TM–102804.

Midden, R. E., and C. G. Miller (1978): *Description and Preliminary Calibration Results for the Langley Hypersonic CF_4 Tunnel,* NASA TM 78800.

Mileshin, V. I. (1986): "Calculation of three-dimensional supersonic flow around air intake in regimes with a detached shock wave," *USSR Comp. Maths. and Math. Physics,* Vol. 26, No. 6, pp. 65–75.

Miller, K. (1981): "Moving finite elements, II," *SIAM Journal on Numerical Analysis,* Vol. 18, pp. 1033–1057.

Miller, K., and R. N. Miller (1981): "Moving finite elements, I," *SIAM Journal on Numerical Analysis,* Vol. 18, pp. 1019–1032.

Molvik, G. A., and C. L. Merkle (1989): "A set of strongly coupled upwind algorithms for computing flows in chemical nonequilibrium," *AIAA,* paper 89–0199.

Moretti, G. (1968): *Inviscid Blunt Body Shock Layers,* PIBAL Rep. No. 68–15, Brooklyn Polytech. Inst.

Moretti, G. (1972): *Thoughts and Afterthoughts about Shock Computations,* PIBAL Rep. No. 72–37, Brooklyn Polytech. Inst.

Nakahashi, K., and G. S. Deiwert (1986): "Three-dimensional adaptive grid method," *AIAA Journal,* Vol. 24, No. 6.

National Research Council (1986): *Current Capabilities and Future Directions in Computational Fluid Dynamics,* National Academy Press, Washington, D. C.

National Research Council (1989): *Hypersonic Technology for Military Application,* Air Force Studies Board, National Academy Press, Washington D. C.

Navier, C.L.M.H. (1822): "Memoire sur les Lois du Mouvement des Fluids," *Memoires de l'Academie des Sciences,* pp. vi, 389.

Nelson, E. S., S-T Yu, and Y-L Tsai (1989): "A reacting LU code for combustors and nozzles," *Sixth National Aerospace Plane Technology Symposium,* pp. 119–128.

Novikov, E. A. (1990): "The effects of intermittency on statistical characteristics of turbulence and scale similarity of breakdown coefficients," *Physics of Fluids A, Fluid Dynamics,* Vol. 2, No. 5, pp. 814–820.

Nyland, F. S. (1962): *The Synergetic Plane Change for Orbiting Spacecraft,* RAND, RM–3231–PR.

Nyland, F. S. (1964): *Analytic Trajectories for AEROSPACEPLANE,* RAND, RM–4357–PR.

Nyland, F. S. (1965): *Hypersonic Turning with Constant Bank Angle Control,* RAND, RM–4483–PR.

Ogawa, S., and T. Ishiguro (1987): "A method for computing flow fields around moving bodies," *Journal of Computational Physics,* Vol. 69, pp. 49–68.

Ominsky, D., and H. Ide (1989): "An effective flutter control method using fast, time accurate CFD codes," *AIAA,* paper 89–3468, Boston Massachusetts.

Orszag, S. A. (1970a): "Transform method for calculation of vector coupled sums: application to the spectral form of the vorticity equation," *J. Atmos. Sci.*, Vol. 27, pp. 890–895.

Orszag, S. A. (1970b): "Numerical simulation of incompressible flows within simple boundaries," *Journal of Fluid Mechanics*, Vol. 49, pp. 75–112.

Orszag, S. A. (1971): "Numerical simulation of incompressible flows within simple boundaries: Galerkin (spectral) representations," *Studies in Appl. Math.*, Vol. 50, pp. 293–327.

Papamoschou, D. (1989): "Structure of the compressible turbulent shear layer," *AIAA*, paper 89–0126.

Passot, T., and A. Pouquet (1988): "Hyperviscosity for compressible flows using spectral methods," *J. Comp. Phys.*, Vol. 75, pp. 300–313.

Patel, V. C., W. Rodi, and G. Scheuerer (1985): "Turbulence models for near-wall and low Reynolds number flow, a review," *AIAA Journal*, Vol. 23, pp. 1308–1319.

Patterson, G. S., and S. A. Orszag (1971): "Spectral calculations of isotropic turbulence: efficient removal of aliasing interactions," *Physics of Fluids*, Vol. 14, pp. 2538–2541.

Peaceman, D. W., and H. H. Rachford (1955): "The numerical solution of parabolic and elliptic differential equations," *J. SIAM*, Vol. 3, pp. 28–41.

Pelz, R. B. (1989): "A parallel Chebyshev pseudospectral method," *42nd Annual Meeting*, Fluid Dynamics Division, American Physics Society, Palo Alto, California.

Peraire, J., M. Vahdati, K. Morgan, and O. C. Zienkiewicz (1987): "Adaptive remeshing for compressible flow computations," *Journal of Computational Physics*, Vol. 72, pp. 449–466.

Peyret, R., and H. Viviand (1975): "Computation of Viscous Compressible Flow Based on the Navier-Stokes Equations," AGARD–AG–212.

Phillips, H. (1983): *Towards a Two-Fluid Model for Flame Acceleration in Explosions, H and SE Explosion and Flame Lab*, Buxton, England.

Poisson, S. D. (1829): "Memoires sur les équations générales de équilibre et du mouvement de corps solids élastiques et des fluids," *Journ. de Ecole Polytechn.*, pp. xiii, 1.

Power, G. D., and T. J. Barber (1987): "Analysis of complex hypersonic flows with strong viscous/inviscid interaction," *AIAA*, paper 87–1189, AIAA 19th Fluid Dynamics, Plasma Dynamics and Laser Conference.

Prabhu, D. K., J. C. Tannehill, and J. G. Marvin (1987): "A new PNS code for three-dimensional chemically reacting flows," *AIAA 22nd Thermophysics Conference*, Honolulu, Hawaii, AIAA–87–1472.

Prozen, R. J., L. W. Spradley, P. G. Anderson, and M. L. Pearson (1977): "The general interpolation method," *AIAA*, paper 76–642.

Pulliam, T. H. (1984): "Euler and thin layer Navier-Stokes codes: ARC2D, ARC3D," Notes for Computational Fluid Dynamics User's Workshop, University of Tennessee Space Inst., Tullahoma, Tennessee.

Pulliam, T. H., and J. L. Steger (1980): "On implicit finite difference simulations of three-dimensional flow," *AIAA Journal*, Vol. 18, pp. 159–167; also in *AIAA*, paper No. 78–10, 1978.

Qian, J. (1986): "Universal energy cascade in two-dimensional turbulence," *Phys. Fluids*, Vol. 29, No. 11, pp. 3608–3611.

Rangwalla, A. A., and B. R. Munson (1987): "Numerical solution for viscous flow for two-dimensional domain using orthogonal coordinate systems," *Journal of Computational Physics*, Vol. 70, pp. 373–396.

Reddy, K. C. (1983): "Pseudospectral approximation in a three-dimensional Navier-Stokes code," *AIAA Journal*, Vol. 21, No. 8, pp. 1208–1210.

Reynolds, O. (1894): "On the dynamical theory of incompressible fluids and the determination of the criterion," *Phil. Trans. A.*, Vol. 186, Papers, Vol. 2, p. 535.

Reynolds, W. C. (1976): "Computation of turbulent flows," *Ann. Rev. of Fluid Mech.*, Vol. 8, pp. 183–208.

Rice, J. R. (1985): "Using supercomputers today and tomorrow," *Proceedings, 3rd Army Conf. Appl. Math. Computing.*

Richardson, L. F. (1922): *Weather Prediction by Numerical Process*, Cambridge University Press, London.

Richardson, P. F., E. B. Parlette, J. H. Morrison, G. F. Switzer, A. D. Dilley, and W. M. Eppard (1988): "Data comparisons between a 3-D Navier-Stokes analysis and experiment for the McDonnell Douglas lifting body generic option #2," *Fourth National Aerospace Plane Technology Symposium*, pp. 53–86.

Ringleb, F. (1940): "Exakte Losungen der differentialglechungen einer adiabatischen gasstromung," *Zeitschriff für angewandte mathematik und mechnik*, Vol. 20, pp. 185–198; abstract in the *Journal of the Royal Aeronautical Society*, Vol. 46, pp. 403–404, 1942.

Rizzi, A., and B. Engquist (1987): "Selected topics in the theory and practice of computational fluid dynamics," *Journal of Computational Physics*, Vol. 72, pp. 1–69.

Roberts, W. W., and M. A. Hausman (1988): "Hypersonic, stratified gas flows past an obstacle: Direct simulation Monte Carlo calculations," *Journal of Computational Physics*, Vol. 77, pp. 283–317.

Rodi, W. (1981): "Turbulence models and their application in hydraulics," *International Association for Hydraulic Research.*

Rodi, W., and D. B. Spalding (1970): "A two parameter model of turbulence and its application to free jets," *Warme und Stoffubertragung*, Vol. 3, p. 85.

Rogallo, R. S., and P. Moin (1984): "Numerical simulation of turbulent flows," *Ann. Rev. of Fluid Mech.*, Vol. 16, pp. 99–137.

Rogers, S. E., D. Kwak, and U. Kaul (1987): "On the accuracy of the pseudo compressibility method in solving the incompressible Navier-Stokes equations," *Appl. Math. Modelling*, Vol. 11, pp. 35–44.

Rotta, J. (1951): "Statistical theory of non-homogeneous turbulence" (in German), *Zeitsch. für Physik*, Vol. 129, No. 547, and Vol. 131, No. 51.

Rudman, S., and S. G. Rubin (1968): "Hypersonic viscous flow over slender bodies with sharp leading edges," *AIAA Journal*, Vol. 6, pp. 1883–1889.

Saint-Venant, B. (1843): *Comptes Rendus*, Vol. xvii, p. 1240.

Saint-Venant, B. (1871): "Theory of unsteady flow, with application to river floods and propagation of tides in river channels," *Comptes Rendus*, Vol. 73, Academy of Science, Paris, pp. 148–154, 237–240.

Salas, M. D., T. A. Zang, and M. Y. Hussaini (1982): "Shock-fitted Euler solutions to shock-vortex interactions," in E. Krause (ed.), *Proc. 8th Int. Conf. Numerical Method in Fluid Dynamics*, Spring-Verlag. pp. 461–467.

Schetz, J. A., F. S. Billing, and S. Favin (1982): "Flow field analysis of a Scramjet combustion with a coaxial fuel jet," *AIAA Journal*, Vol. 20, pp. 1268–1274.

Schetz, J. A., F. S. Billing, and S. Favin (1987): "Numerical solutions of Scramjet nozzle flows," *J. Propulsion*, Vol. 3, No. 5, pp. 440–447.

Schiestel, R. (1987): "Multiple-time-scale modelling of turbulent flows in one point closures," *Phys. Fluids*, Vol. 30, pp. 722–731.

Schiff, L. B., and J. L. Steger (1980): "Numerical simulation of steady supersonic viscous flow," *AIAA Journal*, Vol.18., pp. 1421–1430.

Schmidt, G. H., and F. J. Jacobs (1988): "Adaptive local grid refinement and multi-grid in numerical reservoir simulation," *Journal of Computational Physics*, Vol. 77, pp. 140–165.

Shang, J. S. (1984): "Numerical simulation of wing-fuselage aerodynamic interaction," *AIAA Journal*, Vol. 22, pp. 1345–1353.

Shang, J. S., and S. J. Scherr (1985): "Navier Stokes solution of the flow around a complete aircraft," *AIAA*, paper 85–1509–cp.

Shang, J. S., P. G. Puning, W. L. Hankey, and M. C. Wirth (1980): "Performance of a vectorized 3-D Navier-Stokes code on the CRAY-1 computer," *AIAA Journal*, Vol. 19, pp. 1073–1079.

Shchelkin, K. (1943): *Technical Physics in Soviet Physics*, Vol. 13, p. 520.

Shih, T. H., and J. L. Lumley (1986): "Second-order modeling of near-wall turbulence," *Physics of Fluids*, Vol. 29, pp. 971–975.

Shinn, J. L., H. C. Yee, and K. Uenishi (1986): "Extension of a semi-implicit shock-capturing algorithm for 3-D fully coupled, chemically reacting flows in generalized coordinates," *AIAA 22nd Thermophysics Conference*.

Silberman, I. (1954): "Planetary waves in the atmosphere," *J. Meteor.*, Vol. 11, pp. 29–34.

Sinha, N., and S. M. Dash (1986): "Parabolized Navier-Stokes analysis of ducted turbulent mixing problems with finite rate chemistry," *AIAA*, paper 86–0004.

Sinha, N., and S. M. Dash (1987): "Parabolized Navier-Stokes analysis of ducted supersonic combustion problems," *J. Propulsion*, Vol. 3, No. 5, pp. 455–464.

Sinha, N., W. Krawczyk, and S. M. Dash (1987): "Inclusion of chemical kinetics into Roe upwind/Beam-Warming PNS models for hypersonic propulsion applications," *AIAA*, paper 87–1898.

Sokolnikoff, S. I., and R. M. Redheffer (1966): *Mathematics of Physics and Modern Engineering*, McGraw-Hill Book Company.

Spalart, P. R. (1988): "Direct simulation of a turbulent boundary layer up to $R\theta = 1400$," *Journal of Fluid Mechanics*, Vol. 187, pp. 61–98.

Spalding, D. B. (1967a): "Heat transfer from turbulent separated flows," *Journal of Fluid Mechanics*, Vol. 27, p. 97.

Spalding, D. B. (1967b): "The spread of turbulent flames confined in ducts," *Eleventh International Symposium on Combustion*, the Combustion Inst., Pittsburgh, Pennsylvania, pp. 807–815.

Spalding, D. B. (1969): *The Prediction of Two-Dimensional, Steady Turbulent Flows*, Imperial College, Heat Transfer Section, Rep. EF/TN/A/16.

Spalding, D. B. (1971): "Mixing and chemical reaction in steady confined turbulent flames," *Thirteenth International Symposium on Combustion*, the Combustion Inst., Pittsburgh, Pennsylvania, p. 649.

Spalding, D. B. (1976): "Mathematical models of turbulent flames: A review," *Combustion Science and Technology*, Vol. 13, pp. 3–25.

Spalding, D. B. (1978): "A general theory of turbulent combustion," *Journal of Energy*, Vol. 2, pp. 16–23.

Spalding, D. B. (1979): "Theories of turbulent reacting flows," *AIAA*, paper 79–0213.

Spalding, D. B. (1983): "Chemical reaction in turbulent fluids," *J. Physico-Chemical Hydrodynamics*, Vol. 4, No. 4.

Spalding, D. B. (1984): "Two-fluid models of turbulence," NASA Work Shop on Theoretical Approaches to Turbulence, Hampton, Virginia.

Spalding, D. B. (1986): "The two-fluid model of turbulence applied to combustion phenomena," *AIAA Journal,* Vol. 24, No. 6, pp. 876–884.

Steger, J. L. (1977): "Implicit finite difference simulation of flow about arbitrary geometries with applications to air foil," *AIAA,* paper 77–665.

Stetson, K. F. (1987): *On Predicitng Hypersonic Boundary Layer Transition,* AFWAL–TM–84–160–FIMG, Flight Dynamics Lab., Air Force Wright Aeronautical Lab., Wright-Patterson Air Force Base, Ohio.

Stokes, Sir G. G. (1845): "On the theories of the internal friction of fluids in motion," *Cambridge Trans.,* pp. viii, 289.

Stookesberry, D. C., and J. C. Tennehill (1987): "Computation of separated flow using the space-marching conservative supra-characteristics method," *AIAA Journal,* Vol. 25, No. 8, pp. 1063–1070.

Strange, P. M., and G. J Fix (1973): *An Analysis of the Finite Element,* Prentice-Hall, Englewood Cliffs, New Jersey.

Strawa, A. W., D. Prabhu, and R. Kruse (1988): "A comparison of experiment and computation for slender cones at high mach numbers," *Fourth National Aerospace Plane Symposium,* pp. 115–132.

Su, M. D. (1990): "Algebraic modelling of large eddy simulation and its application," *Science in China,* Series A, Vol. 33, No. 2, pp. 185–195.

Svehla, R. A. (1962): *Estimated Viscosities and Thermal Conductivities of Gas at High Temperatures,* NASA TR–R–132.

Svehla, R. A., and B. J. McBride (1973): *FORTRAN IV Computer Program for Calculation of Thermodynamic and Transport Properties of Complex Systems,* NASA TN D–7056.

Tassa, Y., and R. J. Conti (1987): "Numerical Navier-Stokes modeling of hypersonic laminar wakes behind blunt cones with real-gas effects," AIAA–86–0734, AIAA 25th Aerospace Science Meeting, Reno, Nevada.

Taylor, T. P., R. B. Myers, and J. H. Albert (1981): "Pseudospectral calculations of shock waves, rarefaction waves and contact surfaces," *Comp. Fluids,* Vol. 9, pp. 469–473.

Teare, J. D., S. Georgiev, and R. A. Allen (1962): "Radiation from the nonequilibrium shock front," *Hypersonic Flow Research,* Vol. 7.

Tennekes, H., and J. L. Lumley (1972): *A First Course in Turbulence,* MIT Press, Cambridge, Massachusetts.

Thomas, P. D. (1979): "Boundary conditions for implicit solutions to the compressible Navier-Stokes equations on finite computational domains," AIAA, paper 79–1447, *Proc. AIAA 4th CFD Conference,* Williamsburg, Virginia.

Thomas, P. D. (1987): "Solution-adaptive grid for viscous hypersonic flow," Open Forum Paper AIAA 87–0644, *AIAA 25th Aerospace Sciences Meeting,* Reno, Nevada.

Thomas, P. D. (1988): *Navier-Stokes Simulation of 3D Hypersonic Equilibrium Flows with Ablation, Vol. I: Theory,* AFWAL–TR–88–3020, Flight Dynamics Lab., Air Force Wright Aeronautical Lab, Wright-Patterson Air Force Base, Ohio.

Thomas, P. D., and C. K. Lombard (1979): "The geometric conservation law and its application to fluid dynamic computations on moving grids," *AIAA Journal,* Vol. 17, No. 10.

Thompson, J. F. (1984): "Grid generation techniques in computational fluid dynamics," *AIAA Journal,* Vol. 22, p. 1505.

Thompson, J. F., Z.U.A. Warsi, and C. W. Mastin (1985): *Numerical Grid Generation, Foundations and Applications,* North Holland.

Thompson, M. C., and J. F. Ferziger (1989): "An adaptive multigrid technique for the incompressible Navier-Stokes equations," *Journal of Computational Physics,* Vol. 82, No. 1, pp. 94–121.

Townsend, A. A. (1976): *The Structure of Turbulent Shear Flow,* Cambridge University Press.

Tsien, H. S. (1958): "The equations of gas dynamics," in H. W. Emmons (ed.), *Fundamentals of Gas Dynamics,* Princeton University Press.

Van Driest, E. R. (1956): "On turbulent flow near a wall," *J. Aero. Sci.,* Vol. 23, pp. 1007–1011.

Verwer, J. G., J. G. Blom, and J. M. Sanz-Serna (1989): "An adaptive moving grid method for one-dimensional system of partial differential equations," *Journal of Computational Physics,* Vol. 82, pp. 454–486.

Viegas, J. R., and C. C. Horstman (1979): "Comparison of multiequation turbulence models for several shock-boundary layer interactions," *AIAA Journal,* Vol. 17, pp. 811–820.

Viegas, J. R., and M. W. Rubesin (1983): "Wall-function boundary conditions in the solution of the Navier-Stokes equations for complex compressible flows," *AIAA,* paper 83–1694.

Vincenti, W. G., and C.H.J. Kruger (1962): *Introduction to Physical Gas Dynamics,* Robert Krieger Publishing Company.

von Neumann, J. (1945): "First draft of a report on the EDVAC," Report to the U. S. Army Ordnance Department, University of Pennsylvania.

von Neumann, J. (1958): *The Computer and the Brain,* Yale University Press, New Haven, Connecticut.

Waltrup, P. J. (1987): "Liquid-fueled supersonic combustion ramjets: a research perspective," *J. Propulsion,* Vol. 3, No. 6, pp. 515–524.

Waltrup, P. J., F. S. Billig, and R. Stockbridge (1979): "A procedure for optimizing the design of Scramjet engines," *Journal of Spacecraft and Rockets,* Vol. 16, pp. 163–172.

Waltrup, P. J., G. Y. Anderson, and F. D. Stull (1976): "Supersonic combustion Ramjets (SCRAMJET) engine development in the United States," 76–042, *3rd International Symp. of Air Breathing Engines,* Applied Physics Laboratory, Johns Hopkins University, Laurel, Maryland.

Warfield, M. J., and B. Lakshminarayana (1987): "Computation of rotating turbulent flow with an algebraic Reynolds stress model," *AIAA Journal,* Vol. 25, No. 7, pp. 957–964.

Waskiewicz, J. D., J. S. Shang, and W. L. Hankey (1980): "Numerical simulation of near wakes utilizing a relaxation turbulence model," *AIAA Journal,* Vol. 18, pp. 1440–1445.

Weidner, E. H., and J. P. Drummond (1982): "Numerical study of staged fuel injection for supersonic combustion," *AIAA Journal,* Vol. 20, pp. 1426–1187.

Weinstock, J. (1981): "Theory of pressure-strain-rate correlation for Reynolds-stress turbulence closure. Part 1. off-diagonal element," *Journal of Fluid Mechanics,* Vol. 105, pp. 369–395.

White, M. E., J. P. Drummond, and A. Kumar (1987): "Evolution and application of CFD techniques for Scramjet engine analysis," *J. Propulsion,* Vol. 3, No. 5, pp. 423–439.

Wilcox, D. C. (1988): "Reassessment of the scale-determining equation for advanced turbulence models," *AIAA Journal,* Vol. 26, No. 11, pp. 1299–1320.

Wilcox, D. C., and R. M. Tracy (1976): "A complete model of turbulence," *AIAA,* paper 76–351.

Wilcox, D. C., and W. M. Rubesin (1980): *Progress in Turbulence Modeling for Complex Flow Fields Including Effects of Compressibility,* NASA Tech. Paper 1517.

Wilke, C. R. (1950): "A viscosity equation for gas mixtures," *J. of Chemical Physics,* Vol. 18, No. 4.

Williams, A. F. (1965): *Combustion Theory,* Addison-Wesley.

Wohlenberg, W. J. (1953): "Minimum depth of flame front for stable combustion in a gaseous system at constant pressure," *Fourth Symposium on Combustion,* Williams and Wilkins, Baltimore.

Wray, K. (1962): "Chemical kinetics of high temperature air," *Hypersonic Flow Research,* Vol. 7.

Yakhot, V., Z-S She, and S. A. Orszag (1989): "Deviation from the classical Kolmogorov theory of the inertial range of homogeneous turbulence," *Phys. Fluids, A–1,* Vol. 1, No. 2, pp. 289–293.

Yee, H. C. (1987): *Upwind and Symmetric Shock-Capturing Schemes,* NASA Technical Memo 89464.

Yee, H. C. (1989a): "A class of high resolution explicit and implicit shock capturing methods," *von Karman Inst. Lecture Notes in Computational Fluid Dynamics.*

Yee, H. C. (1989b): "Semi-implicit and fully implicit shock-capturing methods for nonequilibrium flows," *AIAA Journal,* Vol. 27, No. 3, pp. 299–307.

Yee, H. C., and J. L. Shinn (1986): *Semi-Implicit and Fully Implicit Shock-Capturing Methods for Hyperbolic Conservation Laws with Stiff Source Terms,* NASA–TM–89415.

Yee, H. C., G. H. Klopfer, and J. L Montagne (1990): "High-resolution shock-capturing schemes for inviscid and viscous hypersonic flows," *Journal of Computational Physics,* Vol. 88, pp. 31–61.

Yee, H. C., G. H. Klopfer, and J. L. Montagne (1988): *High-Resolution Shock-Capturing Schemes for Inviscid and Viscous Hypersonic Flows,* NASA–TM–100097.

Yeung, P. K., and S. B. Pope (1987): "Lagrangian velocity statistics obtained from direct numerical simulations of homogeneous turbulence," *Proc. 6th Symposium of Turbulent Shear Flow,* Toulouse, Paper 3–7.

York, B. J., N. Sinha, and S. M. Dash (1988): "Computational models for chemically-reacting hypersonic flow," *AIAA,* paper 88–0509.

Zang, T. A., D. A. Kopriva, and M. Y. Hussaini (1983): "Pseudospectral calculation of shock turbulence interactions," *Proc. 3rd International Conference on Numerical Methods in Laminar and Turbulent Flow,* Pineridge Press.

Zang, T. A., M. Y. Hussaini, and D. M. Bushnell (1984): "Numerical computations of turbulence amplification of shock-wave interaction," *AIAA Journal,* Vol. 22, pp. 12–21.

Zienkiewicz, O. C. (1977): *The Finite Element Method,* McGraw Hill Book Company, London.

Zienkiewicz, O. C., and Y. K. Cheung (1965): *Engineers,* pp. 507–510.